ME THESIS

Long-term Performance of Timber-Concrete Composite Flooring Systems

A thesis submitted in partial fulfilment
of the requirements for
Master of Engineering by research

Mulugheta Hailu
University of Technology Sydney
Faculty of Engineering and IT
School of Civil & Environmental Engineering
Centre for Built Infrastructure Research
Broadway, NSW 2007

Principal supervisor: Prof. Keith Crews
Co-Supervisor: Dr Rijun Shrestha

September 2015

CERTIFICATE OF ORIGINAL AUTHORSHIP

I certify that the work in this thesis has not previously been submitted for a degree nor has it been submitted as part of requirements for a degree except as fully acknowledged within the text.

I also certify that the thesis has been written by me. Any help that I have received in my research work and the preparation of the thesis itself has been acknowledged. In addition, I certify that all information sources and literature used are indicated in the thesis.

Production Note:
Signature removed prior to publication.

September 2015

TO MY WIFE NEBYAT

&

MY DAUGHTER MIKAL

Acknowledgements

I would never have been able to finish my dissertation without the guidance of my supervisors, help from friends, and support from my wife.

I would like to express my deepest gratitude to my principal supervisor, Prof. Keith Crews, for opening this opportunity to do research under his supervision and my co-supervisors Dr Rijun Shrestha and Dr Christophe Gerber, for their excellent guidance, caring, patience, and providing me with an excellent atmosphere for doing research. I would also like to thank Prof. Bijan Samali, for his encouragement and advice in the initial period of my enrolments.

This project was funded by STIC (Structural Timber Innovation Company) and I would like to thank them for their financial support and creating this research happen.

I would like to thank also Rami Haddad, Peter Brown together with all Civil engineering laboratory staff for their support and encouragement throughout the research period.

Finally, I would like to thank my wife, Nebyat, She was always there cheering me up and stood by me through the good times and bad and I would never been able to complete without her unfailing support.

List of journal papers

Hailu, M., Shrestha, R., Crews, K., 2015, "Long-term deflection of Timber composite beams in cyclic humidity conditions in bending: Experimental investigation", Journal of Construction and Building Materials, [***To be submitted]***

Hailu, M., Shrestha, R., Crews, K., 2015, "Short-term collapse test of TCC beam after long-term test: Experimental investigation", Journal of Construction and Building Materials, [***To be submitted]***

List of conference papers

Hailu, M., Gerber, C., Shrestha, R., Crews, K., 2012, "Long-term behaviour of Timber-Concrete Composite beams", in "12th WCTE, Proceedings of the World Conference on Timber Engineering, New Zealand, Auckland.

Hailu, M., Shrestha, R., Gerber, C. & Crews, K. 2012, "Residual strength of timber-concrete beams after long-term test", Proceedings, 22nd Australasian Conference on the Mechanics of Structures and Materials, ACMSM 22, Sydney, Australia, 11-14 December.

Hailu, M., Shrestha, R., Crews, K., 2013, "Long-term behaviour of Timber-Concrete Composite Beams in Cyclic Humidity Conditions", Composite Construction VII, Palm Cove, Queensland, Australia, 28-31 July.

Hailu, M., Shrestha, R., Crews, K. 2014, "Long-term deflection of Timber composite beams in cyclic humidity conditions in bending", in "14th WCTE', Proceedings of the World Conference on Timber Engineering, Quebec, Canada.

Hailu, M., Shrestha, Crews, K. 2014, "Timber composite floor beams under 2 years long-term load", Proceedings, 23rd Australasian Conference on the Mechanics of Structures and Materials, ACMSM 23, Byron Bay, Australia, 9-12 December 2014.

LIST OF NOTATIONS

Δ	Deflection (mid-span deflection)
ρ	density
Δ	elastic deflection of the system
δ	deflection
b	floor width
B_c	width of concrete topping
CO_2	carbon dioxide
d	diameter of the shear connector
D_C	theoretical full composite deflection
D_I	measured partial composite deflection
D_N	theoretical fully non-composite deflection
D_w	depth of LVL web
E	modulus of elasticity; efficiency of composite
E_{cj}	mean MOE of concrete at the appropriate age
EI	flexural stiffness
$(EI)_{eff}$	effective bending stiffness
E_x	mean modulus of elasticity of LVL in x-direction
F, P	point load
f'_b	characteristic bending strength
f'_c	characteristic compression strength parallel to grain
f'_p	characteristic compression strength perpendicular to grain
f'_s	characteristic shear strength
f'_{sj}	characteristic shear strength at joint details
f'_t	characteristic tensile strength
f_b	mean bending strength
f_c	mean compression strength
f_{cm}	mean value of the compressive strength of concrete at the relevant age
f_t	mean tensile strength
f_v	mean shear strength

g	acceleration due to gravity (9.81 m/s^2)
G	shear modulus
I	moment of inertia
k	stiffness
$K_1,K_4,k_6,K_7,K_9,K_{11},K_{12}$	Modification factors for timber as per AS/NZS 1720
$k17$	factor for multiple nailed joints
K_{serv}	serviceability limit state stiffness
K_u	ultimate limit state stiffness
L, l	span
L_b	shear-free span between load points
m	mass of the floor ; mass per unit length; mass per unit area
M_i	initial mass of moisture content test piece
M_o	dry weight of moisture content test piece
N^*t	Axial force on timber
M^*	Design bending moment
M^*t	Design bending moment on timber
φN_R	Resisting tensile strength
φM_R	Resisting bending moment
Q_k	strength of shear connectors
s_e	spacing of the shear connectors at the ends of the beam
S_{eff}	effective constant spacing of the shear connectors
s_m	spacing of the shear connectors in the middle of the beam
S_{min}, S_{max}	Minimum and maximum spacing of the connectors
T_c	thickness of concrete topping
T_f	thickness of LVL flange
T_w	thickness of LVL web
W	effective weight of the floor
V^*	Design shear force
w	maximum short-term deflection; uniformly distributed load per unit length (Chapter 7)
γ_c	Partial safety factor for concrete

$\gamma_{.m}$	Partial safety factor for timber
$\gamma_{.con}$	Partial safety factor for connection
γ	reduction factor (gamma)

LIST OF ACRONYMS

BM	bird-mouth
CA	composite action
CoV	coefficient of variation
MOE	modulus of elasticity
FE	finite element
FEA	finite element analysis
FEM	finite element model
Glulam	glue laminated timber
LVDT	linear variable differential transformer
LVL	laminated veneer lumber
LWC	Light weight concrete
MC	moisture content
NS	normal screw
NZ	New Zealand
B-NS	Beam with normal screw connector
B-4N	Beam with four notch and with coach screw connector
B-6N	Beam with six notch and with coach screw connector
B-SFS	Beam with SFS screw as connector
Pty Ltd	proprietary limited
PSL	Parallel stranded lumber
RH	Relative air humidity
SCC	steel-concrete composite
SLS	serviceability limit state
STIC	structural timber innovation company
TCC	timber-concrete composite
TTC	Timber-timber composite
ULS	ultimate limit state
UTS	University of Technology Sydney

Table of contents

Abstract xix

1 Introduction 1

1.1 History and Background of Timber-Concrete composites 1

1.2 Research objectives and scope 3

1.3 Research Significance 4

1.4 Limitations 5

1.5 Outline of the thesis 5

2 Literature review 7

2.1 Timber-Concrete composite structures 7

2.2 Composite action of timber-concrete composite systems 8

2.3 Timber-concrete connections 11

2.3.1 Nails 15

2.3.2 SFS-Screw (VB 48-75x100) 16

2.3.3 Notch-type connection with and without dowel 19

2.4 Enhancement methods for timber-concrete composite structures 23

2.5 Long-term tests on timber-concrete composites 24

2.5.1 Summary of creep and mechano-sorptive behaviour of wood 24

2.5.2 Long-term experimental tests on TCC floors and beams 29

2.5.3 Long-term experimental tests on TCC connections only 38

2.6 Evaluation of the long-term behaviour of TCCs in accordance to Euro code 5 44

2.7 Concluding remarks 48

3 Timber Concrete Composite beams 49

3.1 Characteristics of the composite beams 49

3.2 Initial short term tests on TCC and LVL joists 52

3.2.1 Initial serviceability test on LVL joists 52
3.2.2 Initial Serviceability test on TCC beams 53
3.2.3 Composite efficiency of the TCC beams 55
3.3 Concluding remarks 61
4 Long-term testing of TCC beams 62
4.1 Test set-up 62
4.2 Environmental conditions 64
4.3 Moisture content 65
4.4 Long-term deflection of TCC beams - Discussion 68
4.5 Unloading of two TCC beams from long-term loads 73
4.6 Concluding remarks 74
5 Creep factor and evaluating the long-term deflection according to Euro code 5 75
5.1 Relative deflection of the TCC beams 75
5.2 Analytical fitted curve 77
5.3 Simplified evaluation of the long-term behaviour of TCCs in accordance to Euro code 5 using gamma method 79
5.4 Concluding remarks 81
6 Residual stiffness and strength tests after long-term test 82
6.1 Serviceability tests and loss in stiffness of TCC beams 83
6.2 Ultimate strength tests 87
6.3 Residual stiffness and strength of LVL joists 99
6.4 Concluding remarks 102
7 Long-term performance of timber-timber composite floor modulus 103
7.1 Introduction and Composite beam properties 103
7.2 Long-term test results and discussions 104
7.3 Concluding remarks 110
8 Conclusions 111

9 Future works 115
References 116
Appendix A 128
Appendix B 131
Appendix C 133
Appendix D 143
Appendix E 148
Appendix F 159
Appendix G 162
Appendix H 175

List of figures

Figure 1: Timber-concrete composite floor (adopted from SFS-Holz Beton-Verbundsystem)2
Figure 2**:** The concept of composite action; (a) fully composite action, (b) partial composite action and (c) No composite action..... 9
Figure 3: Graphical representation of the correlation between stiffness of a shear connection and the effective bending stiffness of a composite floor (Dias 2005)..... 11
Figure 4: Setting of a symmetrical push-out test 12
Figure 5**:** load-time curves for tests according to EN 26891(Dias 2005) 13
Figure 6**:** Examples of timber-concrete connections with: nails (A The concept of composite); glued reinforced concrete steel bars (A2); screws (A3); inclined screws (A4); split rings (B1); toothed plates (B2); steel tubes (B3); steel punched metal plates (B4); round indentations in timber ,with fastener preventing uplift (C1);square indentations, (C2); cup indentations and pre-stresses steel bars (C3), nailed timber planks deck and steel shear plates slotted through the deeper planks (C4), steel lattice glued to timber (D1); and steel plat glued to timber (D2) (Ceccotti 1995)..... 14
Figure 7**:** Typical load-slip behaviour for different types of joints. (Dias, 2005)..... 15
Figure 8: SFS VB screw 48-7.5x100 (Lukaszewska 2009) (all dimensions in millimetres) 17
Figure 9: Arrangement of the connectors in bending tests described by (Meierhofer 1992) 18
Figure 10: Beam with SFS screw as shear connector (Van Der Linden, 1999) (all dimension in millimetres)..... 19
Figure 11: Timber-concrete connection with grooved holes and dowels (Linden, 1999) (dimensions in mm) 20
Figure 12: Shear key connection detail (Gutkowski 2004) (dimensions in mm)..... 21
Figure 13: Semi prefabricated “M” section panel (Buchanan et al. 2008) (dimensions in mm) 22
Figure 14**:** Cross-section of the composite beam tested (Lukaszewska 2009) 23
Figure 15: Results from tensile tests made on pine (0.4x5x150 mm), loaded parallel to grain (Eriksson, Noren 1965).The upper figure shows the strain (the initial elastic strain is subtracted), measured on four samples, and the middle figure shows the free shrinkage-swelling, measured on two samples. The lower figure shows the zero-load compensated strain, i.e. the difference between the upper and the middle figure, here the medium values of the four respectively the two samples have been used (Martensson 1994). ... 26

Figure 16: Geometrical characteristics of the composite beam tested by Bonamini, Uzielli & Ceccotti (1990) (measured in mm) 30
Figure 17: Cross-section of the TCC tested at the EMPA laboratory, Dubendorf (kenel & Meierhofer 1998) 31
Figure 18: Timber-concrete composite section (left) and loads disposition (right) (Bou Said et al. 2004) 31
Figure 19: Comparison between calculated and measured mid-span deflections (Bou Said et al. 2004) 32
Figure 20: Longitudinal view and cross-section of the composite beam tested by Ceccotti et al. (2006) (dimensions in cm) 33
Figure 21: Mid-span vertical displacements for the timber beam and average value (Ceccotti 2006) 34
Figure 22; Longitudinal view (a) and cross-section (b) of the notched composite beam (measured in cm) (Fragiacomo et al. 2007) 35
Figure 23: Trend in time of the mid-span deflection after the placement of the concrete (b) and after the application of the dead load weights.(Fragiacomo et al. 2007) 35
Figure 24: The elevation of beam specimen 1a with SP+N* type during long-term test.(Lukaszewska 2009) 36
Figure 25**:** SP+N* connection type (left) and SST+S* type of connection (right) (Lukaszewska 2009) 36
Figure 26: Mid-span deflection of specimen 1a with SP+N* type during long-term test.(Lukaszewska 2009) 37
Figure 27: Mid-span deflection of specimen 2a with SST+S* type during long-term test.(Lukaszewska 2009) 37
Figure 28: Long-term mid-span deflection result (Yeoh 2009) 38
Figure 29: Half cross-section of the push-out specimens(left) and apparatus used in the long-term test to apply a sustained load (right) (dimensions in mm) (Fragiacomo et al. 2007) 39
Figure 30: Three types of connectors for shear tests (Mueller et al. 2008) 41
Figure 31: Details of the three types of connection (Yeoh et al. 2011a) 41
Figure 32: Sustained load test on connections and the cross-section of the TCC beams (Yeoh et al. 2010) 42
Figure 33: cross-section (left) and stress distribution (right) of a composite beam with flexible connection (Eurocode 5) 44
Figure 34: Cross-section of the TCC beam (Typical) (measured in mm) 49

Figure 35: Longitudinal elevation of the TCC beam (measured in mm) (a) B-NS, (b) B-4N, (C) B-6N, & (d) B-SFS 50
Figure 36: (1) Birds mouth with Ø16 mm coach screw, (2) Normal screw type-17 and (3) SFS screw connections 52
Figure 37: MOE test on LVL only 53
Figure 38: TCC beam under short-term test 54
Figure 39: Load vs. mid-span deflection during serviceability test for B_NS 56
Figure 40: Load vs. mid-span deflection during serviceability test for B_4N 56
Figure 41: Load vs. mid-span deflection during serviceability test for B_6N 57
Figure 42: Load vs. mid-span deflection during serviceability test for B_SFS 57
Figure 43: Location of strain gauges during (a) short-term tests on TCC beams 58
Figure 44: Strain readings along mid-span cross section for B_NS (conc. = strain reading on concrete, LVL= strain reading on the timber) 59
Figure 45: Strain readings along mid-span cross section for B_4N (conc. = strain reading on concrete, LVL= strain reading on the timber) 59
Figure 46: Strain readings along mid-span cross section for B_6N (conc. = strain reading on concrete, LVL= strain reading on the timber) 60
Figure 47: Strain readings along mid-span cross section for B_SFS (conc. = strain reading on concrete, LVL= strain reading on the timber) 60
Figure 48: Test set up (measured in mm) 62
Figure 49 Beams under quasi-permanent loads (lead bars) 63
Figure 50: Changes in relative humidity, moisture content and temperature 65
Figure 51 LVL MC Test samples 66
Figure 52 Moisture content of LVL samples versus time 67
Figure 53: Mid-span deflection versus time 68
Figure 54: Mid-span deflection and MC versus time for B-6N and B-SFS beams. 69
Figure 55 A comprehensive plot RH % and MC % and, mid-span deflection with time. 70
Figure 56: The temperature and relative humidity curve during the long-term test. 72
Figure 57: TCC beams unloaded after two years of long-term test 73
Figure 58: The relative creep of the TCC beams. 76
Figure 59: Mid-span deflection and analytical fitted curve using logarithmic function equation based on up to-date experimental results 77
Figure 60: Mid-span deflection and analytical predicted deflection for 50 years using logarithmic function equation based on up to-date experimental results 78
Figure 61: Test set up for serviceability and ultimate failure test of the TCC beams (typical) (in mm) 82

Figure 62: Location of strain gauges along the mid span of the cross section 83
Figure 63: Total load (2P) versus mid-span deflection at serviceability for B_NS 84
Figure 64: Total load (2P) versus mid-span deflection at serviceability for B_4N 84
Figure 65: Strain profiles along the mid-span cross section from serviceability tests for B-NS (tests done before and after the long-term test, LT= long-term test) 86
Figure 66: Strain profiles along the mid-span cross section from serviceability tests for B-4N (tests done before and after the long-term test, LT= long-term test) 86
Figure 67: Total load (2P) versus mid-span deflection at ultimate stress for B_NS 88
Figure 68: Total load (2P) versus mid-span deflection at ultimate stress for B_4N 88
Figure 69: Tension failure of the joist B_NS 89
Figure 70: Tension failure of the joist B_4N 89
Figure 71: Total load (2P) versus slip B_NS 90
Figure 72: Total load (2P) versus slip B_4N 90
Figure 73 Connector close to the right support after the failure test (left) and before the failure test (right) for B-4N 91
Figure 74 Connector close to the right support after failure for B-NS 91
Figure 75: Magnitude of the strain along the mid span cross section during ultimate test on B_NS (the numbers from 1 to 9 refer to the strain gauge numbers given in Figure 62, (-ve) strain in compression and (+ve) strain in tension 92
Figure 76: Magnitude of the strain along the mid span cross section during ultimate test on B_4N [the numbers from 1 to 9 refer to the strain gauge numbers given in Figure 62, (-ve) strain in compression and (+ve) strain in tension] 93
Figure 77: Strain profile along the mid span cross section of B-NS during ultimate test 94
Figure 78: Strain profile along the mid span cross section of B-4N during ultimate test 94
Figure 79: Set-up for bending tests of LVL joist 100
Figure 80: Set-up for tension test of LVL joist 101
Figure 81: Atypical cross section of the composite beams 103
Figure 82: Load versus deflection (Zabihi 2012, Zabihi 2014) 104
Figure 83: Long-term test set up and service loads 106
Figure 84: Timber composite beams in humidity chamber 106
Figure 85: Relationship between the Mid-span deflection, moisture content and relative humidity of the chamber 107
Figure 86 Relationship between deflection and length of exposure cycle (Hearmon and Paton 1964) 128
Figure 87 Deflection of loaded beech beams, Curve A, specimen maintained at R.H. 93%;Curve B, specimen, specimen loaded dry and then ’cycled’; curve, specimen

loaded at R.H.93% and then ‘cycled’. Solid line. R.H. zero; broken line, R.H.93%.(Gibson, 1965) 129
Figure 88 Typical creep curves A, B and C, due to cycling of relative humidity between 90% and 30%, adopted from Epmeier (2007) 130
Figure 89 the lengths of the coach screw, SFS and normal screw used in the connectors .. 131
Figure 90 Location of MC samples in the fog-room 143
Figure 91 General layout of TCC beams in fog-room 143
Figure 92 Relationship between air humidity and moisture content (top) and deflection (bottom) with time 145
Figure 93 Relationship between deflection, moisture content and air humidity 146
Figure 94 Comparison of the MC measurement between small and large samples. 147
Figure 95 Relative creep of TCC beams with time 149
Figure 96 Logarithmic curve fitting 150
Figure 97 Logarithmic curve fitting 150
Figure 98 Magnitude of the Strain measured on tests conducted before and after long-term test for B-NS (LT= long-term test) 160
Figure 99 Magnitude of the Strain measured on tests conducted before and after long-term test for B-4N (LT= long-term test) 161
Figure 100 Connector close to the right support before (right) and after (left) failure for B-4N 171
Figure 101 Connector at L/4 from the left support before (left) and after (right) failure for B-4N 171
Figure 102 Failure patterns on the LVL for B-4N 172
Figure 103 all the four connectors’ investigation after failure for B-4N (N1 left end support, N2 left at L/4, N3 right at L/4 and N4 right support) 172
Figure 104 Connector close to the right support for B-NS. 172
Figure 105: Strain distribution along the beam cross section during short-term test (Zabihi 2012) 175
Figure 106: Relationship between the Mid-span deflection, moisture content and relative humidity of the chamber for timber only floor beams. 178

List of tables

Table 1: Properties of concrete used (Pham 2010) 51
Table 2 Type of connectors, characteristic strength and slip moduli 51
Table 3: The Modulus of Elasticity of the Timber (LVL) (Pham 2010) 53
Table 4 TCC beams bending stiffness (Pham 2010) 54
Table 5 Theoretical bending stiffness of TCC beams at serviceability 55
Table 6 Composite action achieved by TCC beams 58
Table 7 Instantaneous elastic mid-span deflection measured 64
Table 8 Instantaneous elastic deflection and recovery after load removal 74
Table 9 Relative creep values after three years 76
Table 10 Theoretical bending stiffness's using Euro code 5 80
Table 11 Comparison between the predicted theoretical Mid-span deflections according Eurocode 5 with the deflections from the experimental result 80
Table 12 Percentage loss in bending stiffness in TCC beams 85
Table 13 Summary of ultimate tests results for the TCC beams 87
Table 14 Comparison of the theoretical design capacity of the TCC beams using GAMMA method with the failure loads (kN) from experimental results 97
Table 15 Modulus of Elasticity of LVL after long-term test 99
Table 16 Tensile strength of LVL after long-term test 100
Table 17 Percentage loss in MOE of LVL joists 101
Table 18 Relative creep values of the composite beams 109
Table 19 LVL properties (Carter Holt Harvey) 131
Table 20 Shear strength of the connectors used (Khorsandnia et al 2012) 132
Table 21 Slip moduli of the connectors used (Khorsandnia et al. 2012) 132
Table 22 Slip moduli of the connectors used (Gerber et al. 2011) 132
Table 23: Geometric properties of concrete and timber for all the TCC beams 133
Table 24: Properties of concrete used 133
Table 25 Theoretical effective serviceability bending stiffness for B-NS 134
Table 26 Theoretical effective serviceability bending stiffness for B-4N 136
Table 27 Theoretical effective serviceability bending stiffness for B-6N 138
Table 28 Theoretical effective serviceability bending stiffness for B-SFS 140
Table 29 Serviceability design load for TCC beam 144
Table 30 Weights (lead bars) on the TCC beams 144

Table 31: Transformed section properties for B_NS (typical)..... 148
Table 32: Bending stiffness theoretical and experimental..... 149
Table 33: Concrete design creep coefficient (t=3years after loading)..... 151
Table 34: Concrete design creep coefficient (t=0, instant of loading)..... 151
Table 35: Concrete design shrinkage coefficient..... 152
Table 36: Long-term bending stiffness of B-6N..... 152
Table 37: Long-term bending stiffness of B-SFS..... 155
Table 38: Predicted immediate mid span deflection of the TCC beam during loading (Euro code 5)..... 158
Table 39: Predicted mid span deflection of the TCC beam at the end of life (Euro code 5) 158
Table 40 Magnitude of strain along mid span cross section during serviceability test (Pham, 2010)..... 159
Table 41 Magnitude of strain along mid span cross section during ultimate..... 159
Table 42: ULS analysis of beam B-NS..... 162
Table 43: ULS analysis of the beam B-4N..... 166
Table 44: Results of bending test on LVL joist cut from the TCC beam (B-4N) after the ultimate test with 1260 mm clear span..... 173
Table 45: Results of bending test on LVL joist cut from the TCC beam (B-NS) after the ultimate test with 1260 mm clear span..... 173
Table 46: Results of tension test on LVL joist cut from the TCC beam (B-4N) after the ultimate test with 1000 mm clear length between the grips..... 173
Table 47: Results of tension test on LVL joist cut from the TCC beam (B-NS) after the ultimate test with 1000 mm clear length between the grips..... 174
Table 48: Design load for L6-01 and L6-03 beams according AS/NZS 1170..... 175
Table 49: The transformed section properties of the timber composite beams..... 176
Table 50: The analytical long-term deflection for L6-01 and L6-03 beams using GAMMA method and Euro code 5..... 177

Abstract

Timber concrete composites (referred to as TCC beams here onwards) consist of a concrete slab integrally connected to the timber joist by means of a shear connector. The coupling of a concrete layer on the compression side and timber on the tension side of cross-section results in efficient use of both materials. As the timber joist is mainly subjected to tension and bending while the concrete flange is mainly subjected to compression. The connection plays an important role for the composite action in determining the structural and serviceability performance of the system. Use of stiff and strong connection system contributes to a suitable bending strength and stiffness of the TCC together with other mechanical properties..

Design of timber-concrete composite systems requires verification of serviceability and ultimate limit states. With the increasing trend in long span and light-weight construction, design of these floors may be governed by serviceability limit states and deflection under long-term load is one of the serviceability criteria that need to be addressed.

The long term behaviour of timber-concrete structures depends on a number of phenomena taking place in its components. Phenomena such as creep and shrinkage effects in concrete, creep, shrinkage or swelling effects in timber and creep in connection affect long term strength, stiffness and deflection behaviour of timber-concrete composites. Creep due to variation in the moisture (mechano-sorptive creep) plays a major role in the long term behaviour of TCC floors. Few long-term experimental tests conducted so far have been reported in the literature.

The objectives and scope of this study are to conduct long–term experimental test on timber-concrete composite beams, analyse the results to determine the creep coefficient of the composite system and compare the experimental results with the analytical solutions in accordance with Eurocode 5, in which the effective modulus method is used to account the effect of creep.

To achieve the aforementioned objectives, a long-term laboratory investigation was started in August 2010 on four 5.8m span TCC beams with four different connector types. The specimens have been under sustained loads of 1.7kPa and subjected to a cyclic humidity conditions whilst the temperature remains quasi constant (22 °C). During the test, the mid-span deflection, moisture content of the timber beams and relative humidity of the air are continuously monitored. The long-term test is still continuing, two TCC beams were unloaded and tested to failure after 550 days, while the other two TCC beams are still being monitored and this report included experimental results up to the first 1400 days only. The long-term investigation on the two timber only composite floor beams commenced on March 2013 and the results are reported for the first 800 days from their commencement.

1 Introduction

1.1 History and Background of Timber-Concrete composites

Timber is the oldest renewable natural building material and had been the primary structural material until the beginning of the 20th century (Freedman et al. 2002).Timber has a very old history in the construction of the buildings and foot bridges in Australia, Europe and the rest of the world. Timber is a widely available and flexible building material and is the only renewable material used in large quantities in construction. Although construction materials have been dominated by concrete and steel since the 20th century, the shortage and higher cost of steel and concrete materials has opened a renewed interest in the use of timber as a construction material. Wood structures possess least embodied energy and this also played important role in the recent acceptance of timber concrete composites structures. It possess the least embodied energy (the energy required to acquire raw materials as well as to process, manufacture, transport and construct) when compared to similar structures of concrete or steel. Wood structures also consume the least amount of operational energy (energy used for heating, cooling, lighting, etc.). Both embodied and operating energy mainly use non-renewable fossil fuels, which release deleterious greenhouse gases, such as carbon dioxide and nitrous oxide, into the environment (Clouston 2004). The traditional timber floors structures have low stiffness, are susceptible to vibration and have relatively low acoustic insulation due to their inherent low density. The desire to build long-span and light weight constructions coupled with the need for refurbishment of the exiting old traditional timber floors led to the introduction of this new technique of combining concrete with timber. This technique involves connecting a timber joist to a concrete topping with a shear connector between the two materials (the top concrete and bottom timber joist) as shown in Figure1.

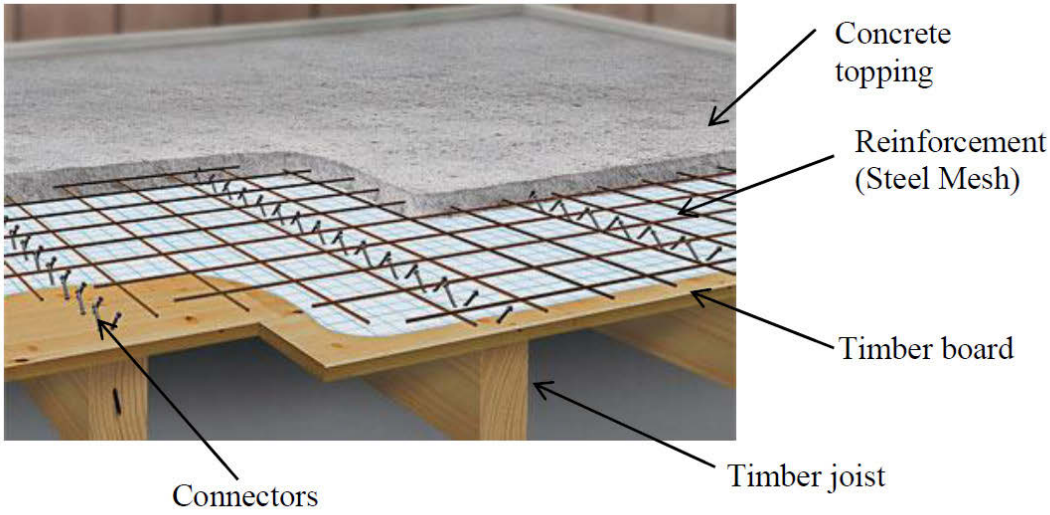

Figure 1: Timber-concrete composite floor (adopted from SFS-Holz Beton-Verbundsystem)

The refurbishment of TCC involves installing the fasteners in the wood members and pouring a concrete slab over the existing timber floor which becomes permanent formwork. Temporary shoring is generally provided to support the weight of the wet concrete prior to curing and achieving composite action. Wooden floors in existing buildings are not the only structures in need of renovation and strengthening. There are, for instance, many deteriorated short-span wooden bridges which were renovated and strengthened by adding a top layer of concrete on old wood structures and as Dias (2005) reported, a large number of timber-concrete bridges were also built in Australia between the 1950's and 80's with lengths varying between 6 m and 37.3 m and in New Zealand in the 70's with spans from 6 m to 24.5 m.

The primary advantage of connecting the timber concrete to the wood is composite action. The wood and the concrete act in unison and thereby achieve overall stiffness and strength that is superior to that of either of the components acting alone.

Some of the beneficial characteristics of these composite systems are;

- They are lighter in weight and therefore the overall weight of the superstructure will be lower than that for concrete structures. This will normally result in reduced foundation sizes.
- TCC system provides good insulation and acoustic performance.

- TCC floors have higher load carrying capacity than traditional timber floors, provided a good shear connection between timber and concrete is achieved.
- TCC floor systems have improved fire performance as compared to timber only structures.

Timber concrete composite system obtained by interconnecting timber joists with concrete slab using a connection system makes it possible to exploit the desirable properties of concrete and timber to the maximum level. The collapse and long-term behaviour of TCC floors is characterised by complex interaction between the components of the floor system, namely, concrete, timber and the connections system.

The long-term behaviour of timber structures depends upon several factors such as stress level, moisture content and temperature. The main long-term design parameter for TCC floors is deflection. It is possible to control the long-term deflection in timber significantly by application of surface treatment against moisture (Ranta-Maunus 2000). However, the long-term performance of TCC floors depends on a number of phenomena taking place in its components. Phenomenon such as creep and shrinkage effects in concrete, creep, shrinkage or swelling effects in timber and creep in the connections, affect long-term strength, stiffness and deflection behaviour of TCC. Creep due to variation in the moisture (mechano-sorptive creep) plays a major role in the long-term behaviour of TCC floors. Factors such as size, surface properties, loading type, length environmental cycle, etc also indirectly affect the long-term behaviour of the TCC floors (Toratti 2004).

The concrete part of the TCCs may be normal weight concrete, light weight concrete, prestressed or pre-cast concrete. The use of different type of concrete affects the interface and the bending stiffness of composite. The use of low shrinkage concrete or precast concrete slabs which are allowed to shrink first before connecting to the timber are some of the possible solutions to reducing long-term deflection for long-term applications (Yeoh 2009).

1.2 Research objectives and scope

The objective of this research work was to experimentally investigate the long-term performance of timber-concrete composite beams under service loads and subjected

to cyclic humidity conditions. To fulfil this objective, the research is subdivided into the following milestones as summarized below;

(i) Conduct Long–term experimental tests of timber-concrete composite beams under cyclic moisture conditions.

(ii) Compare the experimental results with deflection predicted analytically based on the Eurocode 5 calculation procedures for long-term performance of TCC beams.

(iii) Conduct serviceability and ultimate short-term tests on two TCC beams to investigate the residual stiffness and strength after long-term tests.

(iv) Conduct a long-term investigation on timber-timber floor beams to establish a difference of behaviour between TCC and timber only composite beams under identical humidity conditions

Whilst the results can be used for development and validation of models for use in numerical modelling, but this is outside the scope of this thesis.

1.3 Research Significance

The purpose of this research project was to explore the long-term behaviour of TCC beams under cyclic moisture conditions. The long-term performance of TCC beams under service loads is still not well understood and the results of this research will produce valuable information for design engineers to use in the serviceability analysis of these structures.

Some of the specific questions addressed by this works are;

- The behaviour of TCC beams under cyclic moisture conditions under service loads in bending
- The relative deflection of the TCC beams, i.e. the long-term deflection of the beams as a multiple of their short-term deflections.
- The loss in stiffness and/or strength of TCC beams due to the long-term test.

1.4 Limitations

The work presented in the thesis has several limitations, including the following:

- Only the behaviour of TCC under service loads is investigated
- The vertical displacement of the beams at the supports is not measured, and the mid span displacement is not checked (compared) against the support settlement that may be caused by compression of the seatings at the supports. It should be noted that this was not observed to be significant.
- Although the oven-dried method gives accurate moisture content measurement for the test samples, this measurement will give the approximate average MC of the joist but may not give the actual moisture content in the LVL joist in the TCC beams.
- The horizontal displacement (slip) under long-term loading between the LVL and concrete is not monitored and hence no creep coefficient for connection is investigated in the tests.
- The long-term test is limited to LVL 250x45 mm section size.

1.5 Outline of the thesis

The thesis has been divided into seven chapters.

Chapter 1 is introduction and background; it covers the development of the composite systems and also discusses the theory of composite systems. In this section the objectives, scope and the significance of this research are also elaborated.

Chapter 2 is a literature review and serves as the foundation for the thesis. It deals primarily with the short term and long term experimental investigation of various types of TCC beams and connections. It also discussed the guidelines provided for long-term evaluation of TCC beams in procedures using Eurocode 5.

Chapter 3 introduces the properties of the composite beam under investigation as part of this thesis. The characteristics and geometry of the TCC beams are presented in this chapter. This section also discussed the short-term tests conducted on the TCC beams and the composite behaviour achieved through the composite action of the two materials (Concrete and Timber).

Chapter 4 accounts for the full scale long-term experimental investigations that were conducted which is the main focus of the research work. The environmental condition of the humidity chamber and, the behaviour exhibited by the TCC beams under these extreme conditions will be discussed.

Chapter 5 the current design procedure described in Appendix B of Eurocode 5 for timber-concrete composite structures for serviceability and ultimate limit state verifications for the TCC beams is tried. A prediction for long-term deflection of the TCC beams is also presented, and recommendations are also made.

Chapter 6 the short-term collapse tests done on the beams before and after the long-term test is reported here. The residual stiffness and strength of the TCC beams due to the long-term effect are discussed in this chapter. The ultimate strength of the beams is evaluated using Eurocode 5 provisions and compared against the experimental results.

Chapter 7 discusses the long-term experimental result of two timber composite beams and comparison also made with the theoretical long-term deflections expected from the beams.

Chapter 8 presents the conclusions drawn from this work, together with a summary of the findings from each chapter.

Chapter 9 this chapter recommended additional possible research areas that are very crucial to fully understand the long-term behaviour of TCC beams. Some of the proposed future works would involve creep tests on timber-concrete connections to determine the creep coefficients for the connection by measuring slip with time.

2 Literature review

2.1 Timber-Concrete composite structures

Timber-concrete composite structures represent a technique used for building new structures or upgrading the strength and stiffness of existing timber traditional structures. In timber-concrete composite structures, the concrete topping mainly resists compression, while the timber joist resists tension and bending, and the connection system transmits the shear forces between the two components. Although this technique exploits the desirable characterises of the component materials, the different behaviour of the three component material (concrete, timber and connector) in their life time makes the long-term investigation of this structures very complex.

The timber part of the composite can be glue laminated timber (Glulam), laminated veneer lumber (LVL) and parallel strand lumber (PSL) which is then connected to a concrete overlay with a shear connector.

Laminated veneer lumber (LVL) is an engineered timber product, which can be used as beams, plates, members of trusses and shells. It consists of 3-4 mm thick laminates that are glued together. The veneers are made by peeling logs with thickness ranging from 1 to 5 mm. The grain on each veneer runs in the same direction giving orthotropic properties similar to those of sawn timber. Some LVL members are made with a few laminations laid up at right angles to enhance the shear strength which is referred to as cross-banded LVL.

Like other engineered timber products LVL has numerous advantages over sawn timber, such as,

- A defect occurring in one laminate hardly affects the rest of the member. Defects are distributed evenly over the member. Therefore the natural strength reducing characteristics are minimized. This gives LVL higher characteristics strength and more uniform stiffness compared to the raw material. Furthermore the properties show less variation.
- After fabrication, LVL is quite dry with a moisture content of approximately 10-12 %. Thus dimensions are more accurate and moisture related distortion of the shape is not a problem.

- Manufacturing of LVL is not limited by the size of trees and therefore can be produced in nearly unlimited sizes.
- Although LVL is not solid timber it still has nearly the same good architectural appearance as natural timber.

The connection between the two elements (timber and concrete) is the critical part of any composite structure. This component is usually referred to as the shear connector. The most commonly used shear connectors in timber-concrete composite structures include; nails, screws, rebar plates, tubes, hollow steel sections, glue and notched systems. A detailed review of exiting TCC connection systems will be discussed in the next section of this chapter.

2.2 Composite action of timber-concrete composite systems

If a concrete slab is cast freely on top of a beam and the friction is assumed to be negligible, the beam and the slab will act separately to resist flexural actions (Figure 2*c)*. Their separate action will give rise to a slip between the slab and the beam upon loading. By interconnecting concrete and timber, however, this slip can be reduced. Preventing slip results in reduced vertical displacement as well. Thus, by interconnecting two elements, their combined bending stiffness can be increased. This phenomenon of two components working together as opposed to acting separately is known as a composite action. The degree of composite action achieved increases with the stiffness of the connection and the shear connectors are key elements of a composite system. There are two bounds of composite action:

- A lower limit of fully non-composite action, displayed by timber and concrete layers that are not connected and thus work independently, with no transfer of horizontal force (shear) between the two layers through either mechanical bonds or friction *(*Figure 2*c)*. The layers have individual neutral axes and there is discontinuous flexural strain at the timber- concrete interface.
- An upper limit termed as “fully composite action”, displayed by timber and concrete components that are rigidly connected with no interlayer slip and with complete shear force transfer between the layers. The cross-sections

have a single neutral axis and identical flexural strains at the timber-concrete interface *(*Figure 2*a)*. Consequently, the transformed section method can be validly applied to analyse stress in such systems.

Most of TCC connection systems in reality are deformable and allow some horizontal movement "slip" at the interface. Such behaviour is called as "partial composite system" (Yeoh 2010). The single neutral axes splits and as slip between the layers increases the two neutral axes move further apart. Hence slip between the timber beam and concrete slab reduces the efficiency of the cross-section. A rigid connection is difficult to achieve, yet minor slippage between the two layers are also beneficial for stress redistribution along the shear connectors.

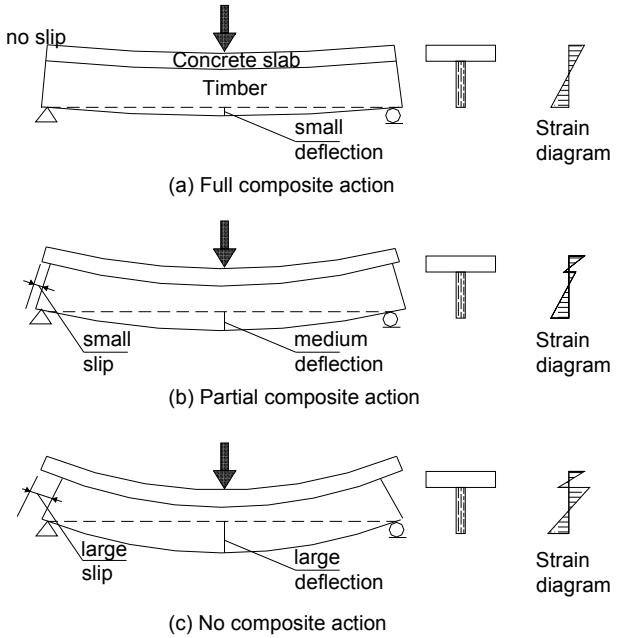

Figure 2: The concept of composite action; (a) fully composite action, (b) partial composite action and (c) No composite action

The amount of interlayer slip and deflection in the composite beam are significantly affected by the strength and stiffness of the interlayer connection system. Balogh et al. (2008) has described composite efficiency as a measure to determine the expected

long term deflection of a TCC beam and the composite efficiency can be quantified using *equation 1*.

$$E = [D_N - D_I \,/\, D_N - D_C] * 100 \qquad \textit{Equation 1}$$

Where: D_C is the theoretical fully composite deflection (calculated by the transformed section method; upper limit), D_N is the theoretical fully non-composite deflection (calculated as a two layered without shear transfer; lower limit), and D_I is the measured deflection for incomplete composite action of the beam. The efficiency can vary between 0 % and 100 % for ideal cases with no connection and fully rigid connection, respectively. It may be also convenient to define the efficiency of a shear connection for a composite beam, using the following equation (Lukaszewska 2009).

$$\gamma = [EI_{real} - EI_0 \,/\, EI_\infty - EI_0] \qquad \textit{Equation 2}$$

Where: γ is the efficiency of the interlayer connection, EI_∞ is the bending stiffness of the beam with a theoretical full composite action, EI_o is the bending stiffness of the beam with no composite action and EI_{real} is the actual bending stiffness of the beam. When shear connection is very stiff EI_{real} tends to EI_∞ and thus $\gamma \rightarrow 1$.On the other hand, for a very flexible shear connection EI_{real} would tend to EI_o and thus $\gamma \rightarrow 0$.

The bending stiffness of a composite system EI can be calculated using the formulas recommended in Eurocode 5 Annex B and is covered in detail in section 2.6 of this paper.

Relatively rigid shear connectors should be used in composite structures to limit deflection; however rigidity is not the only desirable characteristics of timber-concrete shear connectors. In order to avoid sudden brittle failures in the composite structure the shear connector is required to be sufficiently ductile behaviour in addition to ease and cost of manufacturing.

It should be emphasised that the correlation between the bending stiffness of composite structure, often referred to as the effective bending stiffness, and the stiffness of the connection is not linear. Dias (2005) presents the graphical (Figure 3) representation of the correlation between the stiffness of the connection and the effective bending stiffness of a composite beam.

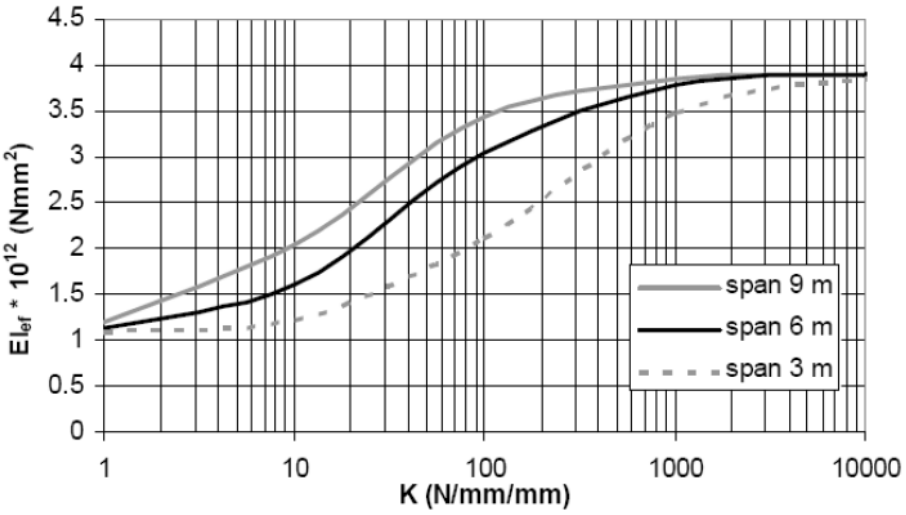

Figure 3: Graphical representation of the correlation between stiffness of a shear connection and the effective bending stiffness of a composite floor (Dias 2005).

As shown in Figure 3, increasing the stiffness of a connection beyond certain limits has no benefit since it has no significant impact on the effective bending stiffness of the TCCs. However, a connection is required to be above certain limits to serve its purpose satisfactorily and Linden (1999) in his study concluded that the bending stiffness could increase up to a maximum of 4 times by introducing composite action. This was only possible using an infinitely stiff connection and certain combinations of geometric and material properties (Dias 2005).

2.3 Timber-concrete connections

The first timber-concrete composite joints used were those adopted from timber joint types (Linden 1999). The relatively low slip modulus of these joints led to the development of new connector types that were especially manufactured to be used in timber-concrete composites. The connection system can be either a discrete mechanical fastener or a continuous system. The discrete mechanical fasteners include coach screws, specific proprietary screws such as SFS screws, nail plates, dowels, rebar, stud connectors such as the "Tecnaria connector" screwed in to the timber, plugs with different shapes (with or without mechanical reinforcement), and notched details. Continuous systems include steel lattices glued and milled into the

timber; punched metal plates glued and milled into the timber, glued in steel meshes such as the HBV system, and punched steel profile screwed into the timber.

The connection element between the concrete and timber components which is referred to as “shear connector” is the critical part of the composite system. In addition to being stiff, a shear connector needs to have certain strength, or shear capacity, in order not to fail. The strength and stiffness of a composite beam is dependent on both the stiffness and strength of its connectors. Increasing the number of connectors could substitute the lack of stiffness and strength of connectors but it will also increase the construction costs (Linden 1999).

The stiffness, strength and post peak behaviour of connectors is often investigated by conducting symmetrical or asymmetrical shear tests. These tests are commonly called as “push-out tests”, since they involve the pushing out of one of the components of the test specimen. Figure 4 shows a typical setup of a symmetrical push-out test (Dias 2005).

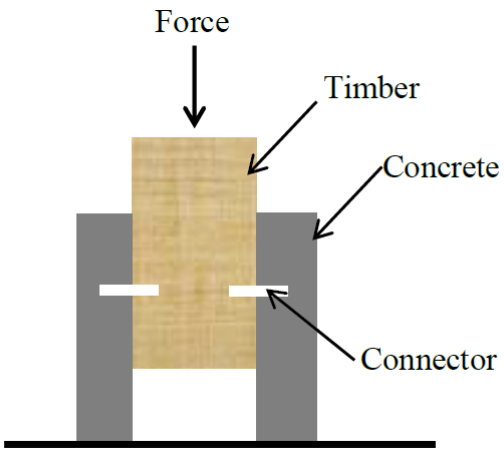

Figure 4: Setting of a symmetrical push-out test

The experimental assessment of strength and deformation properties of timber-concrete connectors is usually done according to the EN26891 (1991). These standards set out the rules and principles for the determination of the strength and deformation properties of timber-timber joints made with mechanical fasteners. However, since there is no specific standard for timber-concrete connector, this procedure is normally used (Dias 2005).

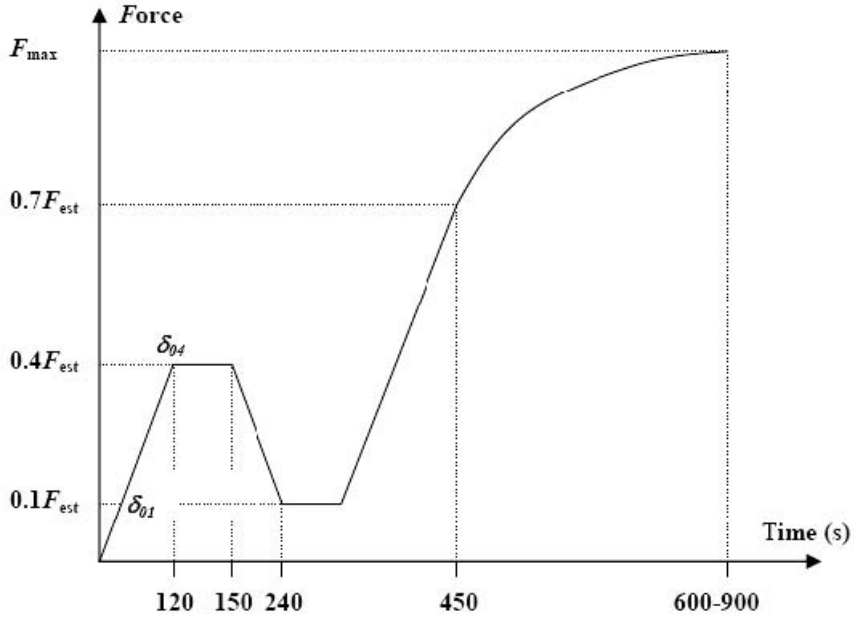

Figure 5: load-time curves for tests according to EN 26891(Dias 2005)

The test is conducted with a loading procedure as shown in Figure 5. After conducting the push-out tests, the shear capacity, stiffness and post-peak behaviour of the connector can be accessed from studying the load-displacement curves. The shear capacity is equal to the peak value of the load in the load-displacement (slip) curve or the load for a displacement of 15 mm as it is indicated in the standards and the stiffness is assessed by determining the slip-modulus "k", of the connector. The post-peak behaviour of the connector can be defined as "the connector's behaviour under loading after failure has occurred". Good post peak behaviour for connectors is considered to be ductile. Since the failure mode of concrete as well as the tensile/bending failure mode of timber can be considered brittle, it would be desirable to have failure occur in shear connector with ductile post peak behaviour. This would lead to a slow increase in deflection before the final failure.

The most commonly used methods of joining concrete to timber, as classified by Ceccotti (1995) are shown in Figure 6. The shear connectors are grouped, according to their stiffness, in four groups: Connections in group-A have the lowest stiffness while connectors in group D are the stiffest (with twice as much bending stiffness as those in group A).With group D type connections, it is possible to achieve full composite action between timber and concrete (Ceccotti 2002).

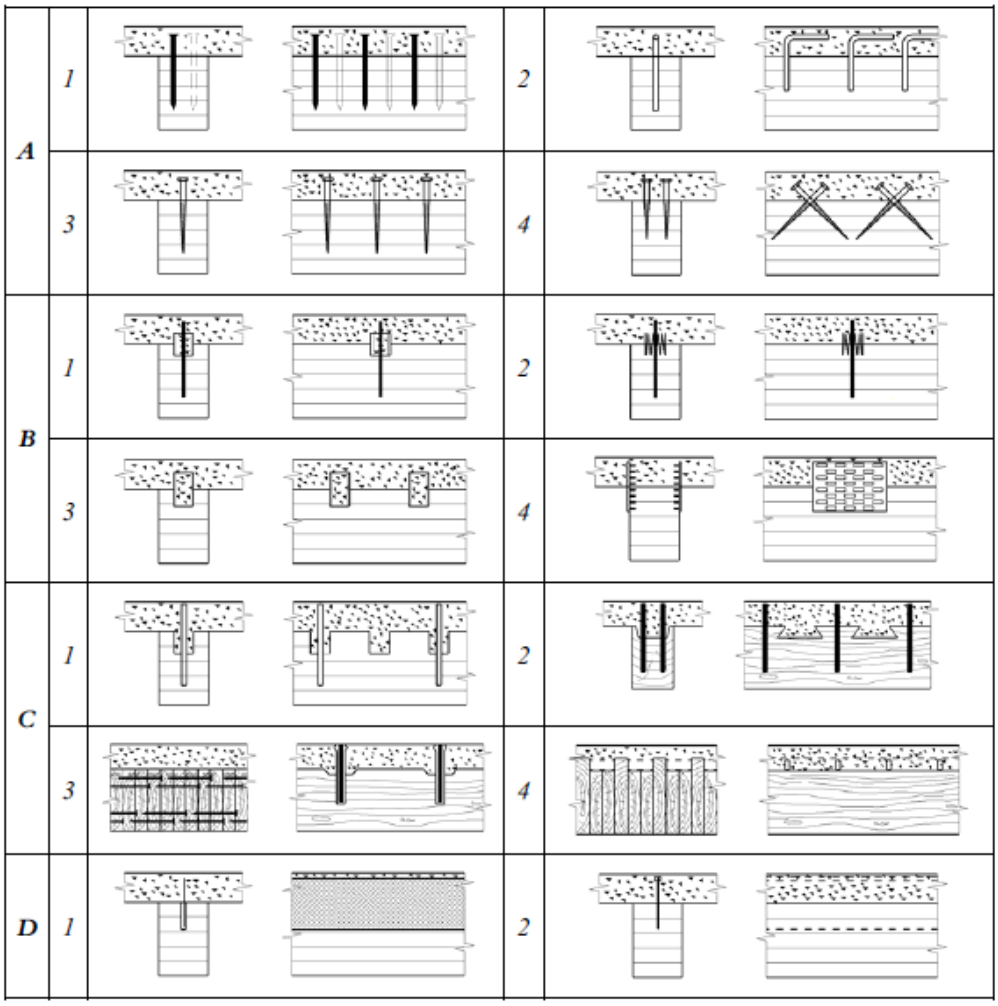

Figure 6: Examples of timber-concrete connections with: nails (A The concept of composite); glued reinforced concrete steel bars (A2); screws (A3); inclined screws (A4); split rings (B1); toothed plates (B2); steel tubes (B3); steel punched metal plates (B4); round indentations in timber ,with fastener preventing uplift (C1);square indentations, (C2); cup indentations and pre-stresses steel bars (C3), nailed timber planks deck and steel shear plates slotted through the deeper planks (C4), steel lattice glued to timber (D1); and steel plat glued to timber (D2) (Ceccotti 1995)

Group D connectors are generally considered to be rigid connections. In this group design calculations for connections can be easily made since there is negligible slip between the concrete layer and timber member and the concrete section can be "transformed" to an equivalent timber section. On the other hand group A to C

connectors are least rigid, they are known as semi rigid connectors or flexible connector which is quite typical for most TCC connections. They are characterised by varying levels of slip and the analysis requires complex design solution. Dias (2005) also presented typical load-slip curves for a number of different joint in order to allow a direct and easier comparison between the different joint systems. As indicated glued and notched connections have higher stiffness's as compare to nail or dowel type of fasteners Figure 7).

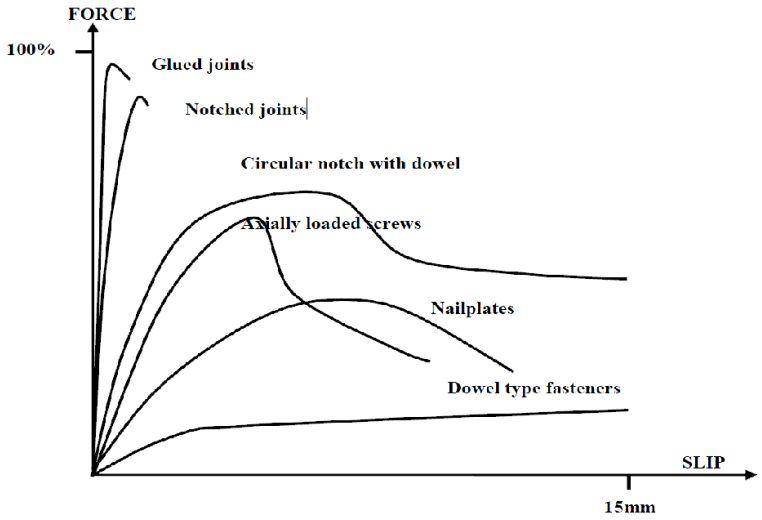

Figure 7: Typical load-slip behaviour for different types of joints. (Dias, 2005)

Existing shear connectors are further discussed in this section in terms of their strength and stiffness as determined in shear tests and observed efficiency in the composite systems. A detailed review of different connector types are presented in Lukaszewska (2009), few of the shear connectors which are relevant to this project are presented here;

2.3.1 Nails

Nails represent the simplest types of shear connectors. Nails are used by embedding them partly into timber, enabling the top to become embedded in the concrete upon casting the slab. Several tests have been carried out on nails as shear connectors. The strength and slip modulus of nail connections depends on the spacing and depth of

penetration. Unnikrishna (1977) used a commercially available 3 mm and 5 mm wire nails as shear connectors and subjected to push-out tests. Nails driven straight and inclined (with the head points towards and in the opposite direction of the shear) were tested. The main conclusions were that the minimum spacing of nails should not be less than 10 times their diameter to avoid damaging the wood, and the length of embedment of the nails in to the concrete should be at least 25 mm in the compressive zone and at least two-third of the length of the nail should penetrate into the timber. Placing the nails at 45° inclination, with the head pointing in the direction of the shear on the timber surface will result in higher strength and lower slip. Push-out tests have shown that the penetration of a nail into wood should be approximately eleven times the diameter in order to reach maximum efficiency. Furthermore, full scale bending test with nails penetrating to this depth show that the load carrying capacity of a floor is doubled while at the same time decreasing deflection (Andreas 2010).

2.3.2 SFS-Screw (VB 48-75x100)

Necessities to reduce the cost of fabrication of the connection led to the development of the RF2000 composite action system. (Meierhofer 1992)

The VB 48-75x100 produced by SFS Intec, commonly known as SFS-screw, is a connector specifically developed for timber-concrete composite structures. Two heads allow for the lower part of the screw to be fixed in the timber joist while the top part is anchored in the concrete. The core of this system is a special high strength steel connector “stadler VB-48-7,5x100” developed by SFS Stadler SA in Heerbugg, Switzerland. This connector (shown in Figure 8) is composed of two parts: the upper 50 mm long part with a diameter of 6 mm acting as the anchor in the concrete and a 100 mm long ‘wood anchor’ with a thread having an outer diameter of 7.5 mm and a core of 4 mm.

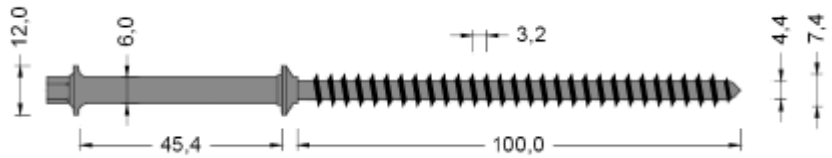

Figure 8: SFS VB screw 48-7.5x100 (Lukaszewska 2009) (all dimensions in millimetres)

Meierfoher (1992) conducted several types of tests to evaluate five different arrangements of connectors with straight and inclined nails at 45° (Figure 9*)*. The highest stiffness was obtained about 60 % with type "d" arrangements and the least stiffness was obtained with connectors arranged vertically with type "a" arrangements. The knowledge acquired with shear test was finally implemented in two series of bending tests on a 4 m span beam. The TCCs with the crossed arrangements of the connectors proved to be more than three times as stiff as the ones with perpendicular arrangements in short-term tests.

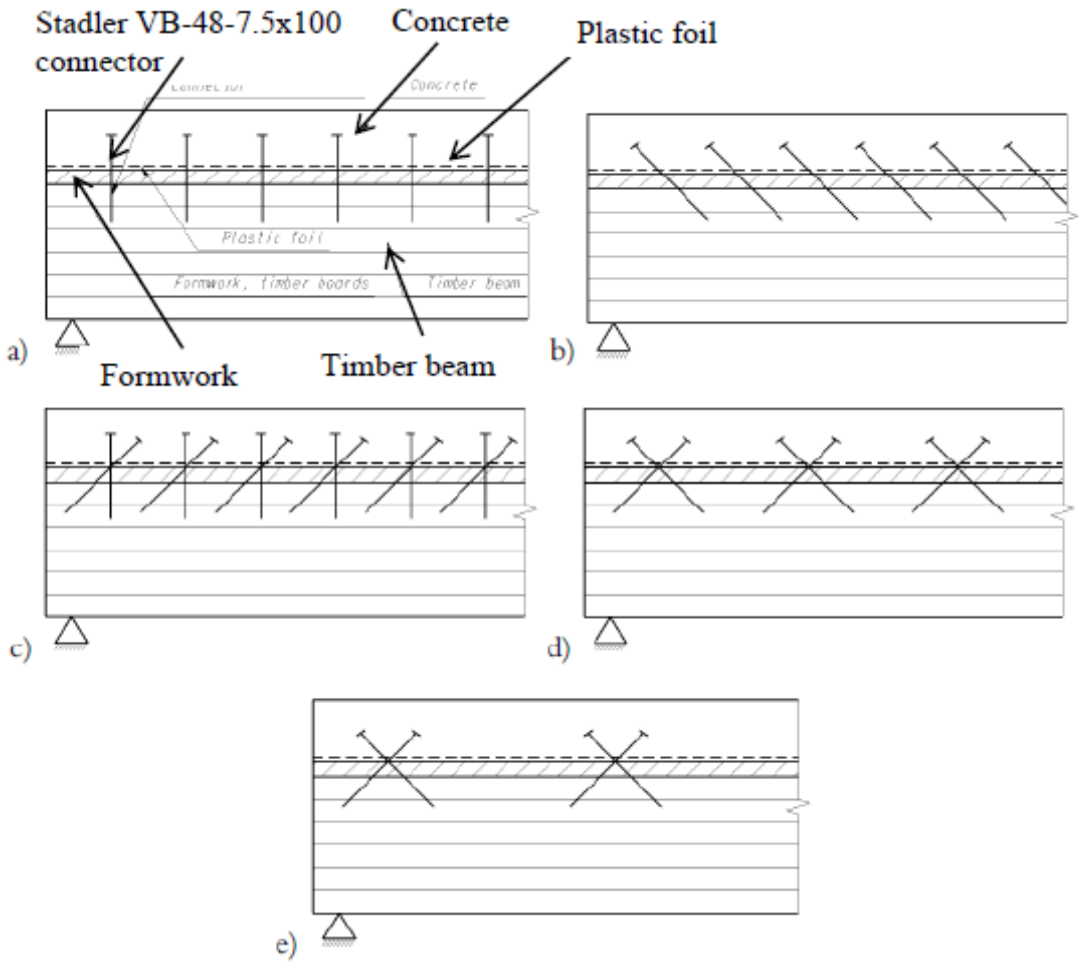

Figure 9: Arrangement of the connectors in bending tests described by (Meierhofer 1992)

Linden (1999) conducted extensive research to determine the load-carrying capacity of timber-concrete composite beams. Four types of timber-concrete composite beams were tested, SFS screws installed at 45°, with an interlayer of 28 mm particle board (Figure 10), nail plates bent at an angle of 90°, reinforcement bar with a concrete notch and grooved connections in LVL.

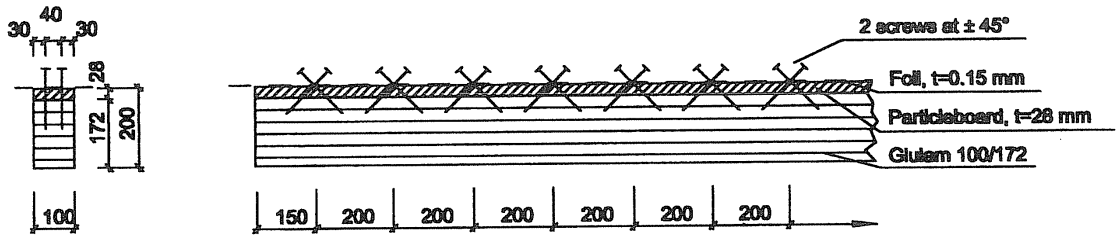

Figure 10: Beam with SFS screw as shear connector (Van Der Linden, 1999) (all dimension in millimetres)

The average strength reached by screws in the shear test was around 30 kN and the strongest composite beams were with SFS screw. The failure load was 38 kN in a 4-point bending test with mid-span deflection reaching 100 mm. In bending tests all the beams failed due to timber tension failure. It was concluded that the connectors satisfied the serviceability and ultimate limit state requirements.
The best performance is achieved when placing the screws pair-wise, inclining the screws, within the pair at 45° and 135°, respectively. This allows the screw tilted in the direction of the shear force to absorb tensile forces, while the screws tilted in the opposite direction acts as a stiffener (Andrews 2010).

2.3.3 Notch-type connection with and without dowel

A very simple type of connector can be created by drilling holes/dimples in the timber beam. Upon casting of concrete, a concrete plug is formed that has the ability to transfer shear forces between concrete and the wood (Andreas 2010). A full composite action can be achieved without the use of any steel connectors, i.e. the small-scale dimples used as shear connectors (which are located in the concrete slab) can provide effective shear transfer (Yttrup 1996).

Linden (1999) also studied grooved connections with dowels (Figure 11), this type of connectors exhibited plastic deformation capability. The maximum shear capacity of the reinforcement bar with concrete notch was reached at a displacement of about 5 mm; with a corresponding load of about 52 kN. The slip recorded was 15 mm at

failure. A 4-point bending test on a 5.4 m span beams was also performed and maximum load was 64 kN with mid-span deflection of 80 mm.

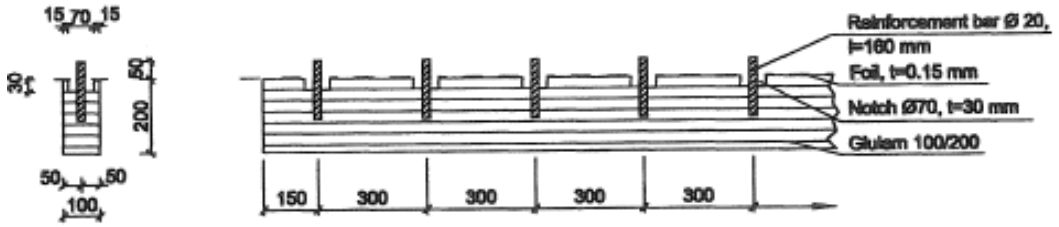

Figure 11: Timber-concrete connection with grooved holes and dowels (Linden, 1999) (dimensions in mm)

Gutkowski (2004) investigated a timber deck and a concrete slab interconnected by a notched shear key/anchor connection detail (Figure 12). Sixty slip test specimens were constructed and tested with three different notch configurations. The highest slip modulus was reached with 152 mm wide and 38 mm deep notch while the lowest slip was reached with 102 mm wide and 25 mm deep notch. From the 4-point bending test (Gutkowski 2007) the composite efficiency measured from mid-span deflection was 57 – 70 % for 3.5 m span with four 32x128 mm notches. The distance from the edges of the beam to the first notch, and the spacing between notches, was 330 mm. The concrete and wood layers (nail planks) were 64 mm and 89 mm thick and 267 and 305 mm wide respectively. The failure was characterized by flexural tensile in the wood and the poor construction of the notch connections resulted in low performance of the system.

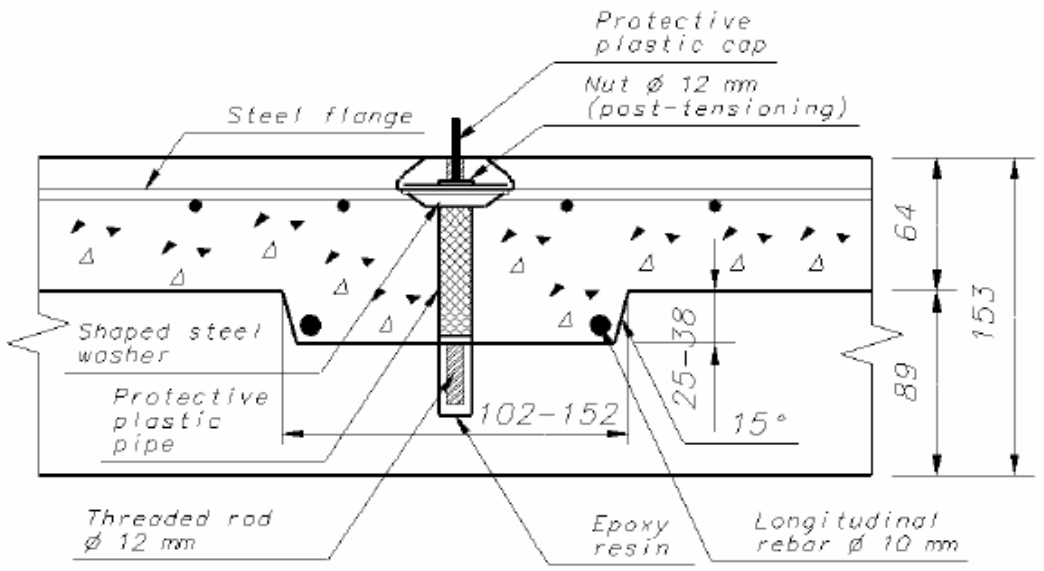

Figure 12: Shear key connection detail (Gutkowski 2004) (dimensions in mm)

Kuhlmann et al. (2004) proposed a connection system consisting of grooves 20 mm deep and 200 mm long in the timber and screws with a diameter of 12 mm at spacing of 250 mm installed and tightened after hardening of the concrete, to handle the tensile force in the connection caused by the resulting eccentric bending moment. The tests showed that the presence of the screws had no significant effect on either the load carrying capacity or the stiffness of the connectors.

Dias (2005) performed a large number of experimental shear-tests on dowel type fasteners and notched joints to evaluate their short-term and long-term mechanical performance. The dowel types were produced from short pieces of steel, smooth or profiled reinforcing bars, with three different types of timber; spruce, maritime pine and chestnut and low strength/light weight normal strength and high strength concrete. The summary of the resulted tabulated showed the strength and stiffness of the dowel joints were affected due to the change in diameter of the dowel and the type of concrete. The use of profiled dowels gave very high strength as compared using smooth dowel types. The influence of timber is more on stiffness than on the strength. Dias (2005) also conducted experimental tests on composite beams with nails to evaluate the approachability of the design procedures proposed by Ceccotti (1995) and concluded that the design procedure can be used to predict the deflection of timber-concrete structures, but with errors in the range of 20-30 %. The

experimental deflections of timber-concrete slabs with nails were around twice as large as the expected deflection for full composite action.

Deam et al. (2008a) and Yeoh et al. (2008) proposed and conducted shear tests on range of shear connectors mostly of notch/plug connector types. The research was to identify the most efficient and cost effective shear connectors for an 8 m timber-concrete composite floor with LVL beam. Concrete plugs reinforced with a screw or steel pipe provided the best stiffness, strength and post-peak behaviour. For 8m long spans, 16 reinforced rectangular concrete plugs, equally spaced along the length of the beam were chosen. Full scale 6 m long specimens with rectangular notches reinforced with lag screw was subjected to quasi-static and dynamic tests to obtain indications of the structural performances of the LVL-concrete composite system. The obtained efficiency at 50 kN load was 93 % and at 150 kN load was 71 % while the failure load was 158 kN (Deam et al. 2008b).The composite system had 295 % greater stiffness ad 74 % greater strength than the bare LVL beam.

Rectangular notches reinforced with coach screw connectors have also been used in a new system for multi storey timber buildings with timber-concrete composite floors developed in New Zealand (Buchanan et al. 2008). The typical section of the TCC system used is shown in Figure 13. Notches are cut from the LVL joist before the plywood interlayer is nailed, the span of between 8 m and 10 m requires six to eight connectors along the length of each joist to provide adequate composite action.

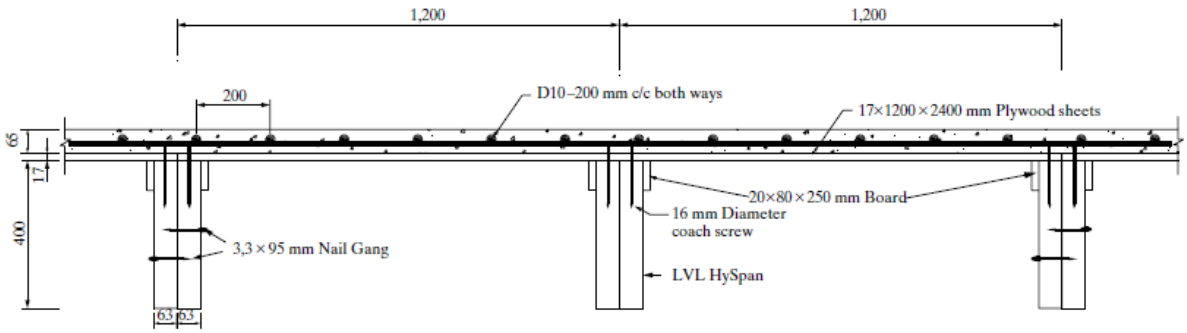

Figure 13: Semi prefabricated "M" section panel (Buchanan et al. 2008) (dimensions in mm)

Lukaszewska (2009) conducted extensive research on seven types of shear connectors to investigate the strength and slip modulus. To assess the mechanical properties and structural performance of the prefabricated concrete composite floors systems, five bending tests to failure were carried out with full-scale 4.8 m span. The TCC floors had a triplet T-sections with glulam joists *(*Figure 14*)*. The concrete slab was prefabricated off-site with mounted connectors. Three specimens had lag screws surrounded by steel pipes whilst two specimens had metal nailed to the glulam joists. The composite action achieved was only 60 % and 30 % with lag screws and metal plates, respectively. The use of a notched connection together with the steel pipe and lag screw is a possible way suggested by the authors of improving the connection efficiency as explained on section 2.2.

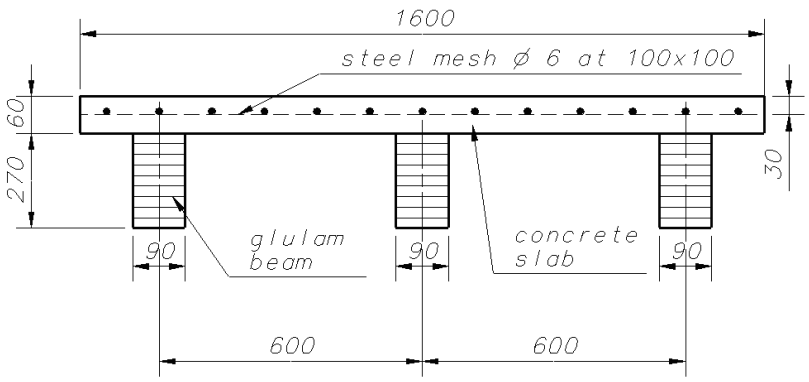

Figure 14: Cross-section of the composite beam tested (Lukaszewska 2009)

2.4 Enhancement methods for timber-concrete composite structures using light-weight concrete

Use of light-weight concrete (LWC) in timber-concrete composite floors could be a possible way to reduce its weight. An even bigger reduction of the overall weight of a building can thus be achieved. The experimental results of Steinberg et al. (2003) suggest that a decrease in the self-weight of a timber-concrete composite by approximately 15 % could be achieved by using LWC instead of regular concrete. However, the lower capacity of LWC would increase the risk of failure in the

concrete. This risk is further increased by LWC's higher tendency to split as a result of the forces concentrated around the shear connectors. On the contrary, Fragiacomo et al. (2007a) also used LWC while testing "Tecnaria" shear connectors. The use of LWC slabs instead of normal weight concrete slabs affected neither the outcome of collapse of the push-out tests nor the long-term tests on the connectors, since the failure in both cases was due to failure in timber.

2.5 Long-term tests on timber-concrete composites

The long-term behaviour of TCC floors is characterised by complex interaction between the components of the floor system, namely, concrete, timber and the connections system. The long-term behaviour of timber structures depends upon several factors such as stress level, moisture content and temperature. The main long-term design parameter for TCC floors is deflection. It is possible to control the long-term deflection in timber significantly by application of surface treatment against moisture (Ranta-Maunus and Kortesmaa 2000). However, the long-term performance of TCC floors depends on a number of phenomena taking place in its components. Phenomenon such as creep and shrinkage effects in concrete, creep, shrinkage or swelling effects in timber and creep in connection affect long-term strength, stiffness and deflection behaviour of TCC. Creep in timber due to variation in the moisture (mechano-sorptive creep) plays a major role in the long-term behaviour of TCC floors. Factors such as size, surface properties, loading type, length of environmental cycle, etc. also indirectly affect the long-term behaviour of the TCC floors (Toratti 2004). A summary of literature on creep and mechano-sorptive effects in wood and investigations on long-term behaviour of TCC beams and connections is presented in this section.

2.5.1 Summary of creep and mechano-sorptive behaviour of wood

A number of studies have been carried out on the mechano-sorptive behaviour of wood. A collection of characteristics of mechano-sorptive behaviour are reviewed by Toratti (1992) and here some of the research results that are important to understand the behavioural response of timber in TCC are summarised in this section;

a) Mechano-sorptive deformation at constant stress is not directly dependent on time. When the moisture content of the loaded wood changes rapidly, deformation increases rapidly, but the final deformation depends on the moisture step and the duration of the process has little effect. The deformation of stressed wood normally increases with any change of moisture content, whatever its direction (Armstrong and Kingston 1960).

b) In bending, the first adsorption and all desorption periods cause increases in deflection, while later adsorption tend to decrease the deflection. This is applicable in cases where the moisture content changes take place within previously attained moisture content limits. The behaviour of wood in bending is the effect of the behaviour in tensile and compressive zones and the observed recovery of deflection in bending is due to the decrease in the zero-load compensated strain in both zones simultaneously. Bending is an effect of the behaviour in the tensile and compressive zones. During desorption the absolute value of the zero-load compensated strain increases in both zones which leads to the expected increase in deflection. An initial absorption leads to an increase in zero-load compensated strain in the tensile zone, if the same holds for the absolute strain value in the compressive zone which would lead to the desired increase in deflection. Later adsorption periods may lead to both increases and decreases in zero-load compensated strain (Martensson 1994).

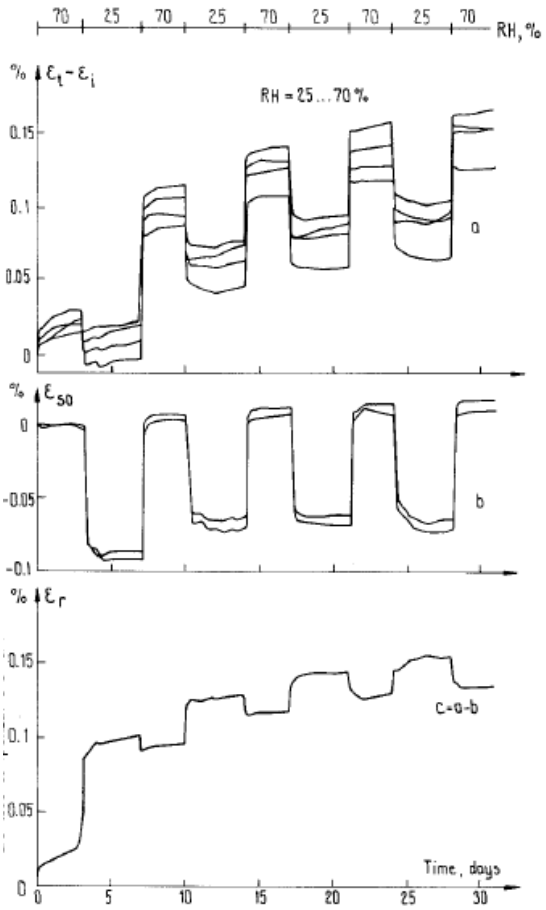

Figure 15: Results from tensile tests made on pine (0.4x5x150 mm), loaded parallel to grain (Eriksson, Noren 1965).The upper figure shows the strain (the initial elastic strain is subtracted), measured on four samples, and the middle figure shows the free shrinkage-swelling, measured on two samples. The lower figure shows the zero-load compensated strain, i.e. the difference between the upper and the middle figure, here the medium values of the four respectively the two samples have been used (Martensson 1994).

c) An effect of stress on the shrinkage-swelling behaviour exists, which leads to decrease in shrinkage-swelling for wood loaded in tension parallel to the grain and to an increase shrinkage-swelling for wood loaded in compression parallel to the grain (Hunt 1988).
d) The effect of moisture content change on total creep deflection is, in general, much greater than the effect of time (Schniewind 1968) and the increase in

deflection was more due to the change in moisture content than to the passage of time (Leicester, 1971).

e) In bending, repeated moisture cycling, even at moderate loads, leads to structural damage and eventually to failure. The strains prior to failure are very high, much higher than maximum strains recorded in short-term tests (Hearmon and Paton 1964), the diagram is presented in Figure 86 in Appendix A. Moisture variation is also known to shorten the time to failure of timber, due to the mechano-sorptive effect (Hoffmeyer 1990).

f) In bending, when the air humidity is cycled the deflection curves also follow a similar pattern. This oscillation of the creep curves (the alternate increase of deflection and recovery of deflection) is the shrinkage strain of wood, since the shrinkage is of much higher in magnitude perpendicular to the cell wall, this would result in higher shrinkage values when wood is compressed and less when tensioned as compared to unstressed state (Toratti 1993).

g) The effect of different constant moisture content on normal creep was found to be insignificantly low (Leivo 1992). A similar finding was also reported by Toratti (1992), that no difference in relative creep behaviour of wood in constant conditions of 45 % RH and 75 % RH was found for clear spruce, and the mechano-sorptive creep is not observed below about 15 % moisture contents, but at high moisture contents the mechano-sorptive effect is very strong.

h) In mechano-sorptive creep, non-linearity starts in compression at about 10-20 % of the ultimate stress, and in tension and bending at about 20-30 % of ultimate stress (Hunt 1989).

i) If, during moisture content cycling under load, the range of change of vapour pressure was made narrower, the changes in deflection during each complete cycle were much less. Nevertheless, a decrease in deflection for each desorption were still found for each cycle after the first (Armstrong and Christensen 1961). The decrease in deflection produced by increase in moisture content could be due to a relative change in the longitudinal components of swelling of the tension and compression components of a beam.

j) Epmeier (2007) investigated the bending creep performance of modified timber. Three modification methods - acetylation, modification with methylated melamine resin and heat treatment in vegetables oil, were tested. It was found that creep behaviour in cyclic climate and with constant loading can behave in three different ways. Type 'A': increasing deformation during drying (desorption) and decreasing deformation during wetting (adsorption), Type 'B': decreasing deformation during drying and increasing deformation during wetting and Type 'C': increasing deformation during both adsorption and desorption or indecisive. The figure showing the creep curves from the author's report is presented in Figure 88 : Appendix A.

k) Gibson (1965) stated the explanation with the widest acceptance, which was produced after investigation into the molecular structure of cellulose, the main constituent of wood. Cellulose consists of long chain type molecules, which in some places from a well ordered, closely packed crystalline array. Adjacent chains are held together by hydrogen bonds (bridges). The hydrogen bonds may include the hydrogen atoms of a water molecule, and these produce a weaker bond than one that does not include water. An increase in moisture will cause new hydrogen bonds to be formed, and existing ones to be broken and reformed with water molecules. A decrease in moisture will cause these bonds to be broken, some reforming without a water molecule. Each temporary break of hydrogen bond leads to a temporary weakening of the structures, which causes an increased strain for a fixed applied stress. Strain recovery occurs during adsorption because of the exothermal heat of adsorption from the vapour phase, although some of this energy is dissipated in swelling and vibration. A change in moisture will cause the hydrogen groups that are formed, which are normally inaccessible to water, to enter into an exchange reaction with water vapour. The amount of this exchange increases as the number of a beam that has been subjected to moisture cycling, which occurs upon unloading and rewetting is said to be due to the loosening of many bonds through water movements and the recovery of the elastic strain.

l) On removal of the load, the instantaneous elastic recovery takes place. This instant recovery is equal to or greater than the magnitude of the immediate

deflection during loading (Gibson 1965; Mohager 1987). Recovering is accelerated by moisture changes or cycling, especially during wetting (Armstrong and Kingston 1961, Grossman 1987). The mechano-sorptive deformation was not recoverable, and increased in magnitude when the load duration was increased (Mohager 1993). The figure showing the deflection curves from Gibson (1965) is presented in Figure 87 : Appendix A.

m) Chemical treatment such as acetylation and formaldehyde cross-linking has been shown to reduce the mechano-sorptive effect (Gowda 1996, Ranta-Maunus and Kortesmaa 2000). Toratti (1992) also reported a similar finding that, in fully coated specimens, the variability of relative humidity did not affect the moisture content of the test specimens.

n) Toratti (1992) reported test results of specimens exposed to variable temperatures. The temperature was cycled between room temperature, 20 ºC, and -5 ºC. The relative humidity of the weather chamber was uncontrolled and varied between 30 – 50 % RH at the same phase with the cycling of temperature. Although the low temperatures slow down the creep rates but no mechano-sorptive effects were noticed.

Some of the mechano-sorptive properties of timber only were discussed in this section that will help us understand the contribution to the long-term behaviour of timber-concrete composite beams which will be discussed in section 2.5.2.

2.5.2 Long-term experimental tests on TCC floors and beams

The time-dependent behaviour of TCC requires careful consideration in order to accurately predict the deflection in the long-term. Although long-term tests are expensive and require a lot of preparation, they are needed in order to validate approximate design procedures and calibrating existing analytical and numerical models. Few long-term tests on TCC structures have been performed to-date and will be reviewed here.

Bonamini, Uzielli & Ceccotti (1990) performed a long-term test at the University of Florence on T-sectioned TCC beams. The geometry of the composite beam is shown in Figure 16. An oak timber from a demolished floor was used as a joist. A steel mesh of 100 x 100 mm and 4 mm diameter bars was used in the concrete slab. The

connector was made of 12 mm diameter dowels drilled into the timber and filled with epoxy resins. After 28 days of concrete pour, dead loads were applied and then removed after 347 days. The relative humidity varied between 48 to 80 % while the temperature was kept quasi-constant at 30° C. The mid-span deflection, the relative slip between the slab and timber over the support and the moisture content at the surface and at 50 mm depth into the timber was monitored.

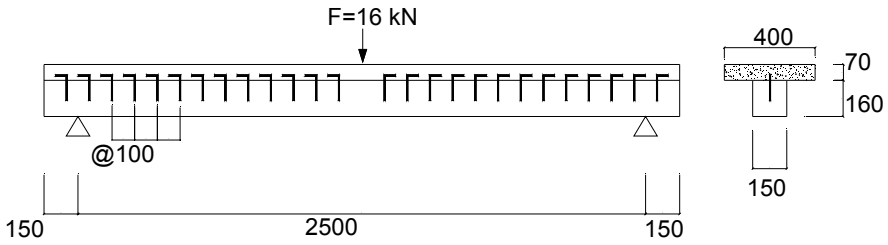

Figure 16: Geometrical characteristics of the composite beam tested by Bonamini, Uzielli & Ceccotti (1990) (measured in mm)

Ahmadi and Saka (1993) tested a simply supported 3.9 m long TCC slab by loading it with a full sustained live load of 2 kPa. The test revealed that the deflection of the composite slab under live load of 2 kPa increased due to creep, shrinkage and changes in temperature and humidity up to four months and then remaining steady. It was noticed that the ultimate long-term deflection under 100 % sustained live load, which rarely occurs in practice, was within acceptable limits set by the building codes.

Kenel and Meierhofer (1998) tested a composite beam made of solid timber with SFS-screw connectors (inclined at 45° with respect to the beam axis) in sheltered outdoor conditions for 4 years in EMPA laboratory in Dubendorf. The cross-section of the beam tested is shown in Figure 17.

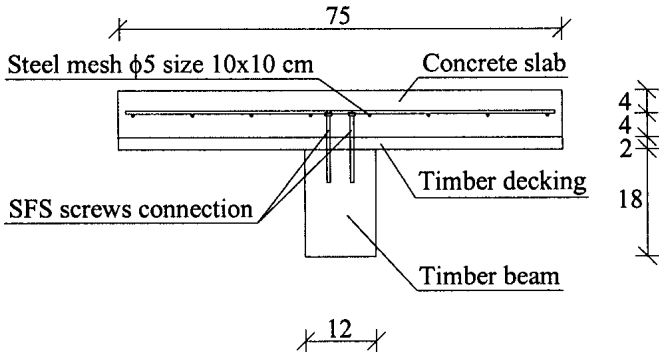

Figure 17: Cross-section of the TCC tested at the EMPA laboratory, Dubendorf (kenel & Meierhofer 1998)

The long-term test demonstrated clearly the superiority of arrangement with the connections inclined under 45° (an arrangement which simulates a truss like connection between the timber and the concrete). The results show a considerable influence of the initial moisture content on the long-term deformation.

Bou Saïd et al. (2004) tested a TCC slab (8 m span) with glued-in connections over a period of two years in sheltered outdoor condition. The relative humidity exceeded 85 % over a number of days. The deflection obtained from the Eurocode estimation was significantly exceeded during the two year period and the limitation on the long-term deflection was also well exceeded. Figure 18 shows the geometry of the specimen and Figure 19 shows the long-term deflection with time.

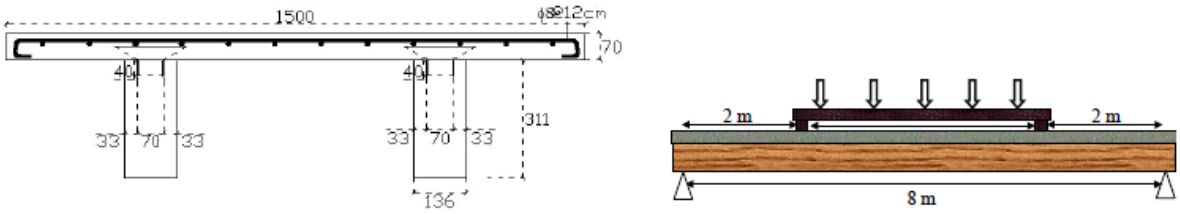

Figure 18: Timber-concrete composite section (left) and loads disposition (right) (Bou Said et al. 2004)

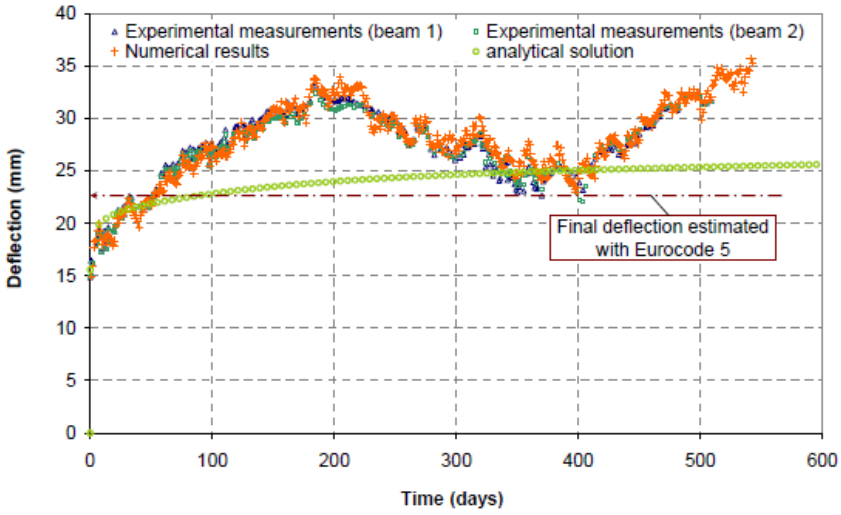

Figure 19: Comparison between calculated and measured mid-span deflections (Bou Said et al. 2004)

Grantham et al. (2004) monitored an upgraded timber-concrete composite floor over a period of 40 days. The tests, however, were aimed at evaluating the benefits of propping the composite floor during pouring of concrete.

Ceccotti et al. (2006) tested a TCC floor system (6 m span) under a uniformly distributed load of 4 kN/m, corresponds to 11 % of the estimated service design load. The connection was provided by 18mm diameter corrugated bars placed inside drilled holes in the timber filled with epoxy resin. Push-out tests were performed to investigate the connection properties. The timber used was European spruce with modulus of elasticity of 10 GPa and the concrete with a cylindrical compressive strength of 30.4 MPa. Figure 20 shows the longitudinal view and the cross-section of the slab tested.

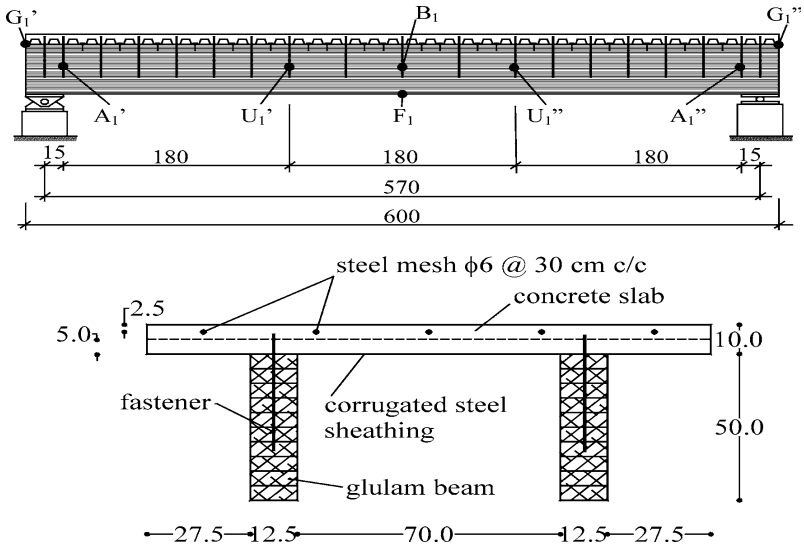

Figure 20: Longitudinal view and cross-section of the composite beam tested by Ceccotti et al. (2006) (dimensions in cm)

The beam was tested in outdoor unsheltered well ventilated conditions and protected from direct radiation from the sun. The test lasted for five years and it was classified as service class 3 as per Eurocode 5. The relative humidity (RH) varied between 40 to 85 % while the moisture content (MC) was in the range of 13 to 18.5 %.The maximum average deflection monitored throughout the test was 3.36 mm as shown in Figure 21, which was almost four times the instantaneous elastic deflection and is well below the limiting value L/300 as per the Eurocode 5. An increase in deflection was observed mainly during the first two years of the long-term test while the slip rose during the whole test period. The environmental variations caused significant influence on all the quantities on both yearly and daily scale. This beam was loaded to failure after the long-term test and it showed good composite action.

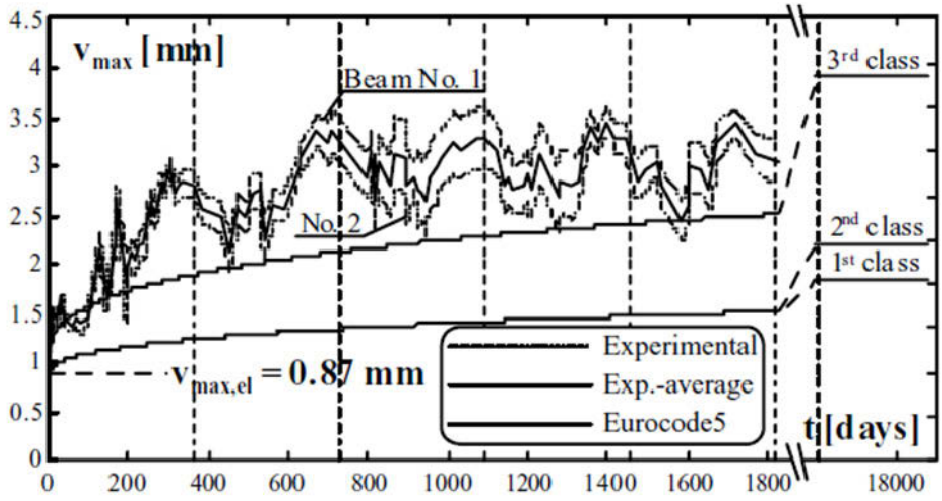

Figure 21: Mid-span vertical displacements for the timber beam and average value (Ceccotti 2006)

Fragiacomo et al. (2007) conducted a long-term test on beam specimens under a quasi-permanent load in an uncontrolled environmental condition for 133 days. The results of the experiment were extended for 50 year service life of the specimens using a purpose built finite element model. The research showed that the increased moisture content due to bleeding of fresh concrete is not an issue for the durability of the wood deck and the type of construction (propped or un-propped) does not significantly affect the structural performance. The rheological phenomenon experienced by the component materials lead to quite large deflections over the entire service life while the variation in stress was not significant. Figure 22 shows the elevation and cross-section of the beam tested and the mid-span deflection with time in Figure 23.

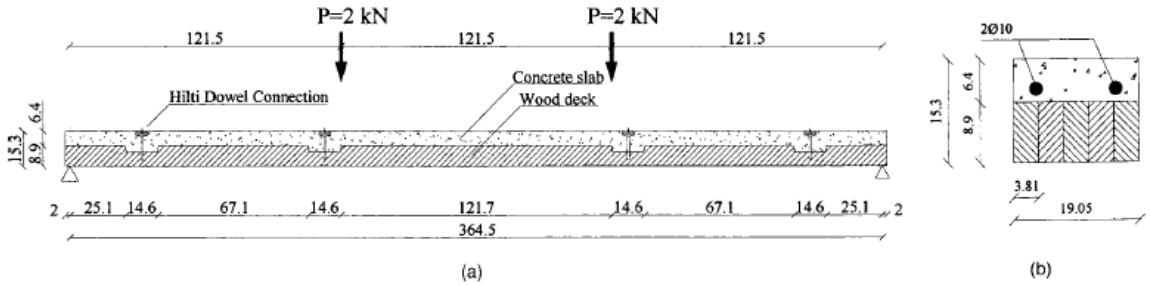

Figure 22; Longitudinal view (a) and cross-section (b) of the notched composite beam (measured in cm) (Fragiacomo et al. 2007)

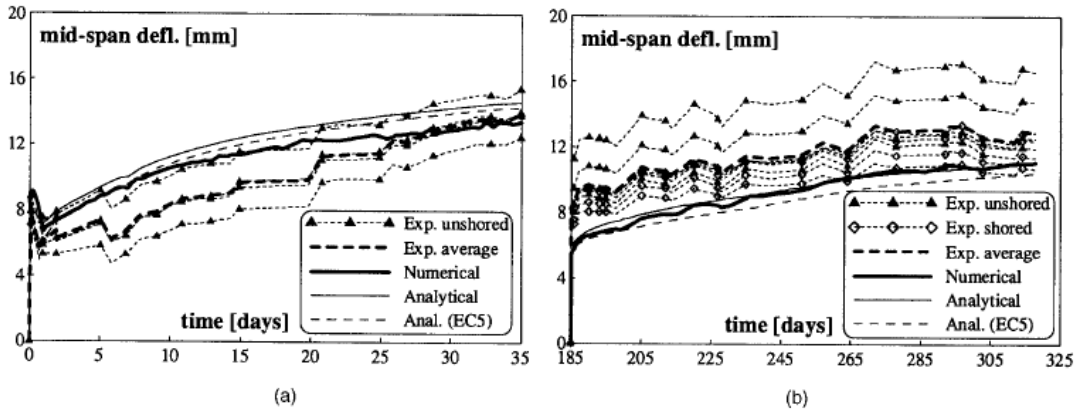

Figure 23: Trend in time of the mid-span deflection after the placement of the concrete (b) and after the application of the dead load weights.(Fragiacomo et al. 2007)

Lukaszewska (2009) performed a long-term test to investigate the time-dependent behaviour of the pre-fabricated timber-concrete composite system at the serviceability limit state. Two 4.8 m long beam specimens, representative of floor strips, were constructed and tested under sustained loading for one year. The first and second beam specimens, denoted as 1a and 2a, respectively, were produced with pre-cast concrete slabs with inserted SP+N* and SST+S* shear connectors shown in Figure 25. Both specimens have a 60x800x4800 mm^2 prefabricated slab of strength class C20/25 according to Euro code 2 and one 90x270x4800 mm^2 glulam joist of Swedish strength class L40, approximately equivalent to strength class GL28c/GL32 according to EN1194. After 172 days of casting, the slab was assembled into a vertically propped glulam beams and left for 68 days. After the props were removed, the specimens were left for 304 days in unconditioned unheated environment in

unloaded condition and no monitoring was done. After 544 days after concrete casting, two concentrated loads were applied as shown in Figure 24 at third point of the beam span.

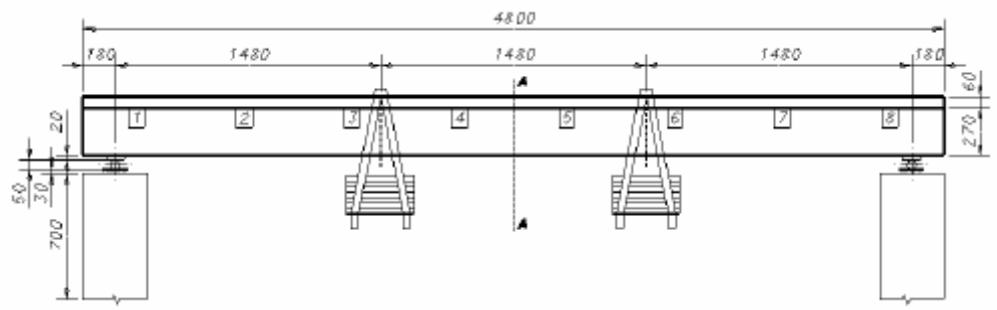

Figure 24: The elevation of beam specimen 1a with SP+N type during long-term test.(Lukaszewska 2009)*

Figure 25: SP+N connection type (left) and SST+S* type of connection (right) (Lukaszewska 2009)*

The temperature and relative humidity, mid-span deflection, relative slip and strains in the concrete slab and glulam beams were monitored throughout the entire test for 339 days of loading and the following 21 days after load removal. The experimental results in terms of mid-span deflection are presented in Figure 26 and Figure 27. The elastic deflection after the live load application was 5.6 mm and 5.4 mm for specimens 1a and 2a, respectively. At the end of the long-term test (339 days after the load application), before the load was removed, the mid-span deflection reached 8.3 mm and 9.5 mm respectively.

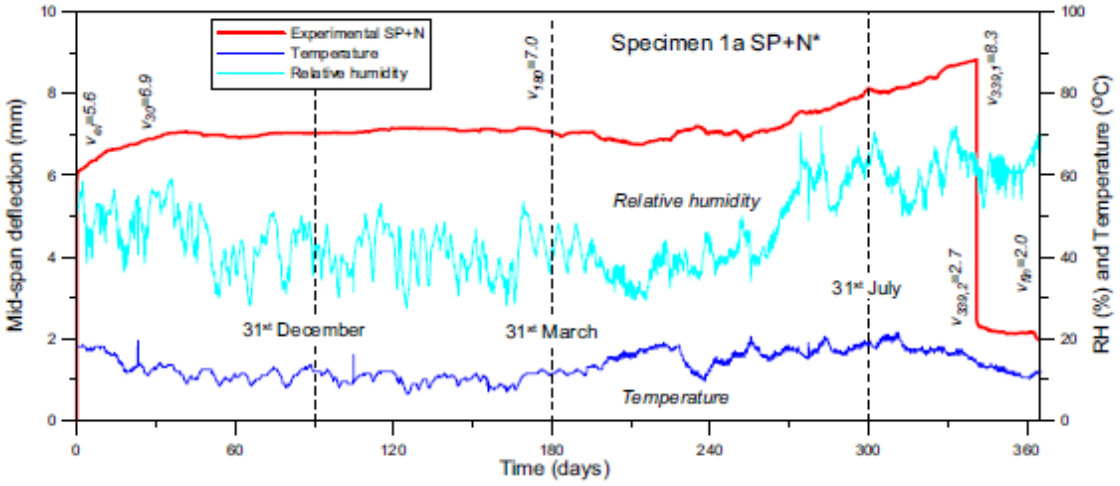

Figure 26: Mid-span deflection of specimen 1a with SP+N type during long-term test.(Lukaszewska 2009)*

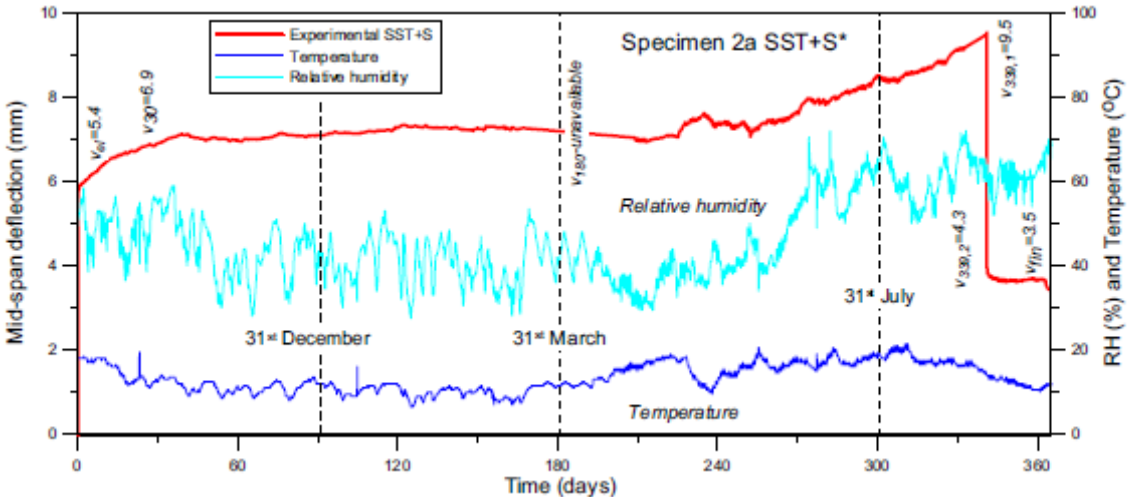

Figure 27: Mid-span deflection of specimen 2a with SST+S type during long-term test.(Lukaszewska 2009)*

Yeoh (2010) conducted a long-term test on three T- section floor beams with 8 m span and three connector types. The beams were subjected to sustained loads for a period of approximately 1.5 years. The long-term tests were conducted in an uncontrolled, unheated indoor environment and classified as service class-3 as per Euro code 5. The LVL joist had a cross-section of 400 mm x 63 mm and normal and low shrinkage concrete were used for the slab. The beams were loaded with a superimposed load of 2.2 kPa. The predicted final deflection exceeded the span/200

deflection limit as shown in *Figure 28*. Yeoh (2010) recommended the use of propping and/or pre-cambering the timber before concreting and use of low shrinkage concrete or precast concrete slabs for long span applications to reduce the long-term deflection. The test result showed largest creep coefficients for plate connection and least with rectangular notch connection. The long-term deflection for beams with normal concrete was larger than the beams with low shrinkage concrete.

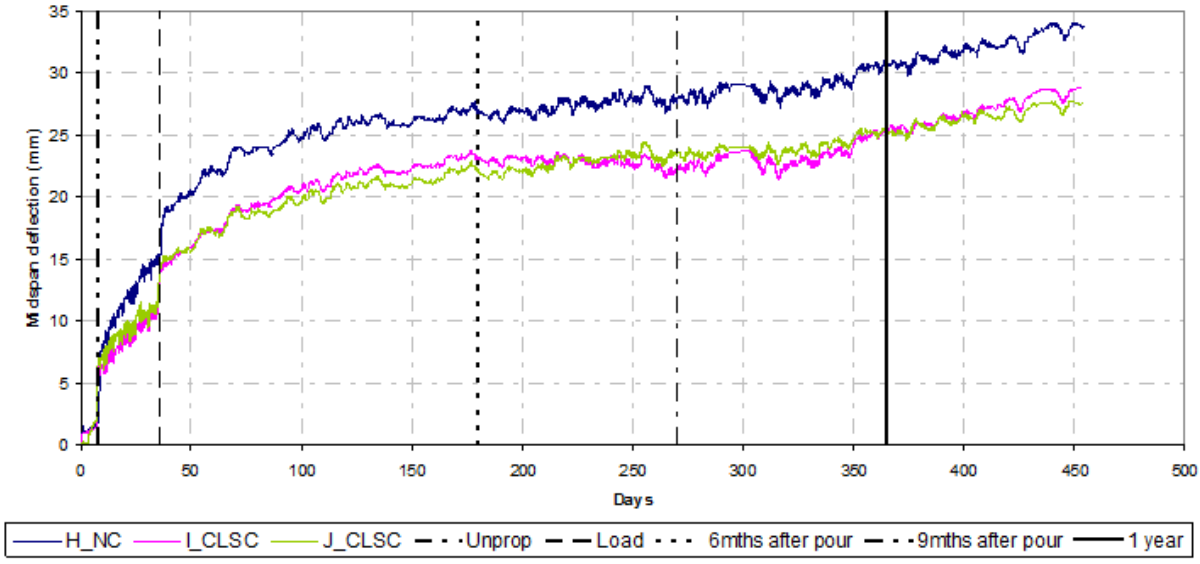

Figure 28: Long-term mid-span deflection result (Yeoh 2009)

2.5.3 Long-term experimental tests on TCC connections only

The long-term behaviour of timber-concrete connections has also been studied in different research programmes. In the few long-term tests on connections performed, however, the authors recognized that the connection creeps, and the amount of delayed slip seems to be affected by the environmental relative humidity. Amadio et al. (2001a) and also reported in Fragiacomo et al. (2007) conducted long-term push-out tests on a special connection system (Tecnaria) using normal concrete and light-weight aggregate concrete. These tests were performed under constant and variable climatic conditions. The constant climatic conditions were characterized by a relative humidity of 70 % and a temperature of 24° C while the variable climatic conditions were characterized by weekly cycles of alternate relative humidity of 50 % and 70 %.

On part of the test specimens, one unloading cycle was also applied. The creep coefficient (delayed slip/elastic slip) after 75 days ranged from 0.33 to 0.60.

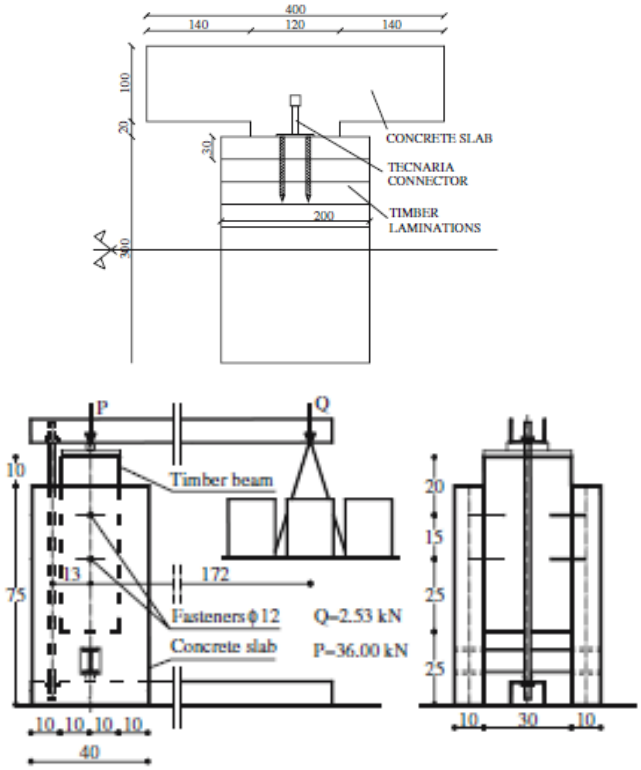

Figure 29: Half cross-section of the push-out specimens(left) and apparatus used in the long-term test to apply a sustained load (right) (dimensions in mm) (Fragiacomo et al. 2007)

Some of the conclusions made from this research were:

The use of light weight concrete slabs instead of normal weight slab does not have a marked effect on the shear strength after long-term loading. And the constant load applied on the specimen for long time did not significantly affect the shear strength, whereas it reduced the initial shear modulus.

The creep coefficients in constant environmental conditions at the end of service life were estimated to be 0.5 under loading and 0.24 for creep recovery when the connection is unloaded. Such values are far less than the long-term creep coefficients of timber and concrete.

The connection system exhibited mechano-sorptive creep i.e. a significant increase of the delayed slips when the loaded specimens were subjected to relative humidity cycles with period greater that seven days and amplitude of 40 % at least.

Based on the experimental test, however, characterized by significant scatter of the results, the final value of the increment in creep coefficient due to the mechano-sorptive effect can be estimated as 1.5.

Kuhlmann and Michelfelder (2004) tested timber-concrete joints made with notches and notches associated with steel fasteners (head and self-tapering screws), testing one specimen for each joint configuration. A load of approximately 30 % of average short-term load-carrying capacity of the joint obtained in short-term shear tests was applied over a period of approximately eight months.

Jorge et al. (2011) tested timber-concrete joints made with inclined screws using different lightweight concretes with and without an interlayer. Five joints configurations were tested in a total of eighteen tests. The test duration varied between 140 days for one joint configuration and 606 days for the other four configurations. The tests were performed in controlled climatic conditions (air relative humidity (RH) 65±5 %, temperature 20±2º C) with a long-term load approximately equal to 30 % of the average short-term load carrying capacity determined in short-term shear tests.

Mueller et al. (2008) conducted experimental shear tests on three different types of connectors (referred as series k, s and x). The shear tests included an experimental program with push-out tests under short term, long-term and dynamic loading. The aim of the short-term shear tests was to determine the stiffness and the ultimate load of each joint. The influence of variations of moisture and temperature on the stiffness of the connectors under long-term loading was analysed by performing long-term shear tests. Figure 30 shows the type of connectors tested; grooves being milled 2 cm deep into the timber and filled with concrete were responsible for the transmission of the shear forces in series k. The stud connectors of series S were composed of a 2 cm thick steel plate with 2 welded studs(diameter 9 mm),Whereas in series x two tension and compression reinforcing bars (diameter 14 mm) were inclined and glued 50 cm into the timber part using a two-component epoxy resin adhesive.

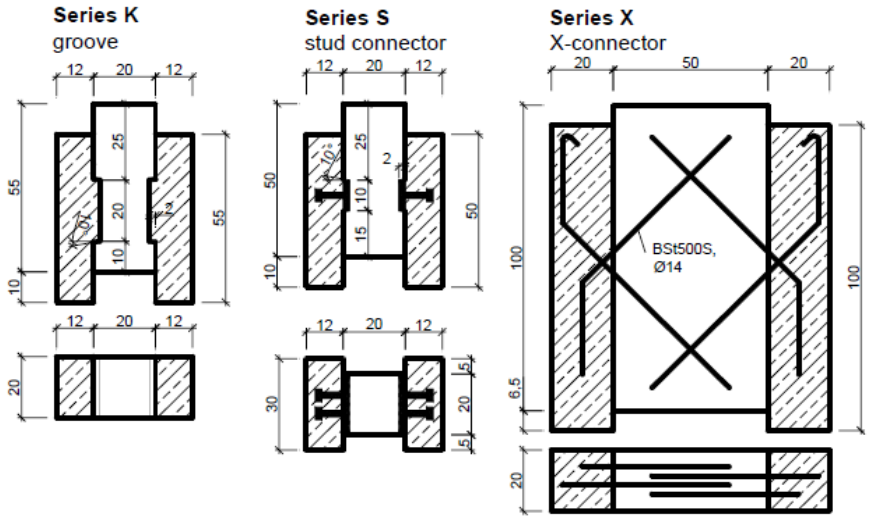

Figure 30: Three types of connectors for shear tests (Mueller et al. 2008)

Yeoh et al. (2011a) tested three types of connection (rectangular notch with 16 mm diameter coach screw referred as "R", triangular notch with 16 mm diameter coach screw designated as "T" and single side tooth metal plate with perforated holes referred as "P") under long-term test. The specimens were subjected to unheated, indoor conditions for 1.5 years. The relative humidity, temperature, moisture content, relative slip of the connections and the mid-span deflection were continuously monitored. The environmental conditions were classified as service class 3 based on Eurocode 5 recommendations. The long-term tests set up and the specimen's details are given in Figure 31 and Figure 32.

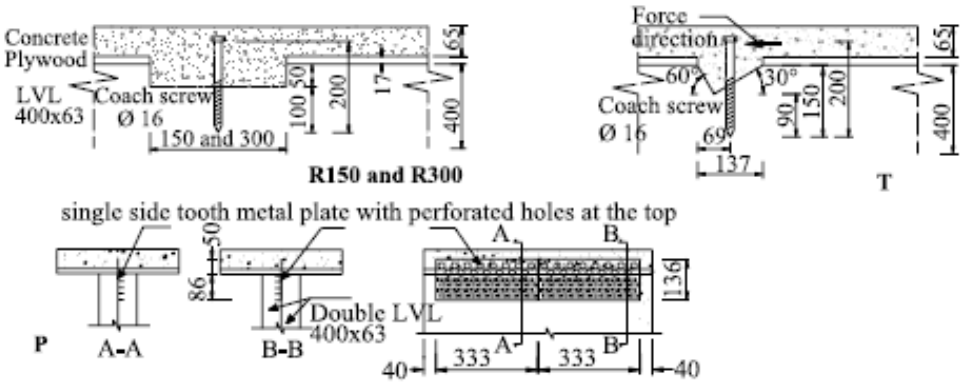

Figure 31: Details of the three types of connection (Yeoh et al. 2011a)

The creep coefficients of the connection were extrapolated to end of service life of 50 years and the corresponding creep coefficients were 2.1 for the triangular notched and coach screw connection, 1.6 for the rectangular notch and coach screw connection and 5.7 for the toothed metal plate connection.

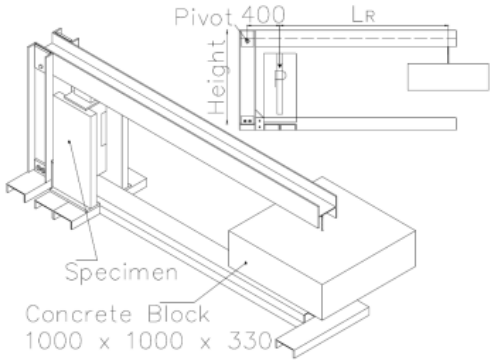

Figure 32: Sustained load test on connections and the cross-section of the TCC beams (Yeoh et al. 2010)

Van de Kuilen and Dias. (2011), conducted experimental investigation on seven different timber-concrete dowel types of fasteners. The tests were conducted in two conditions, uncontrolled in door, non-heated environmental condition and controlled environmental conditions; temperature (20±2º C) and RH (65±5 %) were monitored and controlled using temperature and moisture controlling equipment. The duration of the long-term test varied from 655 days for INT (10 mm profiled dowel with interlayer) and around 1160 days for the rest six types of fasteners (8 mm and 10 mm smooth dowel).The creep values obtained directly from the long-term tests varied between 0.57 to 1.58 for the controlled condition. Although no significant differences were found between creep values obtained for tests in controlled and uncontrolled climatic conditions. The predicted creep values however showed a significantly higher creep values for 10 and 50 years for the test configuration tested in uncontrolled climatic conditions as compared to the controlled conditions.

Some authors derived creep values for timber-concrete joints indirectly from the data for long-term test on timbre-concrete composite beams. Linden (1999) derived

values for the creep coefficients for 4 different types of timber-concrete joints (inclined screws, nail plates and a combination of notches and dowels). These results, however, were not obtained directly from shear tests but derived based on measurements in the composite beam in long-term tests associated with analytical models and finite element models. The creep coefficients derived varied between 1.4 up to 2.4 after 1200 days and from 2.0 up to 3.4 after 18250 days (50 years).

2.6 Evaluation of the long-term behaviour of TCCs in accordance to Eurocode 5

Eurocode 5 is the most commonly used code for design of timber-concrete composite elements. The design of timber-concrete composite structures must satisfy both ultimate and serviceability limit states (ULS and SLS) of design for short- and long-term loads. The ultimate limit state is checked by evaluating the maximum stresses in the component materials (timber, concrete and connection system) using an elastic analysis while the SLS is checked by evaluating the maximum deflection.
Eurocode 5 – Part 1-1, Annex B provides a simplified method for calculating these parameters of mechanically jointed beams with flexible elastic connections *(*Figure 33*)*.

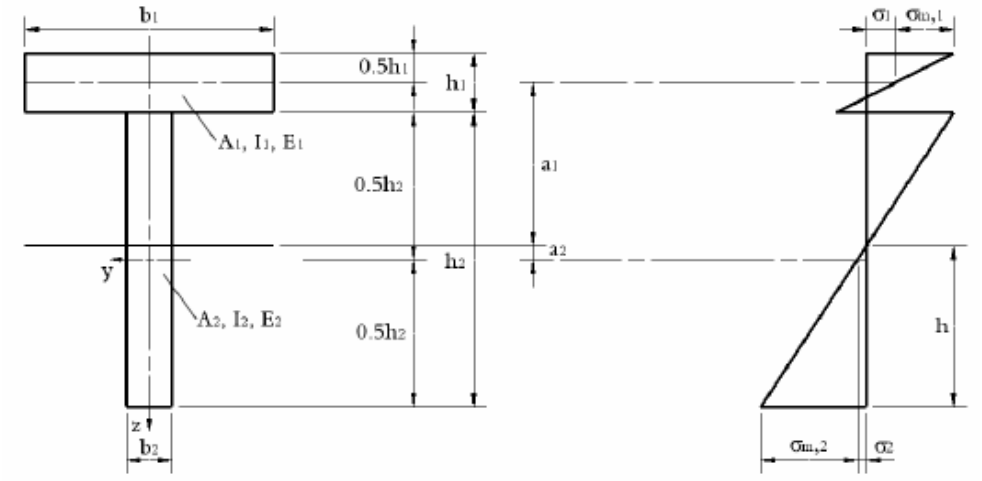

Figure 33: cross-section (left) and stress distribution (right) of a composite beam with flexible connection (Eurocode 5)

These formulas in Eurocode 5 Annex-B, proposed for timber-timber composite beams with flexible connectors, can be effectively used for the design of composite beams and slabs in the short term. The elastic solution for a simply supported composite beam with flexible connection subjected to vertical uniformly distributed

load can be obtained using the simplified method also known as "gamma-method'. This method is based on an approximate solution of differential equation for beams with partial composite action.

In performing the global analysis i.e. calculating internal actions and the consequent stress distribution at ultimate limit state, mean values of material stiffness and slip modulus of connections have to be used. This is because in Eurocode 5 only mean values of slip modulus are given and the characteristic values are not available. Therefore, only the mean values of the modulus of elasticity may be used: In fact, if using at the same time the characteristic value of the modulus of elasticity and the mean value of the modulus of slip the calculated values of the resultant stresses would be on the unsafe side (Ceccotti 1995).

According to the gamma method, the effective bending stiffness EI_{eff} of a simply supported timber concrete composite beam is calculated as:

$$EI_{eff} = E_1 I_1 + \gamma_1 E_1 A_1 a_1^2 + E_2 I_2 + E_2 A_2 a_2^2 \qquad \textit{Equation 3}$$

With shear coefficient γ and distance a_i given by;

$$\gamma_1 = \frac{1}{\left(1 + (\frac{\pi^2 E_1 A_1 S}{KL^2})\right)} \qquad \textit{Equation 4}$$

$$a_1 = \frac{h_c + h_t}{2} - a_2 \qquad \textit{Equation 5}$$

$$a_1 = \frac{\gamma E_1 A_1 (h_1 + h_2)}{2\gamma E_1 A_1 + E_2 A_2} \qquad \textit{Equation 6}$$

Where I_i, A_i and E_i are the second moment of inertia, area, and modulus of elasticity of the concrete slab (i=1) and timber beam (i=2), respectively, s is the connector spacing, L is the beam length, k is the slip modulus of the connector. A coefficient γ equal to 1 indicates full composite action with no slip at the interface between the timber and concrete.

The effective stiffness can be used to calculate the deflection, the stress distribution and the shear load in the fastener using the formulas in Eurocode 5 Annex B. In

using the current procedure for short-term solutions the elastic moduli can be obtained from Equation 7.

$$E_c = E_{cm}(t)\ , \quad E_t = E_{o,mean}\ , \quad K = k_{ser} \qquad \textit{Equation 7 (a,b,c)}$$

Long-term verification of composite beams is more problematic, since concrete creep and shrinkage, the creep and mechano-sorptive of timber and connection and thermal strains of concrete and timber should be considered. Several numerical programs (outside the scope of this thesis) have been proposed to provide accurate solutions, but no consensus among researches has been reached regarding predicting the long-term performance of timber-concrete composite structures (Lukaszewska 2009). The ACI-ASCE joint committee recommends using $E_c/2$ as concrete modulus of elasticity instead of E_c when calculating sustained load creep deflection in steel-concrete composites and AASHTO Bridge Design Specification, Section 10.38.1.4, suggests using E_c /3 (Clouston 2006).The European Code recommends using creep factors developed from load duration studies to reduce the moduli of the respective materials (Eurocode 5).

The simplified approach suggested by Ceccotti (2002) does not account for shrinkage or thermal strain ((Lukaszewska 2009) and is based on the effective modulus method, in which the creep and mechano-sorptive behaviour of the concrete, timber and connection are accounted for by reducing the elastic and slip moduli according to the following Equation 8;

$$E_{c,fin} = \frac{E_{cm}(t_o)}{\left(1+\varphi(\infty,t_o)\right)}, \quad E_{t,fin} = \frac{E_{o,mean}}{\left(1+k_{def}\right)}, \quad K_{fin} = \frac{K}{\left(1+k_{def}\right)} \qquad \textit{Equation 8 (a,b,c)}$$

For the concrete, Eurocode 2-1-1 provided some guidelines for evaluating the creep coefficients $\varphi(\infty,t_o)$, ∞ and t_o being the final and loading instants, respectively. Euro code 5-1-1 provided tables of values of the creep coefficient k_{def} for timber. For the connection the code recommends the same as that of the timber. Kavaliauskas et al. (2005), however, recommends the creep coefficient twice as large as the creep coefficient of the wood i.e. ($2K_{def}$). For concrete analytical formula are suggested by

the CEB-FIP Model code 90.The proposed procedure neglects effects of concrete shrinkage and inelastic strains of concrete and timber due to thermo-hygrometric environmental variations (Ceccotti 2006).

The effective stiffness can be used to calculate the mid-span deflection, using the following equation:

$$\delta = \frac{5qL^4}{384\left(EI_{eff}\right)}$$ *Equation 9*

Where: δ is the mid-span deflection of a simply supported beam, q is the uniformly distributed load.

Kavaliauskas et al. (2005) evaluated the long-term deflection of a TCC beam based on Eurocode 5 by doubling the creep coefficient of timber to account for that of the connection. The Eurocode method only gives the initial and final deformation and several experimental results indicate that the final deformation is often exceeded the limiting deflection (L/250) within the first year for medium and long span floors. In timber concrete composite structures, the concrete is denser than timber in most cases and therefore, concrete stresses tend to decrease in time while stresses on timber tend to increase, and therefore long-term situation is more demanding for timber (Ceccotti 2002). Kavaliauskas et al. (2005) also proposed calculating the creep of concrete and timber separately, with concrete creep deformation calculated using Eurocode 2 and the timber creep deformation calculated using an exponential law proposed by Le Govic. Results from the proposed method showed that the initial deflection prediction was twice that predicted by Eurocode 5 and reached almost its final value over a period of 60 days. The calculated final deflection was 1.5 times that predicted by Eurocode 5.

An extension to Eurocode 5 Annex B formulas for design of timber-concrete composite structures is also proposed by Schanzlin and Fragiacomo (2007). This approach was found to further improve the prediction of the long-term deflection.

Yeoh et al. (2009) used two analytical methods to compare the extrapolated experimental deflections at the end of the service life. The “effective modulus method”, using the separate material creep coefficients for the timber, concrete and connection proposed by Ceccotti (1995) significantly underestimated the

extrapolated experimental deflections. The "effective creep coefficient method" recommended by Schazlin and Fragiacomo (2007) also underestimated the deflection by 40 to 60 %.

2.7 Concluding remarks

The literature review included a general insight into the historical and recent development of timber-concrete composite systems, and it reviewed the existing long-term investigations and the proposed long-term evaluation procedures.

In the design of TCC structures, both serviceability and ultimate limit state has to be checked, and the serviceability limit state of maximum deflection may be the most sever design criterion. Thus it is important to investigate the behaviour of such structures under long-term service loads. Moreover, the three component parts, (the concrete, connector and timber) in TCC demonstrate important but different time dependent phenomena. The creep and shrinkage of concrete, the mechano-sorptive creep in timber, and the creep and mechano-sorptive creep .Hence, experimental investigations to study this complex structural problem is very crucial.

Previous researches reviewed, mainly focused on measuring the strength of various TCC shear connections full scale tests and long-term deflections of structural members due to environmental conditions. However, minimal research has been carried out to assess the impact of extreme variations in humidity on the deflection of TCC beams, which are expected to be indicative of the upper limit for the long-term defection that can be predicted for TCC structures. Dias and Jorge (2011) found out that with a similar properties; specimens tested in test configuration with constant climatic condition lead to creep coefficients that were around half of the values obtained with a test configuration tested in variable climatic conditions. Furthermore, a relationship between the mechano-sorptive effect and the long-term serviceability of TCCs has not yet been established. The literature review also confirmed that the existing analytical methods proposed are found to underestimate the extrapolated long-term experimental deflections.

3 Timber Concrete Composite beams

A long term laboratory investigation was commenced in August 2010 at the University of Technology, Sydney. The test was conducted on four 5.8 m span LVL-concrete composite beams (referred to as TCC beams here onwards) with four different connector types - Type 17 screws, four and six notches with coach screw and SFS screws. The materials used were Laminated Veneer Lumber (LVL) for the beams and 32 MPa concrete for the flanges. The tests and results of short-term investigations on the four TCC beams were reported in Pham (2010) as part of an undergraduate final year project. Several properties were determined from these tests which will be referred throughout this thesis.

3.1 Characteristics of the composite beams

The top slab is made of a normal weight concrete of 32 MPa commercial strength, and the test results for the concrete compressive strength after 28, 56 and 91 days were 39.5, 44.3 and 50.3 MPa respectively, the mean drying shrinkage was 800 μ at 28 days. A standard reinforcing mesh of 7 mm diameter normal strength reinforcement bars at 200 mm spacing was provided in the concrete slab to prevent shrinkage cracks. The properties of the concrete are given in Table 1. Figure 34 illustrates a typical cross-section of the beams under investigation.

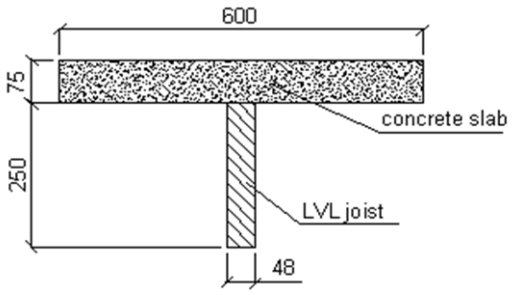

Figure 34: Cross-section of the TCC beam (Typical) (measured in mm)

Four different types of shear connector configurations were used in the four beams. Normal wood screws at 500 mm spacing were used as shear connectors in the first

beam and is referred as (B_NS), in the second beam four bird's-mouth notch connections with minimum of 600 mm spacing between notches with diameter 16 mm coach screw were used and is referred as (B_4N) while in the third beam referred as B_6N, six bird-mouth's notch connections with diameter 16 mm coach screw were used with minimum of 500 mm spacing between the notches, and the fourth beam referred as (B_SFS) was constructed with a pair of SFS crews at ±45° angles at a spacing of 300 mm as shear connectors.

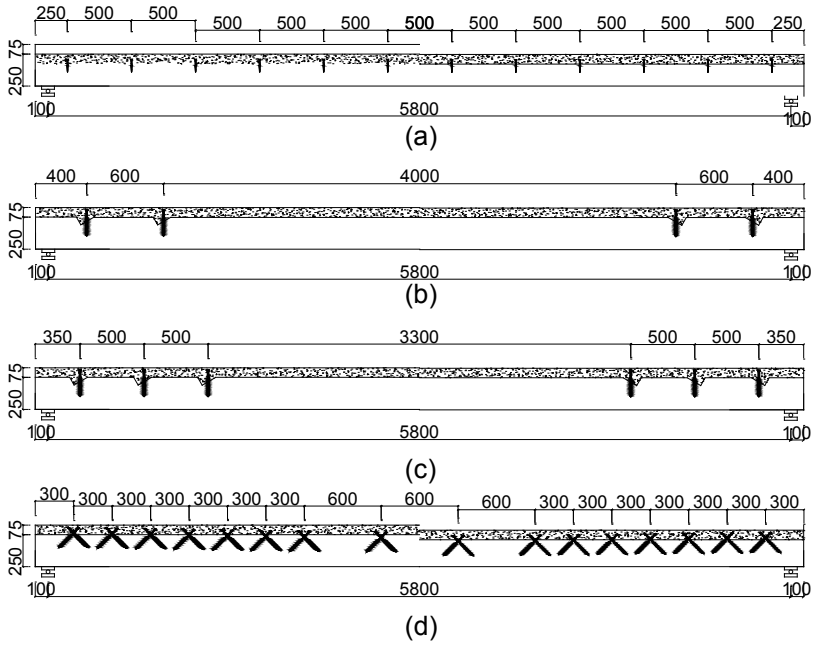

Figure 35: Longitudinal elevation of the TCC beam (measured in mm) (a) B-NS, (b) B-4N, (C) B-6N, & (d) B-SFS

Table 1: Properties of concrete used (Pham 2010)

Age (Days)	Compressive strength (MPa)	Unit mass (kg/m^3)
7	20.76	2378.54
28	39.54	2379.07
56	44.33	2388.79
91	50.33	2390.86

The joists are made of 250 x 45 mm LVL, the mean young's modulus of the LVL was 13.2 GPa and the characteristic bending strength was 48 MPa. The material property values of LVL as supplied by the manufacturer are provided in Appendix B. Push-out tests were carried out to determine slip modulus and characteristic strength (Khorsandnia et al. 2012), the mean strength and slip moduli are shown in Table 2 and more details about the connectors are presented in Appendix B. Figure 36 shows the three types of connectors before the concrete pour.

Table 2 Type of connectors, characteristic strength and slip moduli

Specimen	Slip modulus, $K_{sls,0.4}$, kN/mm	Characteristic strength, $Q_{k,}$ kN
B-NS	45.0	10.9
B-4N	36.9	59.5
B-6N	36.9	59.5
B-SFS	54.9	32.6

Figure 36: (1) Birds mouth with Ø16 mm coach screw, (2) Normal screw type-17 and (3) SFS screw connections

3.2 Initial short term tests on TCC and LVL joists

Short-term serviceability tests were conducted on the LVL joist before assembled into the TCC, and on the TCC beams after 90 days of the concrete pour. The results of those short-term tests will be used in determining and understanding the residual stiffness and strength of the beams.

3.2.1 Initial serviceability test on LVL joists

A short term static test under 4-point bending loads was done to determine the modulus of elasticity of the LVL joist before being assembled for concrete pouring according to AS/NZS 4357:2 (2006). Figure 37 shows a typical test set up for LVL joist. The LVL joists have been tested before and after carving. The reported modulus of elasticity values for the four LVL joists given in
Table 3 are all tests performed after carving as reported by Pham (2010).

Figure 37: MOE test on LVL only

Table 3: The Modulus of Elasticity of the Timber (LVL) (Pham 2010)

Specimen	MoE of LVL (GPa),
B_NS	12.4
B_4N	13.2
B_6N	13.5
B_SFS	12.3

3.2.2 Initial Serviceability test on TCC beams

The TCC beams after cured for ninety days were tested in a four point bending test to determine their bending stiffness. Figure 38 shows the test set up and the data monitored include the magnitude of strain at mid span and defections at mid span and at the load points.

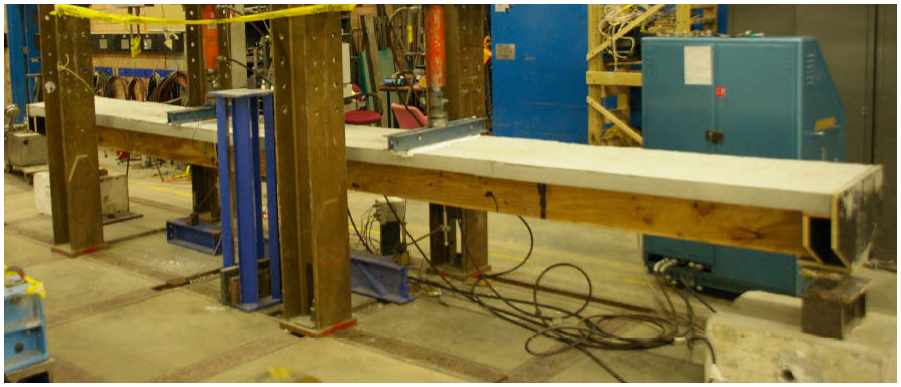

Figure 38: TCC beam under short-term test

The experimental result (Table 4) shows B_SFS with highest bending stiffness and B_NS with least and both B_4N and B_6N in between, the results followed sequence of their composite efficiencies.

Table 4 TCC beams bending stiffness (Pham 2010)

Specimen	Stiffness, (kN/m)	EI (E+12 Nmm^2)
B_NS	802	2.78
B_4N	1178	4.08
B_6N	1254	4.34
B_SFS	1323	4.60

Where: "E" is the modulus of elasticity and "I" is the second moment of inertia of the section.

The effective analytical bending stiffness (EI_{eff}) (Table 5) was also determined by applying the gamma method as discussed in chapter 3.The mean moduli of concrete and timber and the 40% slip modulus of the connection were used. The mean slip modulus at 40 % (K_{sls}, 0.4) is used in computing the bending stiffness of the beam with smeared connection (B-NS and B-SFS), while a fifth percentile slip modulus at 40 % is used in case of notched connector type (B-4N and B-6N). The reason for this is the available redundancy through the parallel action of the connectors in the

interlayer. However, for a small number of connectors as in the case for beams with notched connectors, this redundancy effect vanishes and the 5-percentile value should be taken (Linden 1999). The gamma method underestimated the bending stiffness's values, except B-NS with higher theoretical bending stiffness that the experimental one. This could be due to large slip modulus obtained from this connector type during push-out tests, possibly caused due to high friction in the interface. And, this may not be the case in full-scale beam tests.

Table 5 Theoretical bending stiffness of TCC beams at serviceability

Specimen	S_{eff}	γ_c	EI_{eff} (E+12, Nmm^2)
B_NS	500	0.167	3.97
B-4N	1025	0.074	3.28
B-6N	850	0.088	3.50
B_SFS	375	0.25	4.29

Where: "E" is the modulus of elasticity and "I" is the second moment of inertia of the section

3.2.3 Composite efficiency of the TCC beams

The composite action achievable by interconnecting timber and concrete can be estimated by quantity E, usually defined as composite efficiency, which is given by equation 2.

$$E = [\, D_N - D_I \,/\, D_N - D_C \,] * 100 \qquad \textit{Equation 10}$$

Where: D_C is the theoretical fully composite deflection, D_N is the theoretical fully non-composite deflection, and D_I is the measured deflection for incomplete composite action of the beam.

As shown by the closeness of the top two lines (D_C and D_I) in Figure 39 to Figure 42, the composite efficiency is highest (90 %) for B_SFS and lowest for B_NS beam (51 %); with the notched beams a composite efficiency of 80-84 % (Table 6). The figures also show the stiffness of the LVL joist (timber only), which is falling below the lower limit for the TCC beams i.e. curve D_N a non-composite action case.

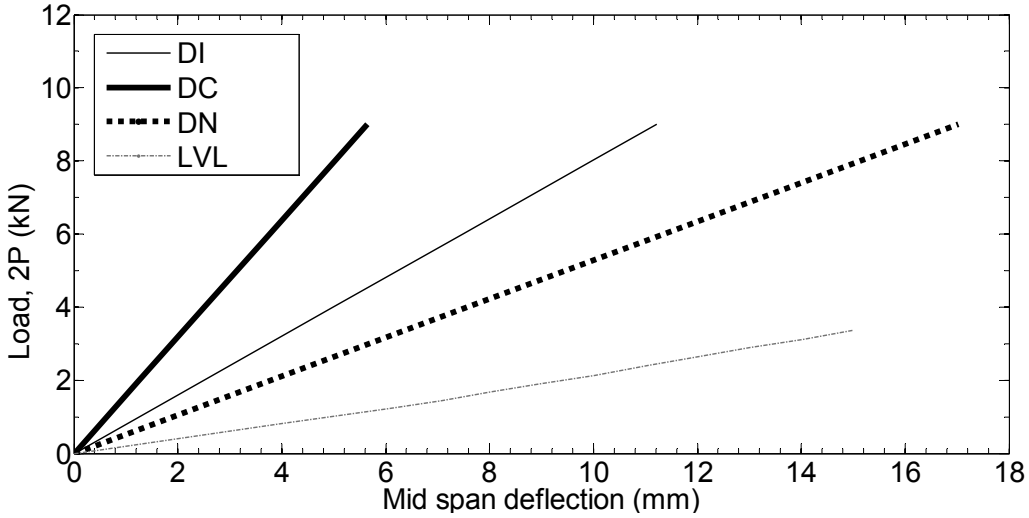

Figure 39: Load vs. mid-span deflection during serviceability test for B_NS

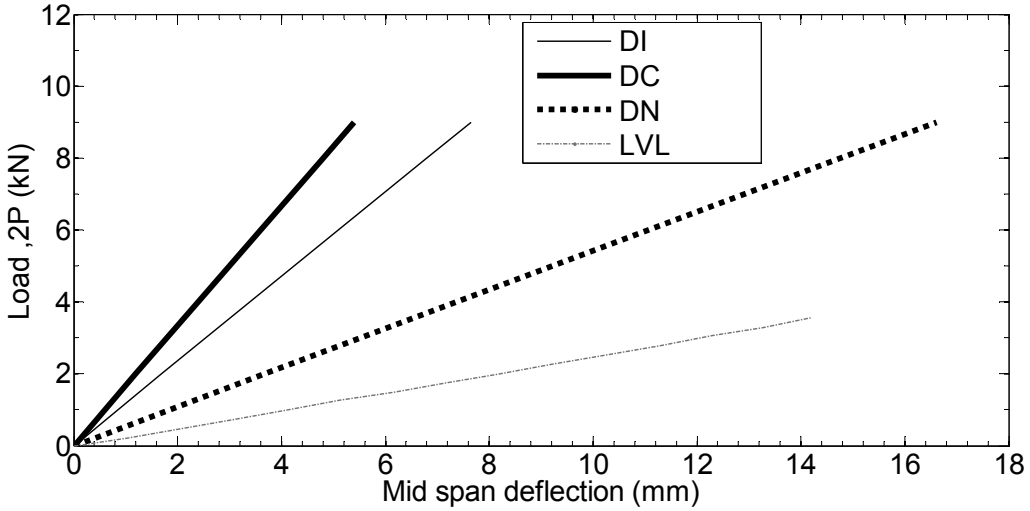

Figure 40: Load vs. mid-span deflection during serviceability test for B_4N

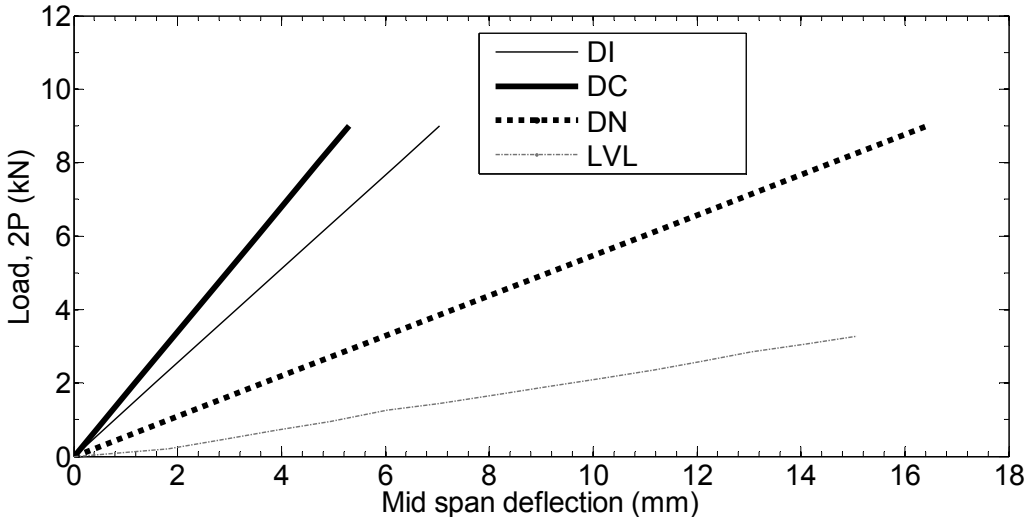

Figure 41: Load vs. mid-span deflection during serviceability test for B_6N

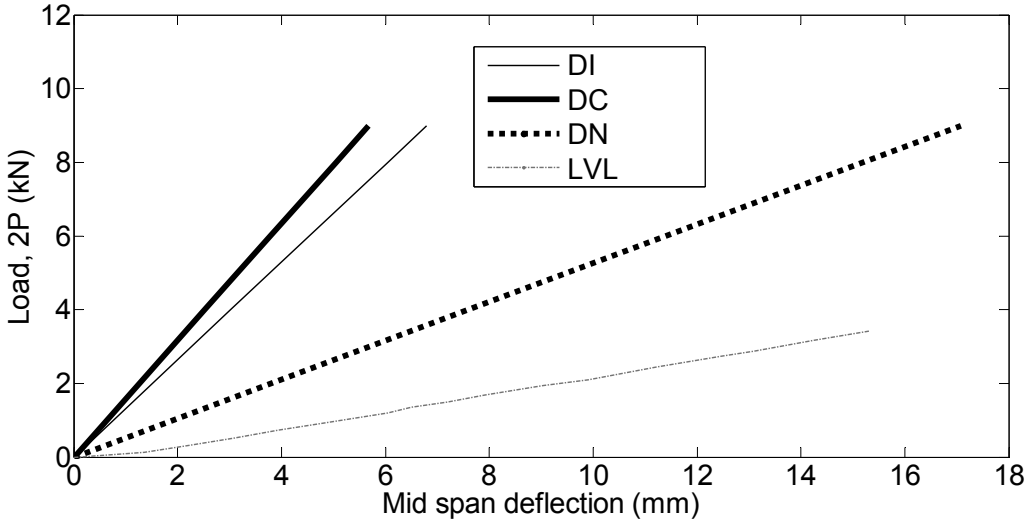

Figure 42: Load vs. mid-span deflection during serviceability test for B_SFS

Table 6 Composite action achieved by TCC beams

Specimen	Composite efficiency (%)
B-NS	51
B-4N	80
B-6N	84
B-SFS	90

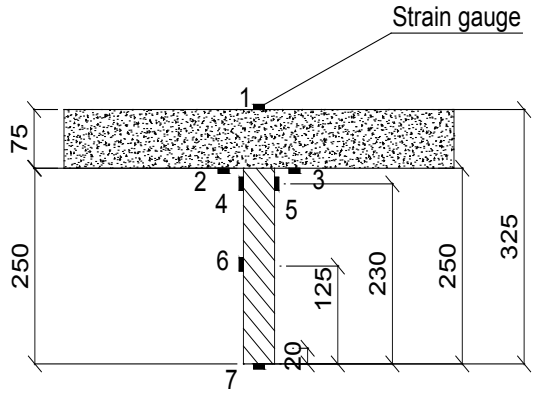

Figure 43: Location of strain gauges during (a) short-term tests on TCC beams

The magnitudes of strains at different points (Figure 43) of mid span cross section are presented in (*Figure 44* to *Figure 47*) for each TCC beams. These strains correspond to a reference total applied load of 8 kN on the beams, the strain magnitudes at this reference load were considered for comparison reasons.

The composite efficiency of the TCC beams can also be investigated from the magnitudes of the strain readings along the cross section of the beam. In all the figures it can be observed that a semi rigid behaviour with both concrete and timber under combined compressive and tensile stresses, with each component having its own neutral axis. This illustrates a significant slip between the concrete and timber. The area of concrete under compression is small for B-SFS beam as compared to the other three beams with larger area under compression is recorded for B_NS beam. The absolute sum of the magnitude of the strains at the interface between concrete

and LVL also indicates indirectly the composite efficiency achieved by the beams; with large magnitude recorded for B_NS revealing large slip and smallest value for B_6N and B-SFS indicating good composite behaviour.

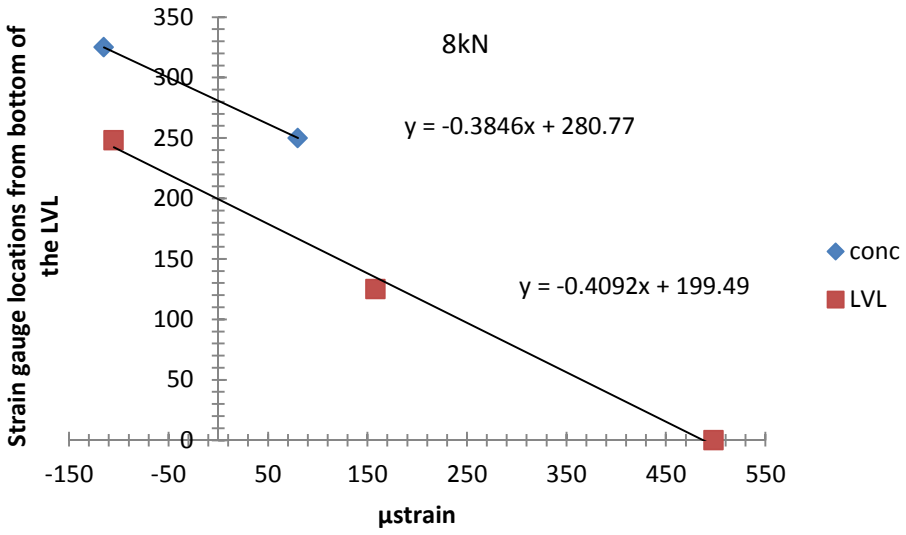

Figure 44: Strain readings along mid-span cross section for B_NS (conc. = strain reading on concrete, LVL= strain reading on the timber)

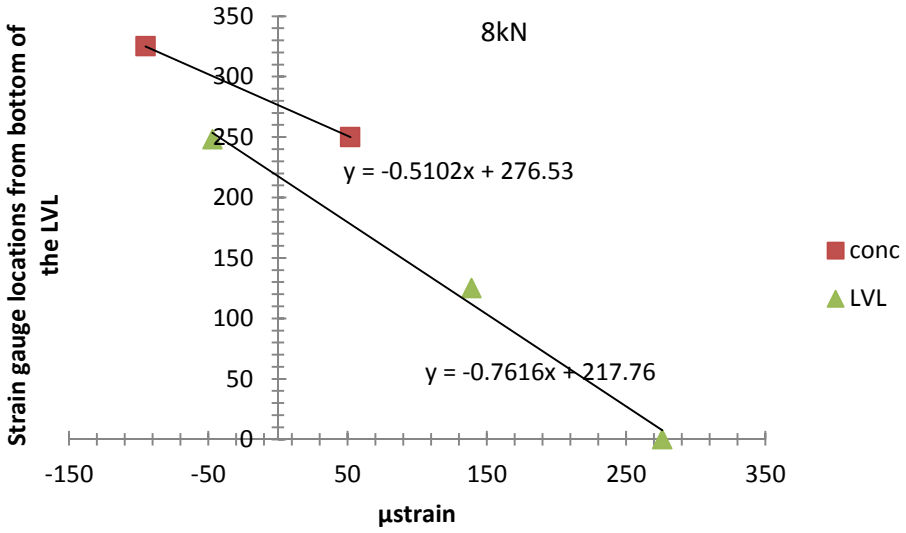

Figure 45: Strain readings along mid-span cross section for B_4N (conc. = strain reading on concrete, LVL= strain reading on the timber)

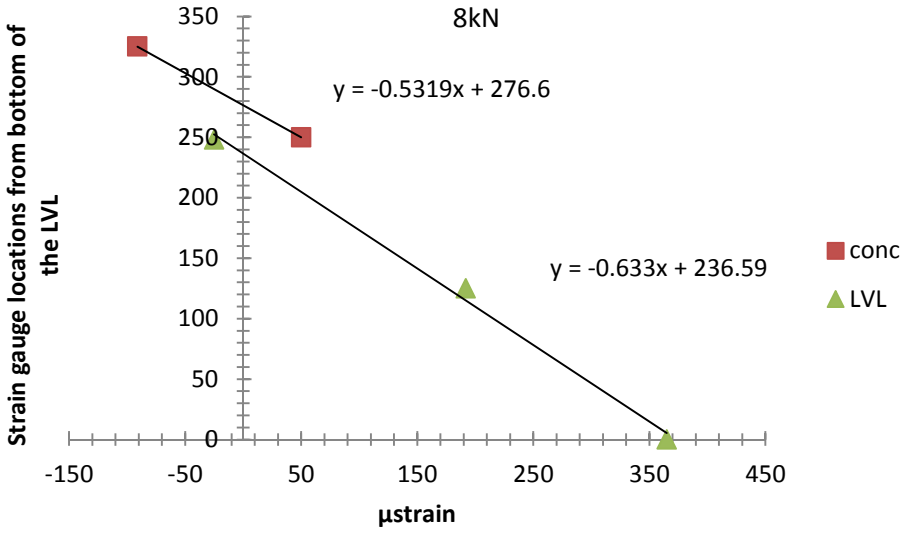

Figure 46: Strain readings along mid-span cross section for B_6N (conc. = strain reading on concrete, LVL= strain reading on the timber)

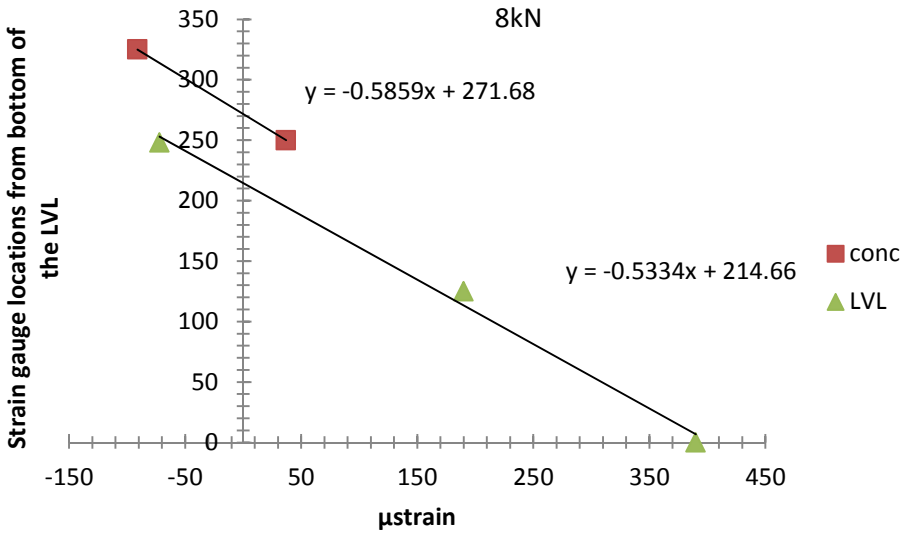

Figure 47: Strain readings along mid-span cross section for B_SFS (conc. = strain reading on concrete, LVL= strain reading on the timber)

3.3 Concluding remarks

The properties of the TCC beams have been discussed in this chapter with references to the experiments conducted by Pham (2010). As the test results show the composite technique (combining LVL and concrete) has achieved higher bending stiffness's as compared the bending stiffness's of the LVL joists before assembled into TCC. The beams exhibited a linear elastic behaviour up to the applied service loads and a good composite behaviour with a composite efficiency of 80-90 % was achieved by three beams (B-4N, B-6N and B-SFS) except beam B-NS. The bending stiffness's were also computed using gamma method in Eurocode 5 and found to under estimate the bending stiffness's as compared to those obtained from the experimental results.

4 Long-term testing of TCC beams

This chapter reports the long-term test of the four TCC beams. The properties of these beams have been discussed in Chapter 3. These beams, each with a clear span of 5.8 m, were tested under long-term tests in the civil engineering structures laboratory at the University of Technology Sydney. The tests were commenced in August-2010, which was 200 days after the concrete pour. The beams were simply sitting in the laboratory area with temperature about (20±2 °C) and relative humidity 60±5 % before put in to the long-term test. Two of the four beams (B-NS and B-4N) were unloaded after 550 days and were then loaded to failure. The other two beams (B-6N and B-SFS) are still under a long-term test at the time of writing the thesis (1400 days).

4.1 Test set-up

The beams were loaded with equally spaced lead bars which were arranged such that the bars apply a uniformly distributed load of 1.05 kN/m (1.7 kPa). The load level is such that no plasticity in any material is expected to occur immediately after the loads have been applied. This applied load is about 43 % of the serviceability long-term design load (G+0.4Q). The set up for the long-term test is illustrated in Figure 48, where the beams were simply supported.

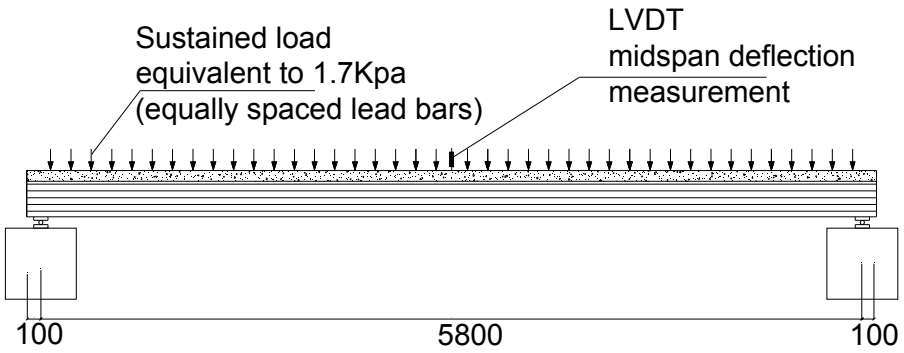

Figure 48: Test set up (measured in mm)

The quantities that have been monitored are;

- mid-span deflection using LVDTs (linear variable displacement transducers) with 1/1000th of mm sensitivity,
- relative humidity and temperature of the room using climate loggers and,
- the moisture content of the timber using small timber blocks placed beneath the TCC beams.

Figure 49 Beams under quasi-permanent loads (lead bars)

The instantaneous elastic mid-span deflections after the application of the load are shown in Table 7, since manual application of the loads took time, these defections were taken once the readings stabilized. Beam B-NS exhibited the greatest amount of deflection 8.4 mm while the other three beams have similar but lesser deflections (4.17 to 4.67 mm). Such difference in the deflection observation is due to limited composite action exhibited by B-NS compared to the other three beams, resulting in slippage between the concrete and the LVL. Beam B-SFS exhibited the least deflection and it demonstrates that this type of connection possesses the greatest amount of composite action. In addition, the SFS screws are uniformly distributed throughout the length of the beam and likewise the slip is more uniformly distributed

throughout the length of the beam and results in least deflection. These values have also been compared with the theoretical deflection obtained using the standard solution based on elementary beam theory. The shear effect on deformation is relatively low in beams of usual structural sizes (Thelanderson 1995), and are not considered in the computation. The instantaneous deflections are calculated using the EI values obtained from the short-term experimental test results (Table 4) and the values were 5.6 mm, 3.8 mm, 3.6 mm and 3.4 mm, respectively. Measurement of the instantaneous deflection was difficult during manual loading of the beams with lead bars and therefore, the instantaneous deflections were taken after the deflections were stabilized.

Table 7 Instantaneous elastic mid-span deflection measured

Specimen	Instantaneous elastic deflection (mm)
B-NS	8.24
B-4N	4.67
B-6N	4.39
B-SFS	4.17

The instantaneous elastic deflection measured after load application (Table 7) are compared with those of calculated, while the results for the three beams (B-4N, B-6N and B-SFS) shows very small difference, however, the measured value for beam B-NS was much higher than the calculated value, and based on the measured instantaneous deflection the corresponding stiffness to induce 8.24 mm deflection is 1.9E+12 Nmm^2 much lower than the experimental bending stiffness measured in Table 4.

4.2 Environmental conditions

The relative humidity (RH) and temperature (T) of the humidity chamber were measured regularly every hour. The changes in RH, T and timber moisture content

(MC) are shown in Figure 50. Air humidifier was used to increase and maintain high RH during the wet periods. The environmental conditions monitored for the last three years showed that the room temperature remains reasonably constant, around 20° C (±1) while, the relative humidity varied between about (50 %) during the dry periods and saturation (100 %) during the wet periods. The length of a humidity cycle varies between six to eight weeks. The moisture content of the MC samples alternated from approx. 10 % at the end of dry periods to above 20 % at the end of wet periods. It can be said that this test is conducted in a semi-controlled environmental conditions.

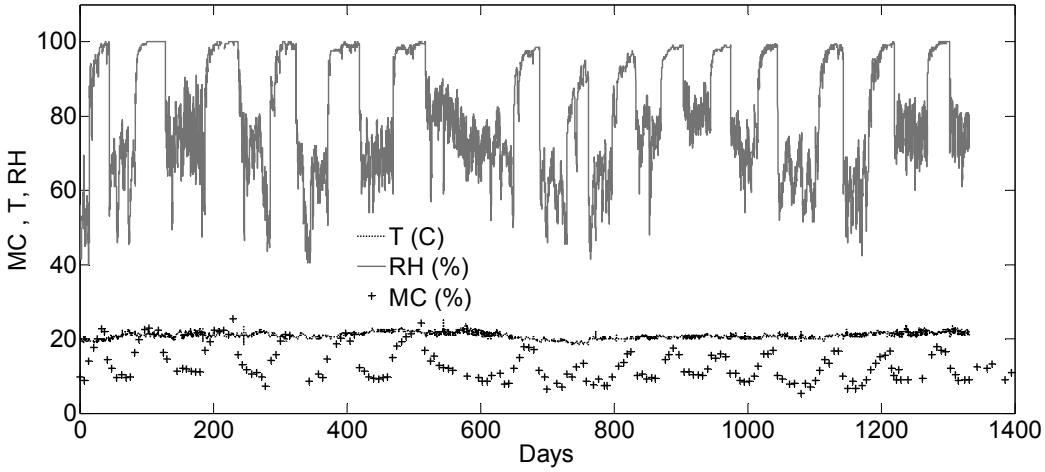

Figure 50: Changes in relative humidity, moisture content and temperature

This environmental condition, based on Eurocode 5, can be assigned to service class 3; it is characterized by moisture content in the material corresponding to a temperature of 20° C and relative humidity of the surrounding air exceeding 85 %. However, in this environment the air humidity exceeded and kept well around 100 % for several weeks and repeated every four to six weeks.

4.3 Moisture content

Separate LVL samples with 100x100x45 mm sizes were kept in the humidity chamber and the changes in the level of moisture were measured regularly to monitor the variation of moisture content in LVL beams. The test samples for measuring the moisture content are shown in Figure 51. The location of the MC samples in the humidity chamber is shown in Figure 90 and Figure 91, Appendix D.

The moisture content obtained from the test samples was initially around 9 % and increased to above 20 % after the humidifier was operated. It was observed from the result that it takes at least two weeks for the moisture content samples to attain 10 % additional moisture content.

The moisture content values are the mean values of moisture content obtained from four samples. However, the actual moisture content along the cross section is not uniform, and may be higher in the surfaces than in the middle of the cross section, which has also been reported by Ranta-Maunus and Kortesmaa (2000). The moisture content measurements on the small samples may not represent the actual moisture in the LVL joist, as small samples admit water faster than the actual LVL joists, hence additional LVL samples of size 600x250x45 mm were placed for comparison. The MC measurements for large samples were done at every start and end of the cycle (i.e. every four weeks mean values of the MC of four samples were taken). These moisture content samples were positioned in the humidity chamber considering the variations of the chamber humidity. A comparison of the MC measured on the small and large samples is shown in Figure 52.

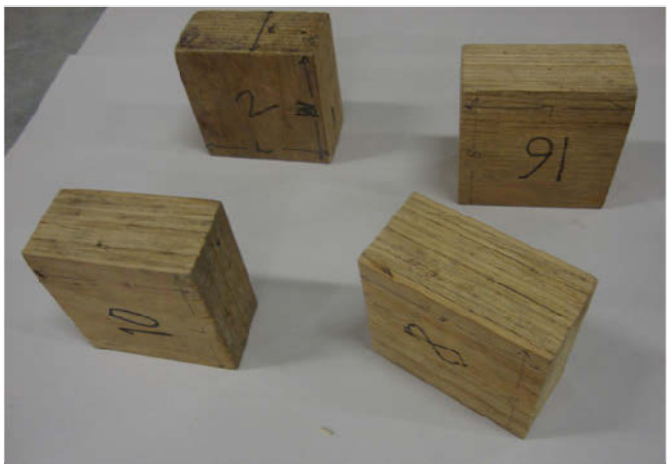

Figure 51 LVL MC Test samples

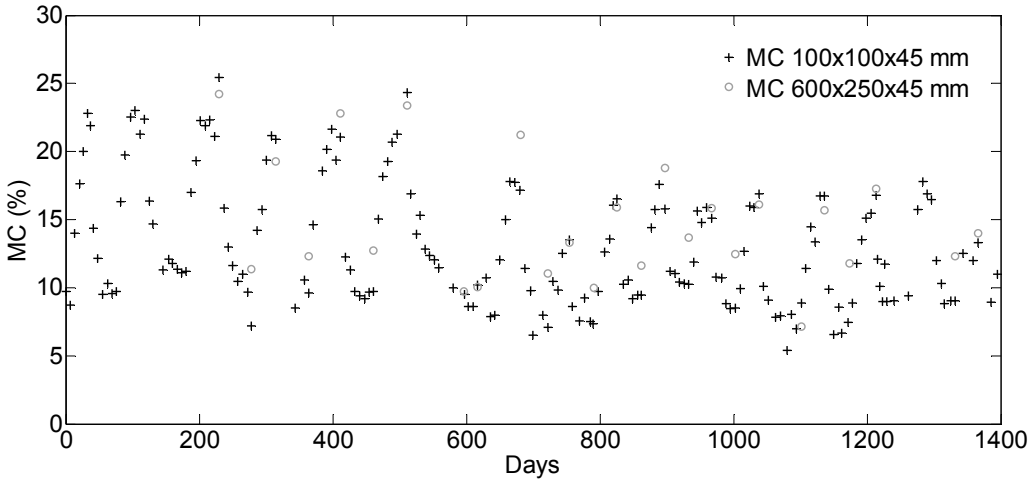

Figure 52 Moisture content of LVL samples versus time

4.4 Long-term deflection of TCC beams - Discussion

The mid-span deflection was measured every minute during loading of the specimen for the initial 24 hours and every hour for the remaining of the long-term test. This section discusses the results of the long-term investigation for the last three years.

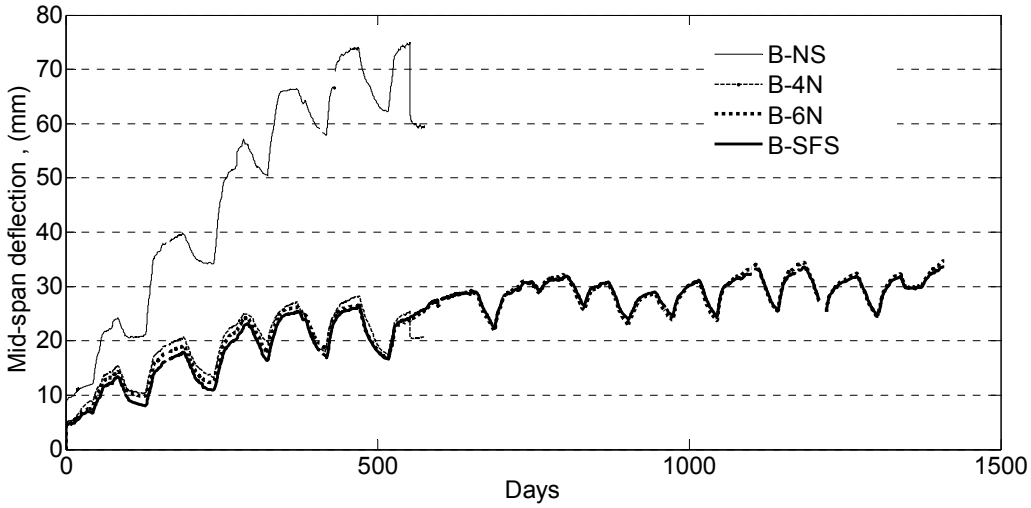

Figure 53: Mid-span deflection versus time

The specimens were loaded when the humidity chamber was at normal room conditions which will be referred as dry state here onwards. Despite the instantaneous elastic deflection due to the applied loads, very little additional deflection due to creep occurred. After approximately one week, water vapour was admitted and the deflection increased in all the beams (Figure 53). This period referred to as wet period is the first absorption period in the test and the beams responded with increase in their deflections. In this wet period the air humidifier was used to increase and maintain the air humidity approximately at 100 %. This was then followed by dry period. The humidity chamber was opened and an air fan was used to increase the ventilation. During this period (desorption), the deflection in all the beams increased sharply with the deflection reaching more than twice their instantaneous defections. When the humidity chamber was kept at this state, the rate of defection increase slowed down tending to reach some limiting values.

The beams were then again exposed to the wet period by admitting water vapour to the chamber, which resulted in recovery of the defection in the beams and the recovery continues as the air humidity was maintained at high RH levels. This procedure was repeated every four to six week except in some instances the duration has been longer due to instrument malfunction and other reasons. The length of the humidity cycle is four to six weeks and is monitored using the moisture content measurements on the moisture content samples.

After approximately six cycles, beam B-NS deflected beyond span/200 and its deflection was five times the deflection attained by the other three beams. The three beams (B-4N, B-6N and B-SFS) behaved relatively in a similar manner with largest deflection being measured for B-4N and least for B-SFS; this followed their respective stiffness's. In addition to its lowest stiffness, B-NS has poor composite behaviour with significant slip and the deflection; this deflection cannot be attained during short term test unless the beam fails. A close visual examination of the beam also shows that there was a visible gap at the interface between the concrete and LVL. Similarly there was a visible gap between the concrete and the LVL at the face of the triangular notches in the beam B-4N. After 550 days, the two beams B-NS and B-4N were unloaded, for determining their residual stiffness and strength and were moved out of the humidity chamber. The discussions from here onwards will focus on the results of the two beams remaining in the humidity chamber (B-6N and B-SFS).

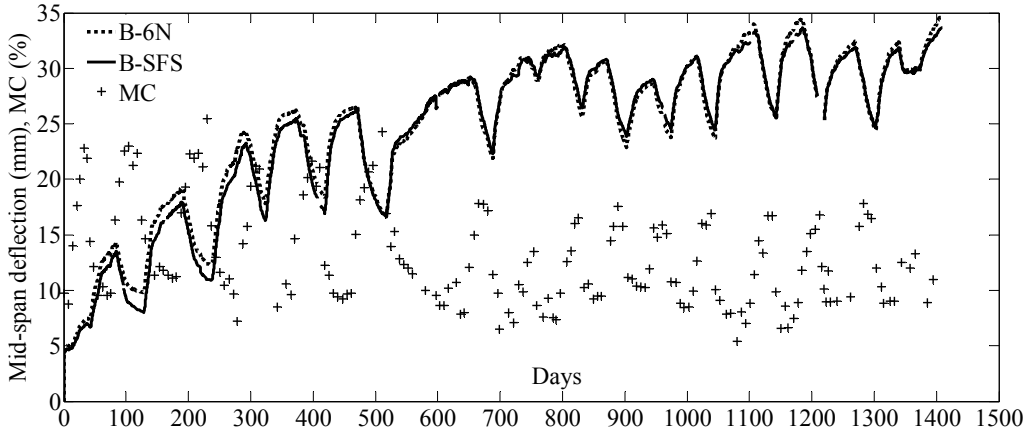

Figure 54: Mid-span deflection and MC versus time for B-6N and B-SFS beams.

The results of the long-term investigation indicates that the long-term deflection of the TCC beams is accelerated due to the variation in air humidity in the humidity chamber and most of the change in deflection occurs within the period when moisture content cycle changes, and is more pronounced during a period when the moisture cycle changes from wet period to dry period (Figure 54). The moisture content of the beams under load, cycled from dry to wet and back to dry again; the deformation also followed a cyclic pattern i.e. the beam deflections fluctuated in response to the cyclic air humidity of the chamber. However, the recovery in each cycle is only partial and the total amount of creep is very large as shown in Figure 55 (similar graph is presented in large scale in Appendix D Figure 93). It should be noted that creep increased during drying and decreased during the wetting cycle with the exception of the initial wetting when creep increased.

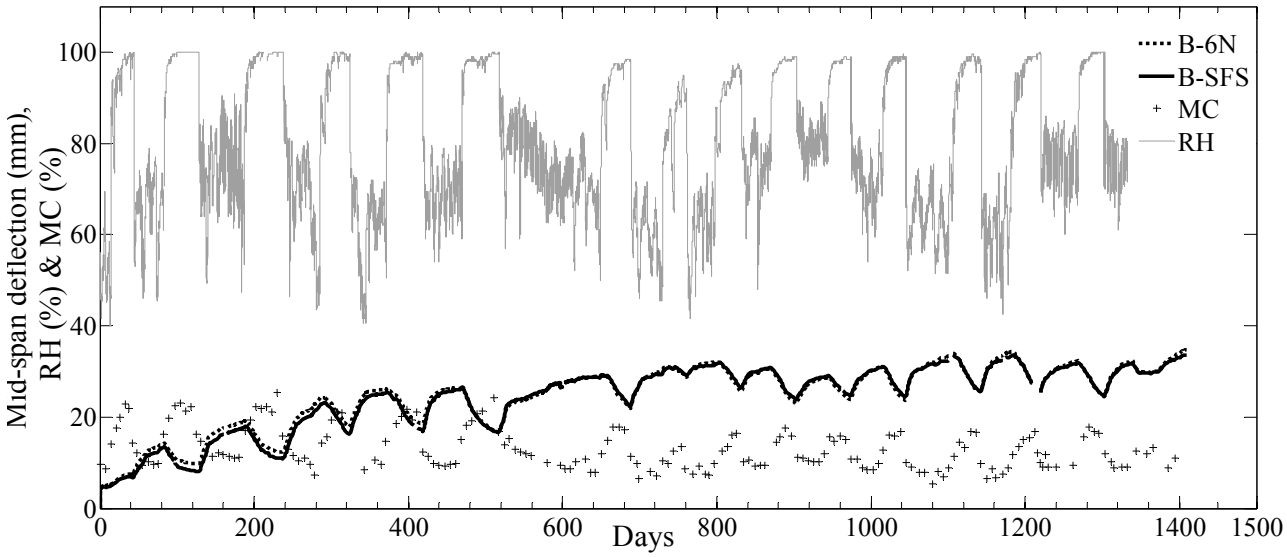

Figure 55 A comprehensive plot RH % and MC % and, mid-span deflection with time.

Three distinct behaviours were observed in the long-term test of these beams;

- increase in RH & MC followed by an increase in deflection in the first one week (first adsorption)

- decrease in RH and MC followed by an increase in deflection in all dry periods (desorption)
- increase in RH and MC followed by decrease in deflection (local recovery) in all wet periods (adsorptions)

The significant MC variation may have contributed to the high creep and deflection. The findings from this test show that it is not just the level of the moisture content that affects creep deflections. The rate of change , number and length of the cycles have a pronounced effect on the deflections, with rapid changes in moisture content (air humidity) producing more sever creep under bending loads also reported in Yeoh et al, (2012). The rapid response to the change in MC is pronounced when the humid cycle changes from wet to dry, during this transition the moisture leaves the surfaces at faster rate than from the middle cross section of the LVL, causing a faster reaction from the beams. Moreover, in dry period the defection was increased faster initially and then followed by a very slow rate when the environment is maintained in the dry conditions and showing tendency to flatten at some point. However, this is not the case when the humidity changes from dry to wet.

In this experimental investigation which is characterized by moisture cycling; except the first cycle in all other subsequent cycles, increase in air humidity causes an increase in timber moisture content, which causes recovery of deflection while in the contrary a decrease in air humidity causes loss of moisture from the timber, which causes a rapid increase in the deflection of the TCC beams. However, in some literatures on the long-term tests of TCC beams, which were conducted in naturally varying environmental condition in bending, an increase in the ambient relative humidity of the air causes an increase in timber moisture content, which is followed by an increase in deflection (Capretti & Cecotti, 1996, Kenel & Meierhofer 1998, Lukaswezkas, 2009 and Yeoh 2009). Although there are hardly any available literatures on the long-term experimental investigations on TCC beams subjected to cyclic humidity conditions in bending, this behaviour has been reported as typical creep behaviour of wood in bending (Armstrong and Kingston 1960, Gibson 1965, Hearmon and Paton 1964, and Toratti 1993). The oscillation of the creep curves (the alternate increase of deflection and recovery of deflection) as reported in Toratti (1992) and Toratti (1993) is due to the differential shrinkage and swelling of the LVL joist.

The stiffness of the TCC beams is much more dependent on the composite action between the concrete and the LVL joists, and the long-term deflection of these beams was significantly influenced by the variation of the MC, concrete creep and the various interactions of shrinkage and creep, shrinkage and swelling of the LVL, and creep of the connection system (Cecotti et al. 2006, Fragiocomo 2007, Lukaswezka 2009, Yeoh et al. 2012).

Both the beams (B-6N and B-SFS) have attained most of the deflection with in one and half years, as was also found out by several researches that most of the deflection developed during the first one and half to two years, after which the deflection tends to either plateau or to increase much more slowly (Cecotti et al. 2006, Yeoh et al. 2012). However, the deflection from these beams is showing a distinct increase throughout the period, with minimal reduction in the rate of deflection increase to the end of this reporting period. Similar finding was also reported in Kenel et al. (1998).

A change in temperature is also found to significantly affect the long-term deflection of the TCC beams (Lukaswezka 2009, Yeoh et al. 2012). However, in this investigation, the temperature of the humidity chamber remained quasi-constant (20±2 °C) as shown in Figure 56, with little or no variation in temperature throughout the test period and negligible influence on the creep deflections.

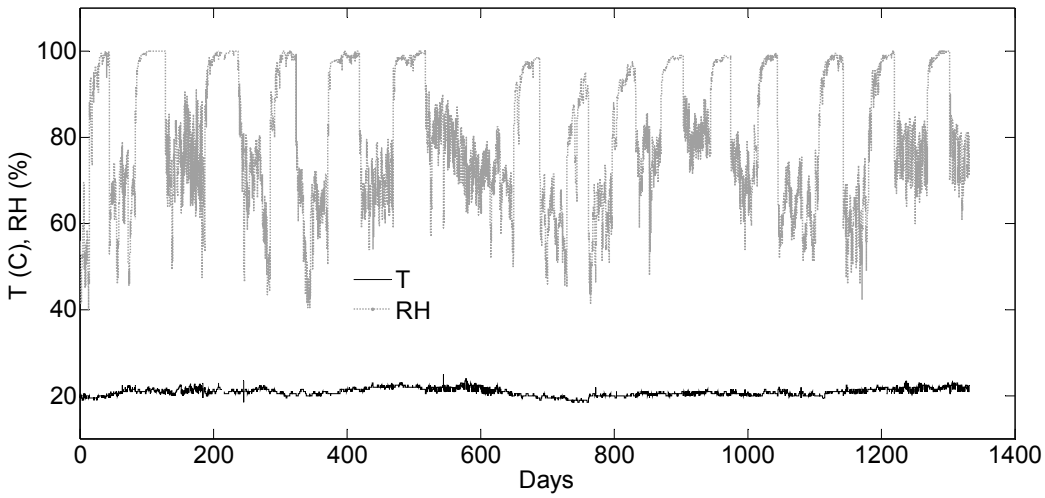

Figure 56: The temperature and relative humidity curve during the long-term test.

4.5 Unloading of two TCC beams from long-term loads

To determine the loss in stiffness and residual strength, two TCC beams (B-NS and B-4N) were unloaded from their long-term loads after 550 days of the test and when these two beams had reached 9.0 and 6.0 times of their elastic deflections, respectively. The measured immediate elastic recovery after load removal (Figure 57), were 13.4 mm and 4.6 mm for beams B-NS and B-4N, respectively. The elastic recovery was approximately 62 % higher for B-NS and 1.2 % lower for B-4N, than the initial elastic deflection when the beams were loaded. After the load was removed, the deflection fell sharply and then declined much more slowly during the following days. Gibson (1965) and Mohager (1987), have found out that the magnitude of the recovery of timber structures after the loads are removed is usually equal to or greater than the magnitude of the initial deflection when the loads are applied, the results obtained from this investigation are found to support the findings. More recovery could have been achieved if the beams were passed through a series of humidity cycles. The beams were then moved for short-term test and were placed in the test location to be conditioned in the laboratory.

.

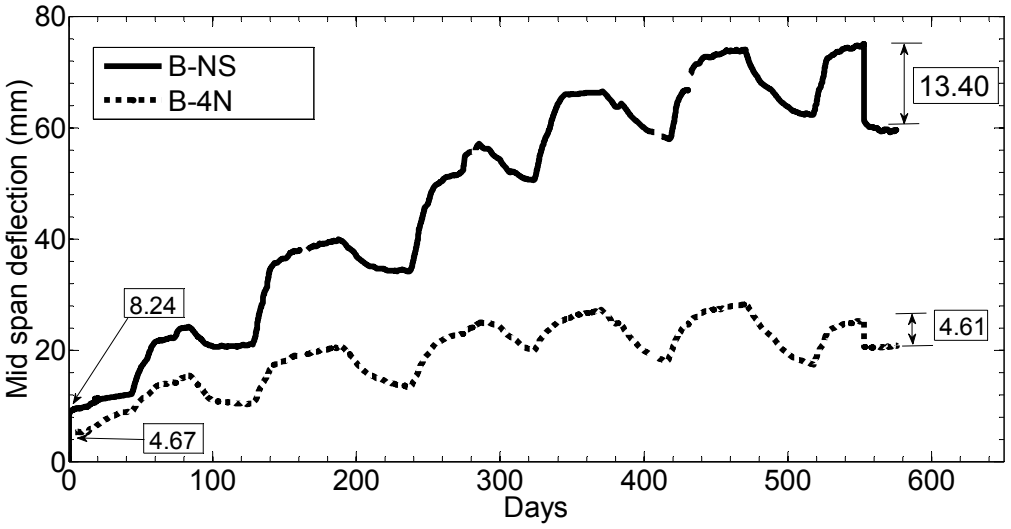

Figure 57: TCC beams unloaded after two years of long-term test

Table 8 Instantaneous elastic deflection and recovery after load removal

Specimen	Elastic deflection (mm)	Elastic recovery (mm)
B-NS	8.2	13.4
B-4N	4.8	4.6

4.6 Concluding remarks

The long-term test conducted on the four beams was reported in this chapter. All the four beams exhibited similar behaviour under a sustained load in sheltered indoor conditions and subjected to cyclic humidity condition. The moisture content of the loaded beams cycled from dry to wet and back to dry condition again. Deformation of the beams also followed a cyclic pattern. The deflection from these beams showed a distinct increase throughout the period, with minimal reduction in their rate of deflection increase to the end of this reporting period. The most important quantities such as mid-span deflection, moisture content, relative humidity and temperature of the environment were continuously monitored through-out the test.

The conclusions made from the test observations are (i) the relative humidity monitored during the long-term test varied from 45 % to 100 % while the timber moisture content fluctuated in the range of 7 % to 20 % and temperate remained quasi constant (21 °C±1), (ii) cycling the humidity accelerated the creep response of the beams and induced very high deflection more than seven times their initial deflection, (iii) the mid-span deflection markedly augmented with in two years of the long-term test, with a final value well above the limits usually adopted by national regulations.

5 Creep factor and evaluating the long-term deflection according to Eurocode 5

The experimental results were fitted with a logarithmic equation and extended to the end of service life of the TCC beams and also a simplified evaluation for the long-term deflection using Eurocode 5 is used to predict the final deflection. This chapter also discusses the relative deflection of the TCC beams.

5.1 Relative deflection of the TCC beams

Creep can be quantified by a number of time-dependent parameters, of which one is the relative creep (creep coefficient). In composite beams, this total creep factor (preferably called as gross creep factor) is regarded as a system property that depends on the interactions between the materials, which is also affected by the thermal, moisture strain and drying shrinkage of concrete as explained in Yeoh (2010). According to Eurocode 5, the instantaneous elastic deflection under an action load should be calculated on the basis of mean values of the appropriate modulus of elasticity. Creep is calculated considering the combined effect of moisture content (service class) and load duration, and it is quantified for different materials by the factor, k_{def}, which considers neither the size nor the quality (strength class) of the timber. The creep part of deflection is equal to the instantaneous deflection multiplied by the creep factor (Morlier and Palka 1994). The creep factor in case of TCC beams, which is the overall creep factor of the composite can be defined as; Relative creep = Total deflection / Elastic deflection. The highest relative creep values (Figure 58) recorded for the TCC beams under investigation for the last three years are given in

Table 9. The relative creep values shown are also denoted as "j_2" in AS1720.1: 2010.

Table 9 Relative creep values after three years

Specimen	Instantaneous deflection (mm)	Total deflection (mm)	Relative creep
B-6N	4.4	34	7.7
B-SFS	4.2	33	7.9

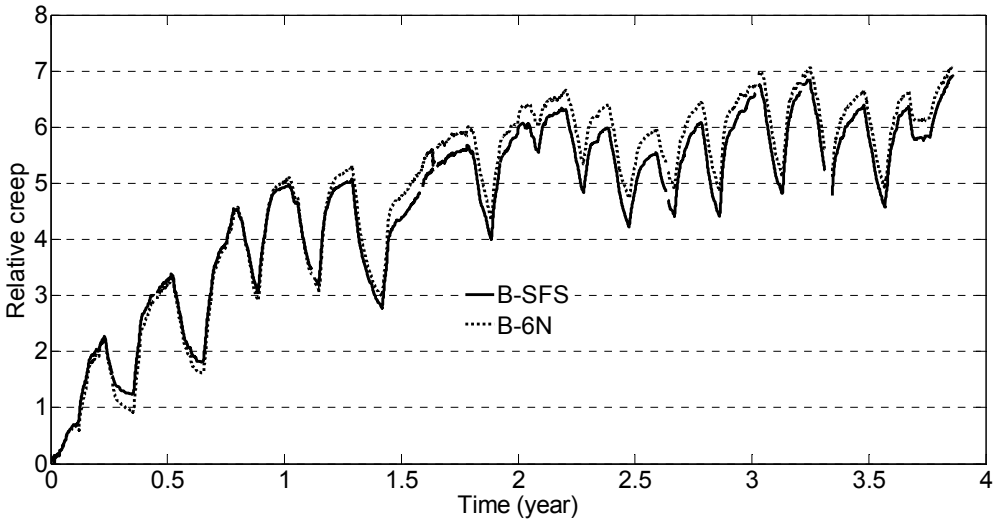

Figure 58: The relative creep of the TCC beams.

5.2 Analytical fitted curve

The experimental results have also been tried to fit using a logarithmic function equation in order to predict the long-term deflection at the end of service life as indicated by the Equation 11. The time value, t is in years and the total mid-span deflection, Δ is in mm. whilst the equation gives a general trend of the progress of the deflection through time, it does not accurately represent the real adjustment as the deflection is influenced by the sinusoidal-like moisture variation. Therefore, the final deflection from the equation must be corrected to include the magnitude of the amplitude of the oscillation. Additionally, the current data does not show a clearly defined tendency to stabilize.

Equation 11

$$\Delta = 6.5\ Ln(t+0.07)+ 21$$

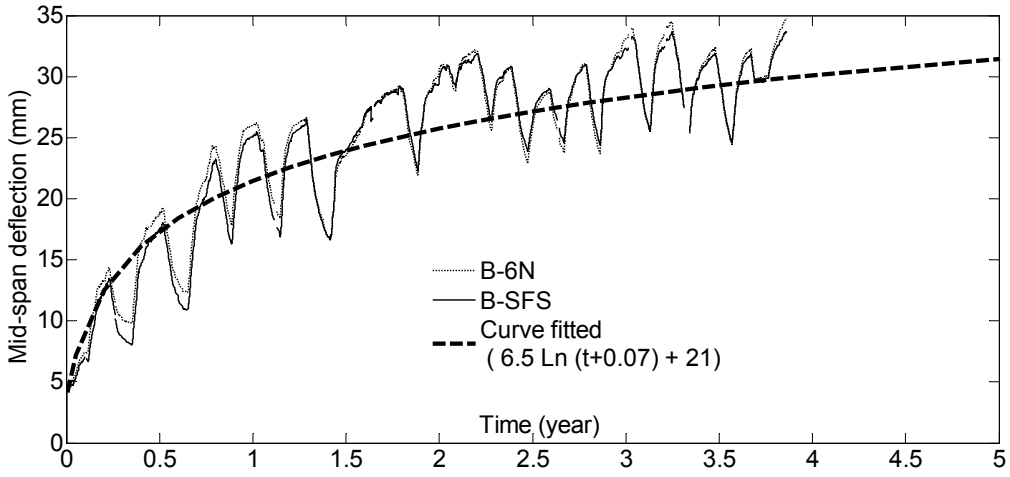

Figure 59: Mid-span deflection and analytical fitted curve using logarithmic function equation based on up to-date experimental results

Based on the above equation the predicted deflection is plotted against the experimental results (Figure 59). The predicted results fall (oscillate) in between the upper and lower range of the experimental results. Hence, the results obtained from

the equation will be adjusted by an equivalent amount to the amplitude of the oscillation, which is approximately ± (4-5) mm. The predicted mid-span deflection for 50 years after corrected for the fluctuations, may reach approximately 51.4 mm (Figure 60). These predictions are too approximate and overestimate the deflection, because the equation is highly governed by the general trend of the curve which is increasing. However, a close look into the results show that the rate of deflection increase is diminishing with time, with more tendency to plateau as observed in the results from 1000th to 1400th days. Hence, in order to avoid over estimating the long-term deflection, the beams need to be monitored for more years and the next couple of years will likely produce results that best define the nature of the curve for better prediction.

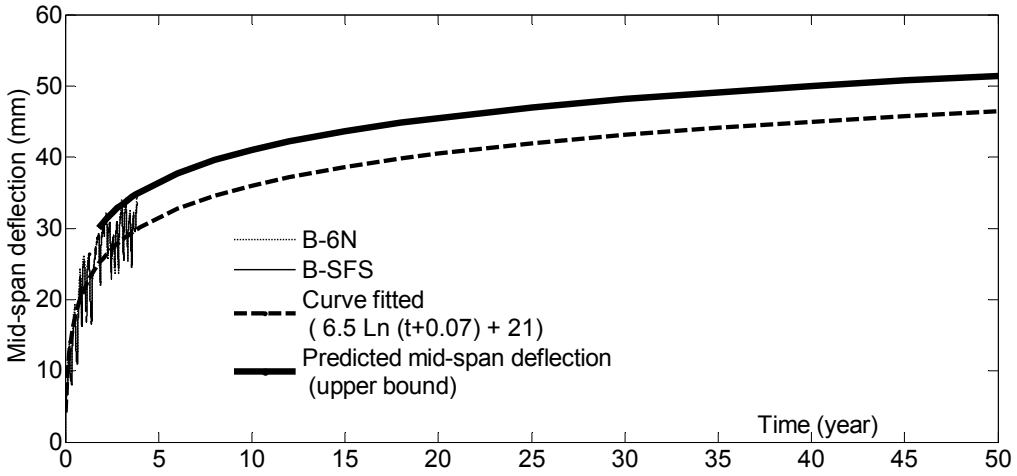

Figure 60: Mid-span deflection and analytical predicted deflection for 50 years using logarithmic function equation based on up to-date experimental results

5.3 Simplified evaluation of the long-term behaviour of TCCs in accordance to Eurocode 5 using gamma method

Eurocode 5 is the most commonly used method for design of timber-concrete composite elements and for estimating the long-term performance of the TCC beams. The simplified approach recommended by Ceccotti (1995) according to Eurocode 5 provisions has been employed here. The method has been discussed in detail in section 2.6 of this report. In this section, the long-term deflection of the two TCC beams (B-6N, B-SFS) will be evaluated. The simplified approach (commonly called gamma method) does not account for shrinkage or thermal strain ((Lukaszewska, 2009) and is based on the effective modulus method, in which the creep and mechano-sorptive behaviour of the concrete, timber and connection are accounted for by reducing the elastic and slip moduli according to Equation 12:

$$E_{c,fin} = \frac{E_{cm}(t_o)}{(1+\varphi(t,t_o))}, \quad E_{t,fin} = \frac{E_{o,mean}}{(1+k_{def})}, \quad K_{fin} = \frac{K}{(1+2k_{def})} \qquad \textit{Equation 12 (a,b,c)}$$

Using this method the long-term deflection of the TCC structures for time t = 0 and t = ∞, can be evaluated. The material creep coefficient and the reduced elastic bending stiffness's for all the beams are presented in Appendix E. The creep coefficient of LVL (K_{def}), depends on the service class which in turn depends on the climate in the humidity chamber, is given in table 3.2 of Eurocode 5 (2008), for this investigation k_{def} = 2.0 is used for LVL considering the environment where the beams are exposed equivalent to service class 3. For the connection systems, the creep coefficient recommended is twice as large as the creep coefficient of the LVL (Kavaliauskas et al. 2005); this assumption is used in the evaluation because there is no experimental investigation on the creep coefficients of the connections used. The creep and shrinkage coefficient of concrete are calculated from the procedures suggested in AS3600: 2009, which considers the environment conditions and the age of the

concrete at time of loading. The result of this computation gives a creep factor for the concrete in the dry period twice as much as in the wet period. The values of the creep coefficient in the dry period are found to influence more significantly as compared to the wet conditions. However, the environmental condition in the humidity chamber is moderate conditions and an interior environment could be a fair representation to compute the creep and shrinkage coefficients of the concrete. The creep and shrinkage coefficients and the reduced moduli are given in Appendix for all the beams. Based on these coefficients the effective bending stiffness of the TCC beams at time of loading (t=0) and at the end of life (t =∞) is given in Table 10 and a detailed computations are presented in Appendix D.

Table 10 Theoretical bending stiffness's using Euro code 5

Specimen		S_{eff} (mm)	γ_c	EI_{eff} (Nmm^2)
B-6N	t = 0	825	0.109	3.38E+12
	t = 50	825	0.063	0.99E+12
B-SFS	t = 0	375	0.29	4.11E+12
	t = 50	375	0.181	1.28E+12

The final deflections using the EI values for initial and end of life period are given for the two beams (B-6N and B-SFS) using gamma method in Table 11. These two beams are still under long-term test.

Table 11 Comparison between the predicted theoretical Mid-span deflections according Eurocode 5 with the deflections from the experimental result

Specimen	Instantaneous deflection (mm)	End of life deflection (mm)	Experimental deflection (mm)
B-6N	4.6	33.5	34.0
B-SFS	3.8	25.9	33.0

The deflection after 50 years was found to be 33.5 mm and 25.9 mm for beams B-6N and B-SFS, respectively, approximately seven times, the instantaneous deflection of the beams. Eurocode 5 suggests limit values of L/250 to L/200 for long-term deflection of beams on two supports, L being the span length. The deflections at the end of the service life were L/170 and L/220, for beam B-6N and B-SFS, respectively; indicating beam B-6N exceeded the acceptable upper limit. The long-term deflection predicted to be less than the deflection attained by the B-SFS beam in three years i.e. the gamma method underestimated the long-term deflection of the B-SFS by about 21 %.

5.4 Concluding remarks

The long-term deflection observed to-date as a multiple of the initial short- term; deflections were presented in this chapter. The relative deflection of the beams reached about 7.7 time their initial deflections. The experimental result was also fitted with a logarithmic equation and extended to the end of service life. The result from the logarithmic curve overestimated the final long-term deflection of the TCC beams, while the Eurocode 5 simplified evaluation methods for TCC beams underestimated the final deflections, however, this is a results of a single beam and with extreme environmental conditions. For a better prediction, the TCC beams will be monitored for more years until their rate of deflection stabilises.

6 Residual stiffness and strength tests after long-term test

This chapter reports the result of a short term experimental investigation on two TCC beams following the long term test. The two beams were unloaded after 550 days of creep loading (section 4.5) these beams were B-NS and B-4N and were tested for serviceability and ultimate failure. The beams were conditioned in the laboratory for three months before being tested.

The tests were performed under displacement control, and the load was applied at a constant rate until failure, according to the loading protocol recommended by AS/NZS 4063.1 (2010) and EN 26891 with a preloading cycle up to a 40 % of the estimated load, unloading to 10 % of the estimated failure load, and ramp loading to failure. The test set up is shown in Figure 61.

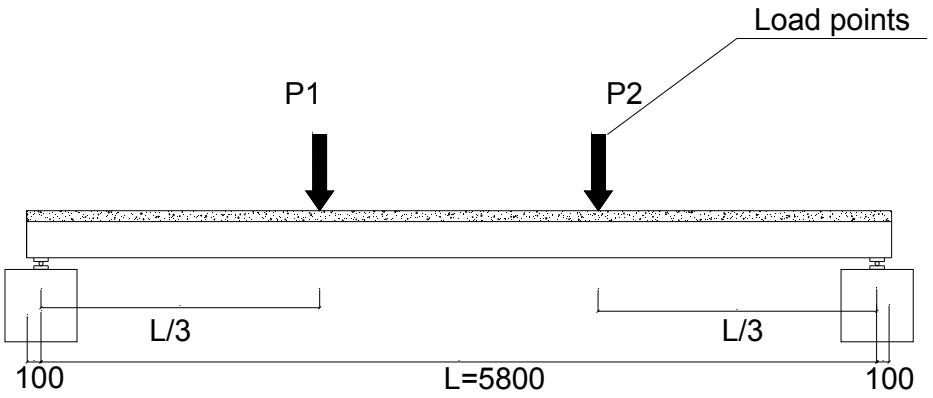

Figure 61: Test set up for serviceability and ultimate failure test of the TCC beams (typical) (in mm)

During this test the following measurements were taken;

- mid-span deflection, deflection at third point beneath the two load points using LVDT's,
- relative slip between concrete flange and timber web over the supports using LVDT's and

- the strains on timber at mid-span at the bottom, at 20 mm from bottom fibre, at the middle and 230 mm from bottom fibre; and mid-span concrete strains at the upper and lower fibres using strain gauges (Figure 62).

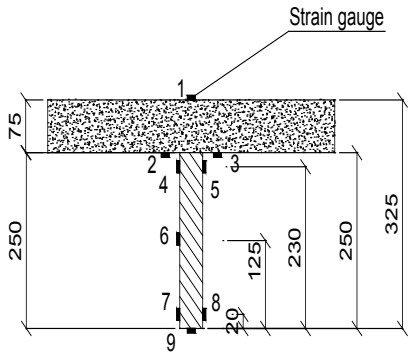

Figure 62: Location of strain gauges along the mid span of the cross section

6.1 Serviceability tests and loss in stiffness of TCC beams

The four-point bending test conducted on two TCC beams before and after an extended exposure to an environmental conditions equivalent to Service Class 3, as per Eurocode 5, provided valuable information to understand the behavioural response of TCC in serviceability. As a consequence of the long-term testing and their exposure to extreme environmental conditions, both beams experienced reduction in their bending stiffness's (Figure 63 and Figure 64). Stiffness of the non-notched beam (B-NS) reduced by 53 % and 20 % reduction in stiffness of the four notched beam (B-4N) was observed (Table 12). B-4N has initially higher stiffness and high composite efficiency as compared to B-NS and also showed lower amount of loss as compared to B-NS. The loss of bending stiffness has a contribution from all component parts (concrete, timber and the connection), and to investigate the possible loss due to the long-term test, tests were conducted on the LVL which were cut from the tested TCC beams to determine their properties after long-term test and will be discussed later in this chapter.

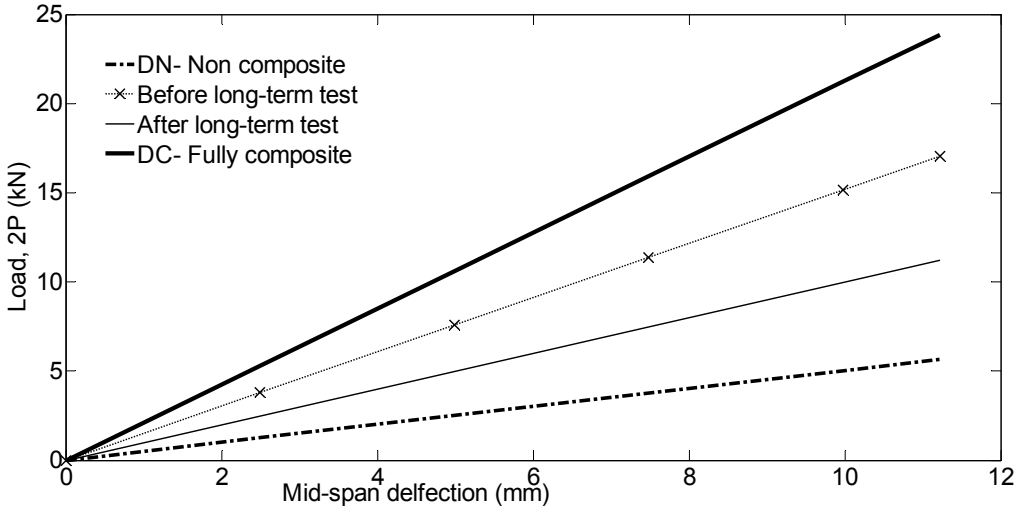

Figure 63: Total load (2P) versus mid-span deflection at serviceability for B_NS

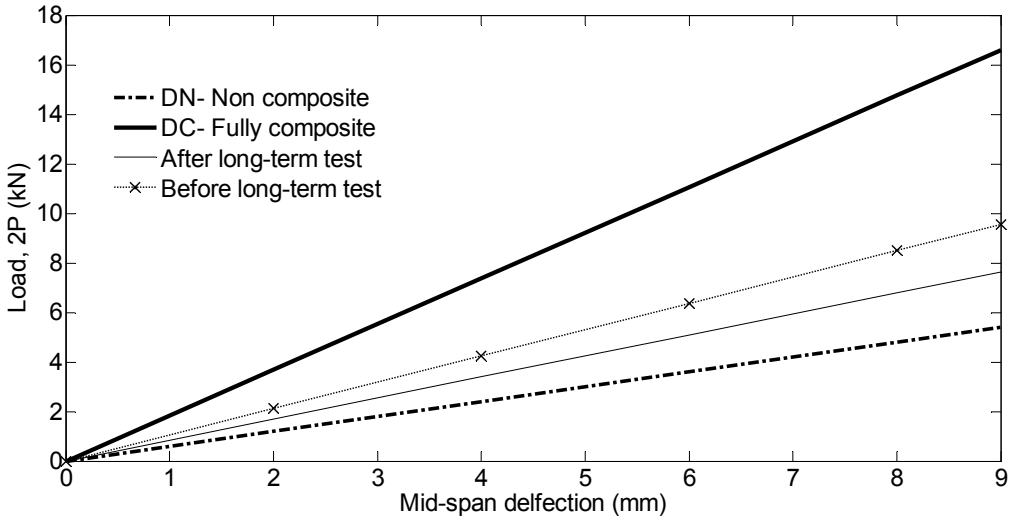

Figure 64: Total load (2P) versus mid-span deflection at serviceability for B_4N

Table 12 Percentage loss in bending stiffness in TCC beams

	EI (E+12 Nmm^2)		Loss (%)
	Before LT	After LT	
B-NS	2.78	1.31	52.9
B-4N	4.08	3.26	20.0

Note: LT = long-term test

The magnitude of the strain reading along the cross section of the TCC beams for both the serviceability tests conducted before and after the long term test (Figure 65 and Figure 66) are compared up to certain target loads and a detailed results are presented in tables and diagrams in Appendix F , The figures show increased strain magnitude for tests after long term exposure. This increase is large for timber in its tensile zone and at the interface, while little change is on the tensile and compressive zones of the concrete. As shown in Figure 65, for B-NS, there is significant increase in magnitude in both the timber tensile zone and also in the interface, and there is a shift in the neutral axis towards its geometric centre as if the LVL was independently acting. This shows a loss in the composite action on B-NS. Although similar increase in magnitude on the timber tensile zones is observed for B-4N but little increase in the interface indicating this beam performed better.

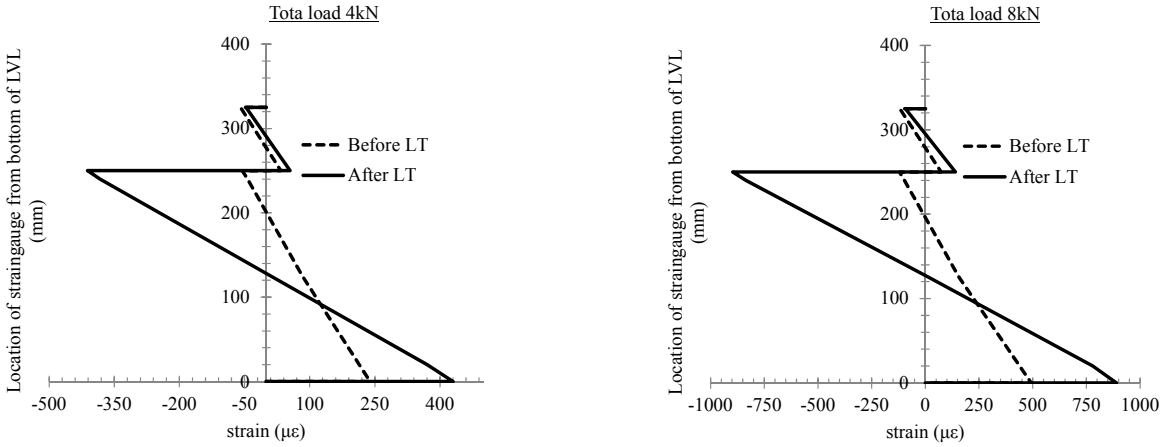

Figure 65: Strain profiles along the mid-span cross section from serviceability tests for B-NS (tests done before and after the long-term test, LT= long-term test)

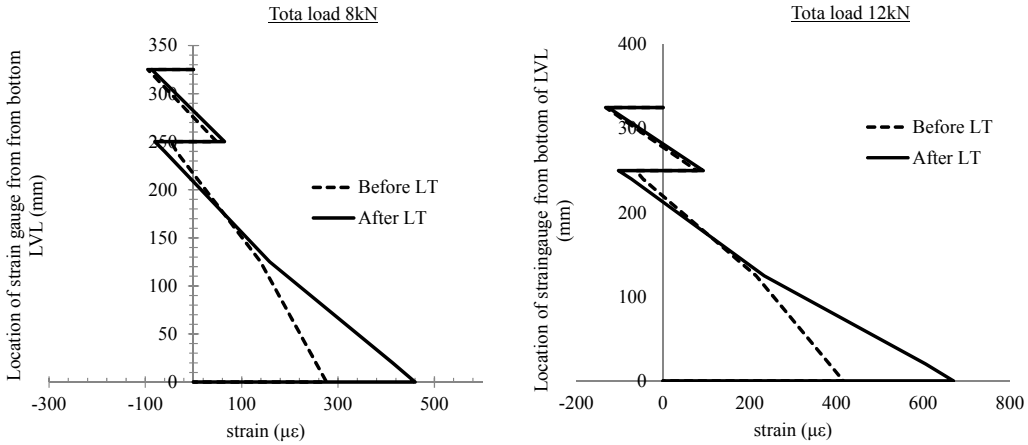

Figure 66: Strain profiles along the mid-span cross section from serviceability tests for B-4N (tests done before and after the long-term test, LT= long-term test)

6.2 Ultimate strength tests

After the serviceability test the beams were finally loaded to failure. During the test, the following observations were made; the presence of any cracks on the connections, the time and level of the load the first crack was detected, and the nature and failure patterns. The failure loads corresponding to the resultant of the point load (2P) and the maximum mid-span deflections at failure are reported in Table 13, and the relationship between the total load and the mid-span deflection for beams B-NS and B-4N are also shown in Figure 67 and Figure 68, respectively.

Table 13 Summary of ultimate tests results for the TCC beams

Specimen	Failure load (2P) (kN)	Mid-span deflection (mm)
B-NS	22.8	98.4
B-4N	34.6	48.0

Both the beams showed linear behaviour approximately up to 20 mm of their mid span deflections and after wards behaved in non-linear manner up to failure (Figure 67 and Figure 68). Both the composite beams failed due to tensile rupture of the timber initiated in the weaker region of the lamination and progressed further to the mid depth (Figure 69 and Figure 70). The strength and stiffness of the timber beam are the most important parameters that influence the behaviour of the composite beam (Linden 1999) after the shear connector. Both the timber-concrete composite beams in this experiment fail, because the timber tensile strength is reached at the outermost tensile fibre. The timber modulus of elasticity determines to a large extent what tensile stresses will appear in the timber tensile zone and consequently, determines the load carrying capacity of a timber-concrete composite beam.

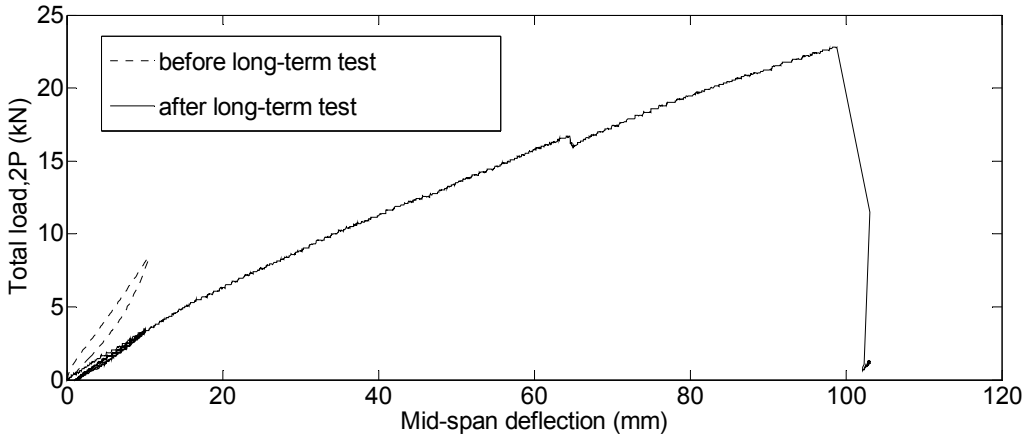

Figure 67: Total load (2P) versus mid-span deflection at ultimate stress for B_NS

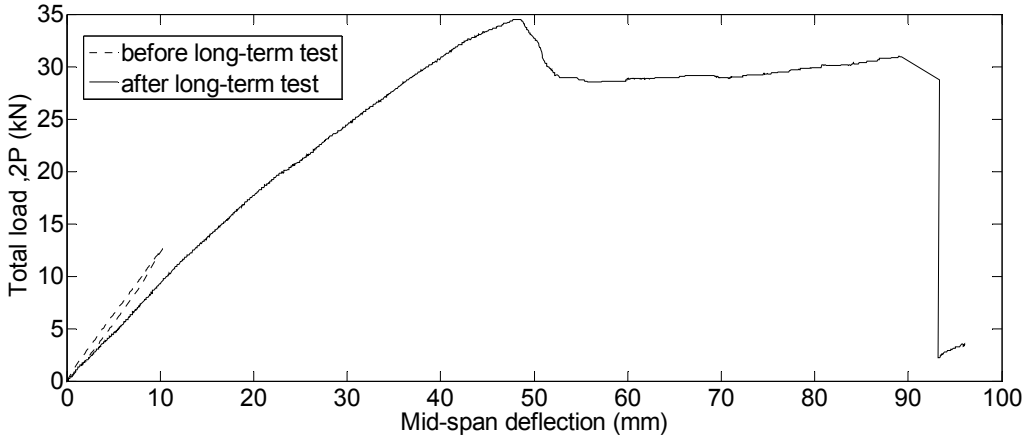

Figure 68: Total load (2P) versus mid-span deflection at ultimate stress for B_4N

Although in both the beams the timber joists exhibited brittle failure in the tensile zone, B_4N showed a good plastic behaviour before total collapse occurred. This behaviour was caused by the connector (notch with coach screw) that had an elasto-plastic load–slip relationship. Usually in TCC structures, the furthest connectors reach its maximum shear strength and then, redistribution takes place to the adjacent connectors until they also become plastic. Once the shear connectors lose their stiffness's, the timber bears the entire load up to failure.

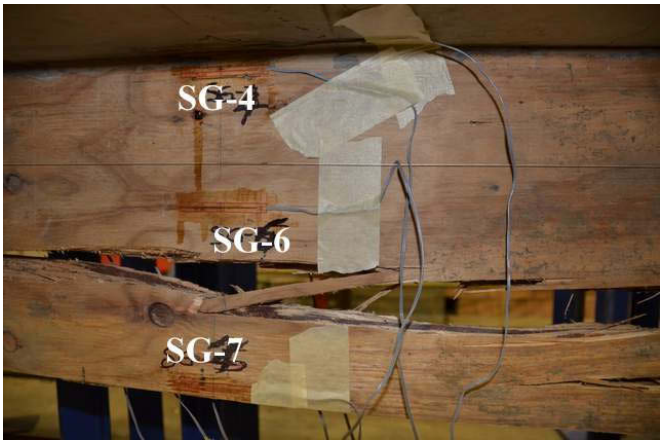

Figure 69: Tension failure of the joist B_NS

Figure 70: Tension failure of the joist B_4N

Figure 71 and Figure 72 show load slip curve for B_NS and B_4N, respectively. The shear connector in B_NS behaved in a brittle manner while a ductile behaviour is observed for B-4N shear connector. The maximum slip measured at failure was 6.4 mm on the left and 12.2 mm on the right support for B-NS and 1.6 mm on left support and 1.4 mm on right support for B-4N. During testing beam B-4N, the LVDT on the left side of the support was in contact with the supporting frames and the slip readings showed erroneous data immediately after failure (Figure 72).

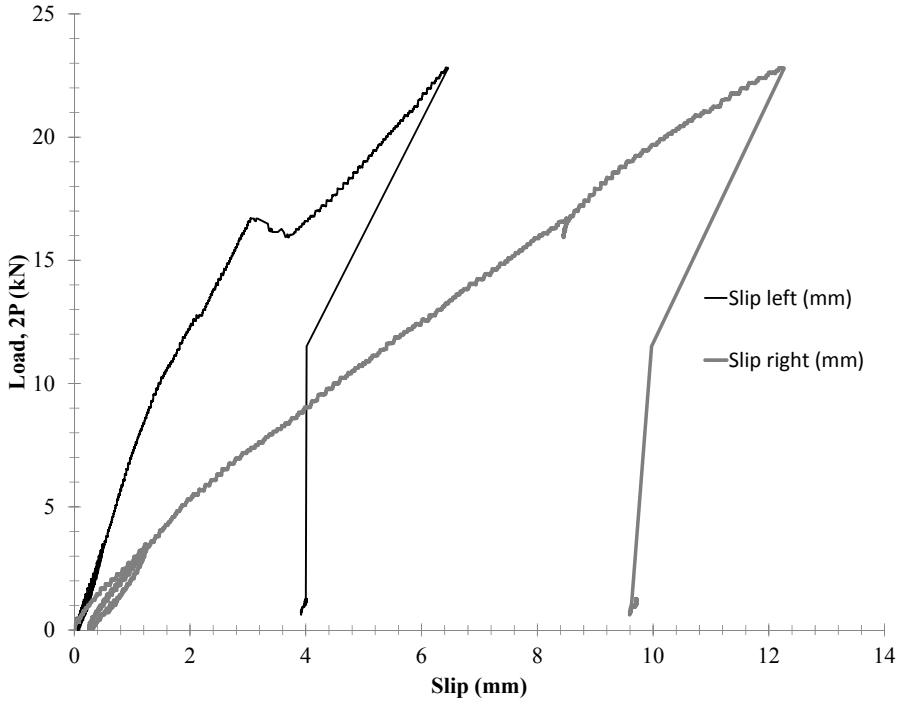

Figure 71: Total load (2P) versus slip B_NS

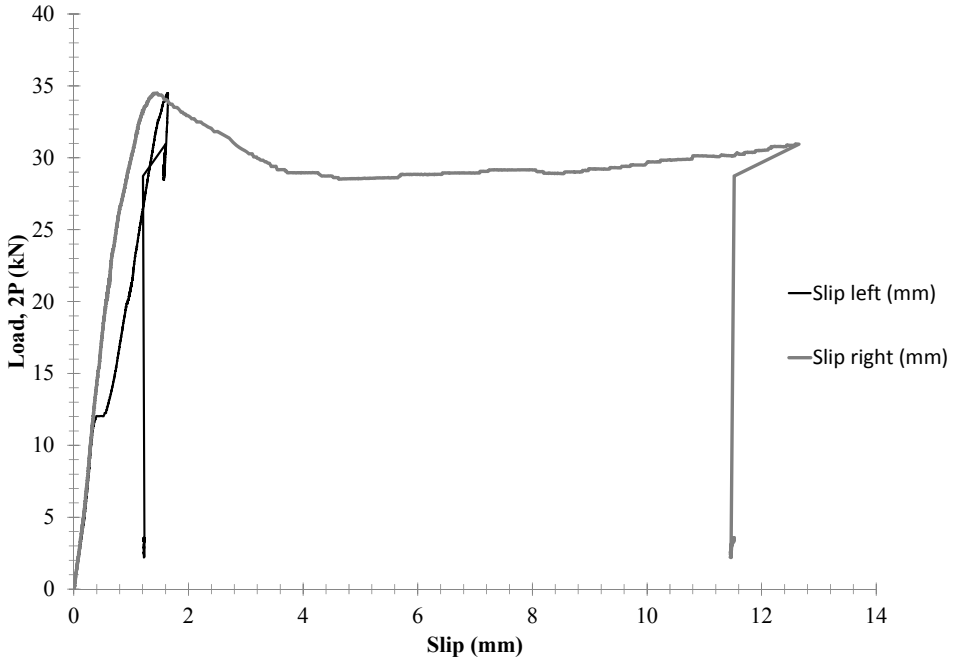

Figure 72: Total load (2P) versus slip B_4N

Figure 73 Connector close to the right support after the failure test (left) and before the failure test (right) for B-4N

Figure 74 Connector close to the right support after failure for B-NS

Investigations after the beams failed, in order to understand the failure patterns, revealed that the two connectors on right side of beam B-4N designated as N3 and N4 (Figure 73) failed due to crushing of the concrete in the notch and the slip reading on those connectors was also significantly large. The screws on the right support for beam B-NS were found broken when observed after the concrete was removed (Figure 74). The maximum slip values obtained for the composite beams indicate that the limit slip value in the joint recommended by EN 26891 for which the load ought to be determined if the maximum load has not already been reached (15 mm) is too high. The composite beams do not have sufficient plastic deformation capacity to deform to a slip of 15 mm (Figure 71 and Figure 72). These finding are consistent with that of Dias (2005) that the maximum slip of various tested beams with span length up to 10 m ranged from 0 to 8 mm. Dias also concluded that the slip is

unlikely to be higher than 8 mm in timber-concrete composite structures built and loaded according to the design rules.

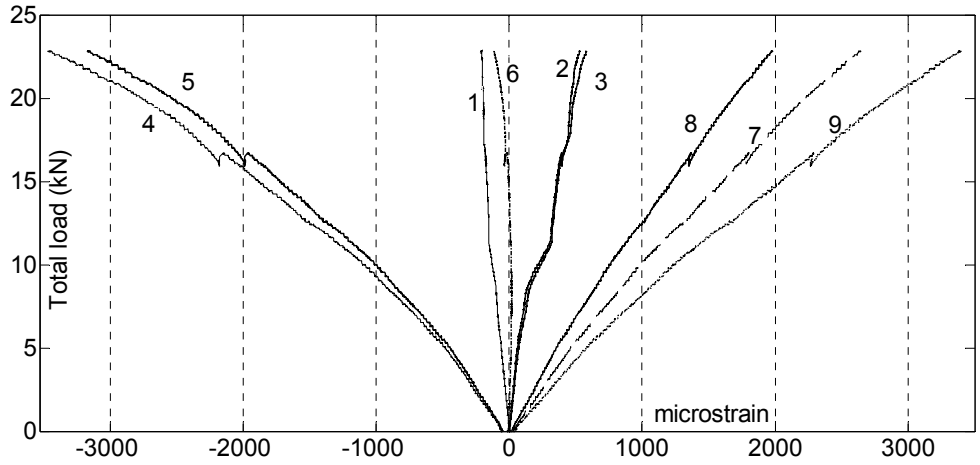

Figure 75: Magnitude of the strain along the mid span cross section during ultimate test on B_NS (the numbers from 1 to 9 refer to the strain gauge numbers given in Figure 62, (-ve) strain in compression and (+ve) strain in tension

)

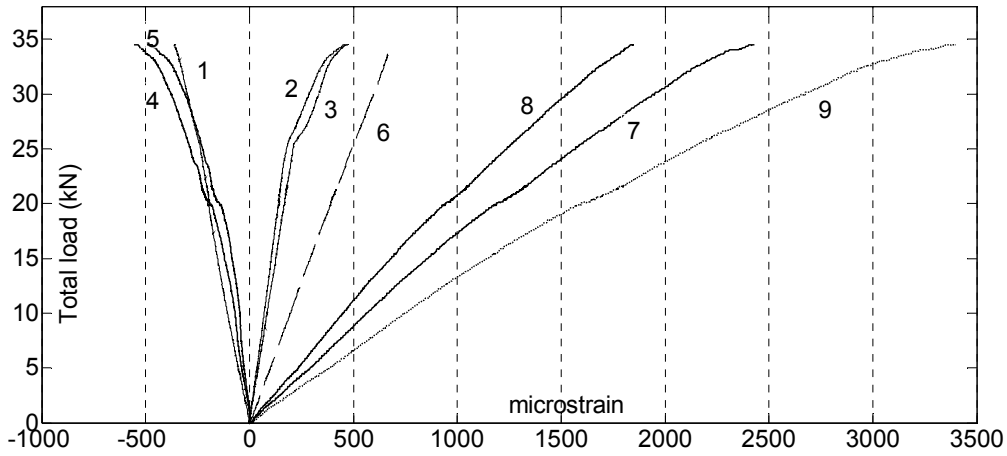

Figure 76: Magnitude of the strain along the mid span cross section during ultimate test on B_4N [the numbers from 1 to 9 refer to the strain gauge numbers given in Figure 62, (-ve) strain in compression and (+ve) strain in tension]

During the ultimate short term test, magnitudes of the strain were measured along cross-section of the beam at the mid-span. The location of the strain gauges is shown in Figure 62. The strain evolution across the mid span of the composite section throughout the loading regime is shown in (Figure 75 and Figure 76). The strain profiles are also displayed in Figure 77 for B-NS and in Figure 78 for B-4N. The strain profile for B-4N shows that for the initial elastic response of the composite system the neutral axis (NA) of the timber is positioned near the interface of the concrete and timber, and the majority of the timber beam is working in tension. However, as the load is increased, and the connection begins to yield, the axial force in the timber beam remains approximately constant, whilst the bending moment continues to increase. The neutral axis in the timber beam drops towards mid-depth and the stiffness of the composite section degrades. The strain profile for B-NS however shows, NA of the timber positioned from the beginning near its mid depth and maintained in this position through the test. This difference in the strain profiles in the two beams shows a lack of composite action in beam B-NS. Additionally the area of the concrete under tensile stresses is much larger in B-NS as compared to B-4N. However, no failure of concrete in tension was observed in both beams.

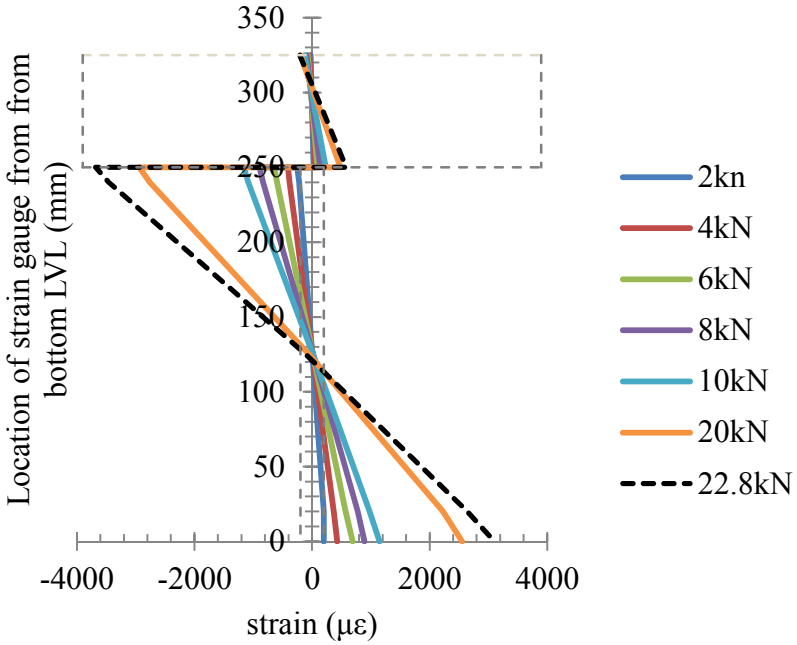

Figure 77: Strain profile along the mid span cross section of B-NS during ultimate test

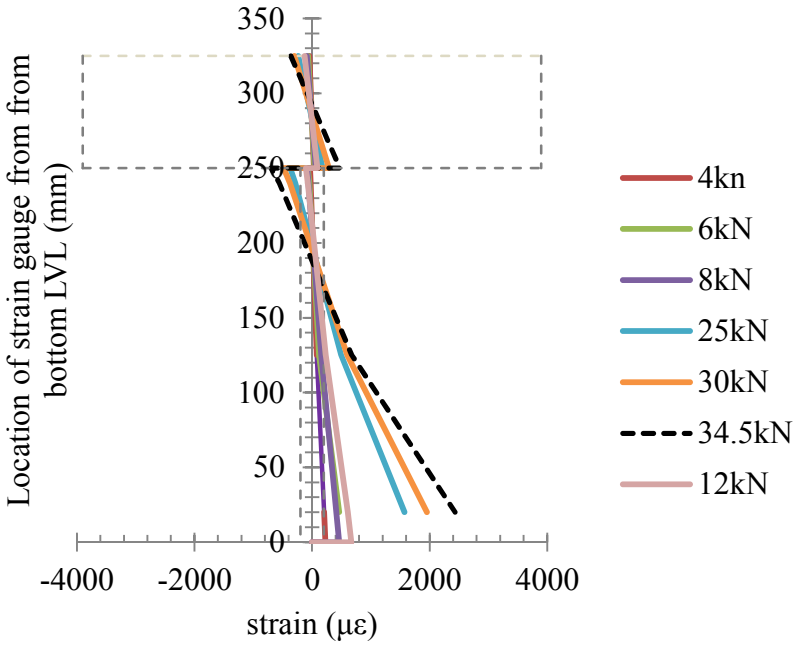

Figure 78: Strain profile along the mid span cross section of B-4N during ultimate test

The failure loads of the TCC beams were also estimated using gamma method according Eurocode 5 in order to try to compare with the experimental results. The

mean values of the mechanical properties (modulus of elasticity and strength) of the materials were used in the analysis. For LVL the modification factors for load duration, moisture content and size effects are used as recommended in AS/NZS 1720 (Appendix G) and secant slip modulus of $K_{ULS0.6}$ is used for the connections. In order to better estimate the loss in strength, the analysis was assumed in periods before the beams were subjected to long-term loads (i.e. after 200 days of the concrete pour).

For ultimate design verification of TCC beams, the bending strength of concrete and timber, flexural shear and bearing strength of timber and strength of the connection interfaces must be checked.

The normal stress on the concrete due to axial force is given by Equation 13 and due to bending moment is given in Equation 14.

$$\sigma_{c,} = \frac{\gamma_c E_c a_c M^*}{(\mathrm{EI})_{eff}.} \qquad \textit{Equation 13}$$

$$\sigma_{b,c,} = \frac{E_c h_c M^*}{2(\mathrm{EI})_{eff}.} \qquad \textit{Equation 14}$$

$$-\sigma_{c,} - \sigma_{b,c,} \le \frac{f'_{c,c,d}}{(\gamma_c)} \qquad \textit{Equation 15}$$

$$-\sigma_{c,} + \sigma_{b,c,} \le \frac{f'_{c,t,d}}{(\gamma_c)} \qquad \textit{Equation 16}$$

Hence, the stresses on the top and bottom fibre of the concrete should be obtained using Equation 15 and Equation 16 , respectively. Where M* is the design moment, $f'_{c,c,d}$ is the design compressive strength of concrete, $f'_{c,t,d}$ is the design tensile strength of concrete and γ_c is the partial safety factor for concrete = 1.5.

The tensile stresses in the concrete are not important and can be neglected, moreover nominal steel mesh is provided on the tension side of the concrete.

The timber or LVL strength demand should meet the following conditions; the axial force on timber (Equation 17*),* the timber bending moment (Equation 18*),* and also the the combined bending and tension ratio (Equation 19).

$$N^*_{t,} = \frac{\gamma_t E_t a_t M^*(A_t)}{(\mathrm{EI})_{eff.}}$$ *Equation 17*

$$M^*_{t,} = \frac{E_t h_t M^*}{(\mathrm{EI})_{eff.}}$$ *Equation 18*

$$\frac{N^*_t}{(\phi N_r)} + \frac{M^* t}{(\phi M_r)} \leq 1.0$$ *Equation 19*

Where; $\phi N_r = \phi N_d / \gamma_m$, ϕN_d is the design tensile strength of timber and γ_m is the partial safety factor for timber (1.2 for LVL).And $\phi M_r = \phi M_d / \gamma_m$, ϕM_d is the design bending strength of timber, A_t is the cross sectional area of the timber.

The timber should also fulfil the design shear strength demand as shown in Equation 20. Where ϕV_s is the shear strength of the timber, $f_{s,d} = f_{s,d}/\gamma_m$, is the design shear stress, hence; ϕV_s >= V*, where V* is the design shear force due to the applied load.

$$\phi V_s = f_{s,d}(2A_t / 3)$$ *Equation 20*

$$\phi V_s \geq V^*$$ *Equation 21*

The largest stresses occur where the normal stresses are zero. The conditions in Equation 17 will be the most important condition for the strength of a TCC beam.
The maximum forces in the connections should also fulfil the requirement in Equation 23.

$$F = \gamma_c E_c A_c a_c SV^* / (EI)_{eff}$$ *Equation 22*

$$F \geq Q_{kd} / \gamma_{con}$$ *Equation 23*

Where Q_{kd} is the design strength and γ_{con} is the partial safety factor for the connections and is equal to1.3.

The design strength of a connector ($Q_{kd}/\ \gamma_{con}$) equals the mean strength of that connector type in case of B-NS, instead of the 5-percentile value as in case of the notched type (B-4N). The reason for this is the available redundancy through the parallel action of the connector in the interlayer. However, for a small number of connectors as in the case for beam B-4N, this redundancy effect vanishes and the 5-percentile value should be taken. This amount depends on the variability in strength of the connector type, the type of load and of the reliability level desired. If S and V* (Equation 22) vary along the beam axis, the connector with the largest value for V* times S should be checked. The first connector near the support will often be the decisive one since V* often reaches a maximum value at the support.

Since there is no experimental result of the failure loads of the TCC beams before they were subjected to the long-term tests, the strength demand for concrete, timber and the connector were computed using the gamma method in order to compare and investigate a possible loss of strength of the TCC beams. The two TCC beams were tested to failure after the long-term test. The calculated theoretical capacities based on mean timber strengths are given in Table 14 above and also detailed computations are presented in Appendix G (Table 42 and Table 43).

Table 14 Comparison of the theoretical design capacity of the TCC beams using GAMMA method with the failure loads (kN) from experimental results

Beam	Theoretical design capacities			Experimental Failure loads
	Concrete	Timber	Connector	
B-NS	90.4(5.5)	43.1	13.0	22.8
B-4N	112(8.1)	46.1	36.3	34.6

Note. The values in parenthesis are the tensile loads in the concrete and the results given for the connections are at the support.

As shown in this Table 14, the shear force on the connectors (composite check) governs the capacity of both beams, however the strength demand on timber is also detrimental, once the shear connectors' yield and lose their composite behaviour, because the load is then carried out by the timber only. The tensile failure on the concrete only means that micro cracks will develop. They have little or no effect on the load capacity of the TCC beam, moreover the steel mesh are provided in the concrete to resist these cracks and hence the strength demands by the connector governed the capacity of the beams. In case of B-4N the experimental failure load is closer to the estimated theoretical capacity with very little difference. The theoretical capacity of the beam before being exposed to the long-term test is found to be about 95 % (Table 14) of the experimental failure load after the long-term test, indicating very little or insignificant strength loss. However, as explained previously there is no experimental test on ultimate capacity done on the beams before the long-term test to verify this loss in strength. The results obtained for beam B-NS however show that the theoretical capacity is only about 57 % (Table 14) of the experimental failure load. This could be due to under estimation of the ultimate slip modulus of the connector for B-NS.

6.3 Residual stiffness and strength of LVL joists

The effect of the long-term test on the stiffness and strength of the composite beam has been discussed in section 6.1 and section 6.2 above, and it was found a loss in stiffness and strength of the composite beams. In order to investigate whether the long-term exposure also affected the stiffness and strength of the component materials a further test have been conducted. This section will present results and discussion on tests conducted on the timber joists.

The LVL joists from the tested TCC beams were cut into smaller sizes in areas where there was little or no damage due to the test. The tests were performed according to the test procedure outline in AS/NZS 4063.1(2010) and the test set up is shown in Figure 79 for the bending test and in Figure 80 for the tensile test on the LVL joists. Table 15 and Table 16 show the test results for bending and tensile strength tests for both the beams, respectively. The peak loads are the maximum loads and also the loads at failure, a detailed tabulated result are presented in *Figure 44* - *Figure 47*: Appendix G.

Table 15 Modulus of Elasticity of LVL after long-term test

Specimen	Width, (mm)	Depth (mm)	Peak load (kN)	Avg. Stiffness (kN/mm)	Mean E (GPa)
LVL-B_NS	48	70	8.01 (0)	488(4)	13.1(7)
LVL-B_4N	48	70	9.56 (9)	474 (2)	12.2 (2)

Numbers in brackets show the percentage of the coefficient of variation (COV)

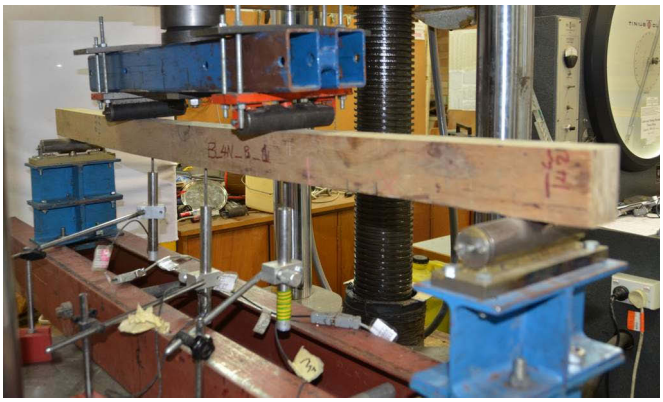

Figure 79: Set-up for bending tests of LVL joist

Table 16 Tensile strength of LVL after long-term test

Specimen	Width, (mm)	Depth (mm)	Peak load (kN)	E (GPa)	Tensile strength (MPa)
LVL-B_NS	48	70	117 (12.8)	13.3 (0.2)	35 (12.8)
LVL-B_4N	48	70	128 (6.8)	11.6 (0.2)	38.1 (6.8)

Numbers in brackets show the percentage of the coefficient of variation (COV)

However the loss in stiffness of the LVL beams based on material tests (Table 17) on the LVL cut from the joists is only 7.5 % compared to the overall stiffness loss observed in the TCC beams. It has to be noted that the number of test samples cut from the joists was small and making definitive conclusions as to whether the reduction is from the variability of the properties of the LVL joist or as a result of the long-term exposure to humidity cycle is difficult. The results from the specimens cut from B-NS joist, however, indicate no significant noticeable reduction in stiffness of the LVL.

Figure 80: Set-up for tension test of LVL joist

Table 17 Percentage loss in MOE of LVL joists

Specimen	MOE (MPa)		Loss (%)
Specimen	Before LT	After LT	
LVL_B-NS	12402	13125	-
LVL_B-4N	13153	12158	7.5

Note: LT = long-term test

Hence, the losses in the stiffness in the TCC beams observed is a results of the loss in the composite behaviour of the beams mixed with the loss in slip modulus of the connectors. However, no long-term tests were conducted on the connectors' and the possible loss in slip modulus on the connector cannot be justified at this stage. Long-term experimental investigation on connectors is required to confirm this.

6.4 Concluding remarks

The short term experimental tests conducted on two beams were reported here. These two beams (B-NS and B-4N) were kept in the humidity chamber for over 550 days. The four-point bending test conducted on these two TCC beams before and after an extended exposure to an environment equivalent to Service Class 3, as per Eurocode 5, provided valuable information to understand the behavioural response of TCC to serviceability. Significant deflections were observed in the specimens during the long-term tests, some of which was not recovered after removal of the load.

Loss of stiffness was also observed. As a consequence of the long-term testing, both beams experienced some reduction in their bending stiffness to a magnitude of up to 52.9 %. This loss is related to losses in stiffness and strength in the concrete, timber and/or connector. The loss in strength and stiffness observed in the TCC beams is also governed by loss of stiffness and strength in the connectors and to some extent in the concrete. The loss in stiffness for connection is arguably demonstrated by the loss of composite action observed for both the beams. On the other hand, the strain value taken on the concrete member before and after long-term tests indicated that the concrete has not been significantly affected. Because there was no experimental test on the strength of the TCC beams before the long-term test, comparison was not made for the possible loss in strength of the TCC beams due to the long-term exposure. However, the comparison made between the theoretical design capacities and the failure load from the ultimate test for B-4N indicates a possible loss of strength.

7 Long-term performance of timber-timber composite floor modules

7.1 Introduction and Composite beam properties

This chapter reports the long-term experimental investigation conducted on two composite timber floor beams with 6 m clear span. These timber composite beams were made of laminated veneer lumber (LVL), with the web and the flanges of the composite timber section connected using screw-gluing technique Figure 81 shows a typical cross section of the composite beams. Short-term tests under service loads were conducted on the beams by Zabihi (2014) to determine their bending stiffness. The long-term investigation on the beams which commenced on March 2012 is still on-going during this reporting. The aim of the test was to investigate the long-term behaviour of these composite timber beams under cyclic moisture conditions. Moreover, the experimental result also produced a valuable finding that complements behaviours observed on TCC beams and a difference of behaviour between TCC and timber only composite beams can be established under identical humidity conditions.

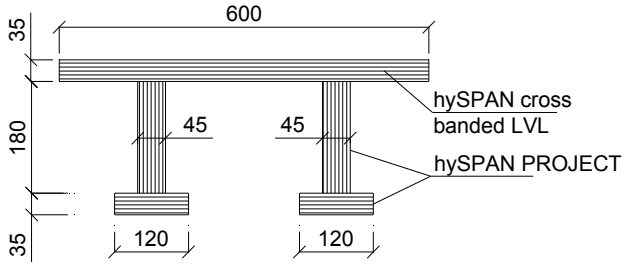

Figure 81: Atypical cross section of the composite beams

Before the commencement of the long-term test, the timber beams were subjected to four-point bending test (Figure 82) under service load up to 40% of the estimated failure load, to determine their bending stiffness. The apparent bending stiffness (EI)

was $4.21x10^{12}$ and $4.24x10^{12}$ Nmm^2 for beams L6-01 and L6-03, respectively (Zabihi 2014), and the load versus deflection the composite beams have a linear elastic behaviour as shown in Figure 82. The location of the neutral axis (NA) with the assumption of a theoretical fully composite behaviour compared with location of the NA from the experimental result shows a 5% deviation and the values of the coefficient R^2 shows a strong correlation between the strain distribution over the depth of the system (about 0.99) as shown in Appendix H. Hence, the composite beams will be treated as a fully composite in further discussions and the properties of the transformed section are presented in Appendix H.

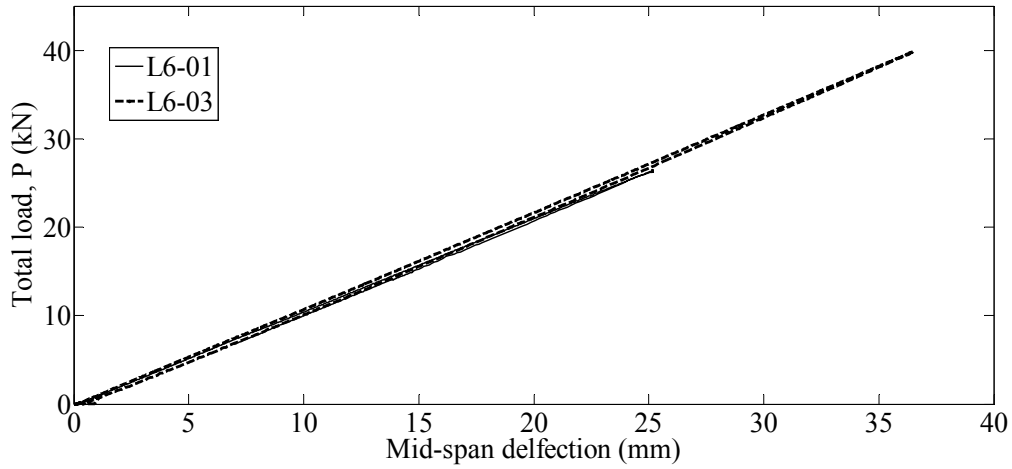

Figure 82: Load versus deflection (Zabihi 2012, Zabihi 2014)

7.2 Long-term test results and discussions

The long-term test set up is shown in Figure 83 where the beams were placed on a simply supported arrangement and a long-term load was applied using lead bars evenly spaced on the top of the beams. The lead bars were applied manually on the top of the beams and it took more than 30 minutes before all the loads were applied, for this reason the instantaneous deflections were read as soon as the deflections stabilized. The serviceability loads applied are equivalent to a uniformly distributed load of 2.1 kPa. This applied load is about 34 % of the short-term ultimate design

load (1.2G+1.5Q) expected for the beams. The instantaneous mid span deflections after the application of the loads were 6.5 mm for L6-01 and 6.2 mm for L6-03. The slight difference between their instantaneous deflections could be due slight variations on the spacing of the lead bars along the length of the beams and/or variations on the individual masses of the lead bars. The stresses developed due to bending along the cross section of the composite beams immediately after the load application are; 2.6 MPa, 2.2 MPa, 3.5 MPa and 4.6 MPa, on the top flange, top web, bottom web and bottom of the flange, respectively. These stresses range from 5 to 11 % of the design capacities of the members and are obtained using the transformed section method assuming a fully composite section. Creep of wood exhibits linear behaviour with respect stress up to stress levels of about 40-50 % of the short-term strength in constant environment conditions. This has been reported in compression, tension and in bending (Toratti, 1992). In mechano-sorptive creep, the non-linearity of wood starts at about 10-20 % of the ultimate stress in compression and at about 20-30 % of the ultimate stress in tension and bending (Hunt, 1989), with generally larger the creep deformations under compression load under tension load (Bengtsson, 2001).The shrinkage and swelling due to moisture changes also indirectly affects the deformation which consequently affects the modulus of elasticity. Hunt (1988) found that the shrinkage and swelling decreases for wood loaded in tension parallel to grain while it increases for wood loaded in compression parallel to grains. Large part from the cross section of the composite beams under this investigation lies under compression and bending zones and hence, is expected to behave in similar manner to behaviours observed by wood under compression and/or bending stresses. And for LVL the creep perpendicular to the grain was found to be significantly larger than the creep parallel to grains as reported in Matthew (2008). It means that the flanges and webs will have higher creep than the webs and the stresses on the webs will also increase with time. However, no experimental measurements were conducted to verify this in this investigation.

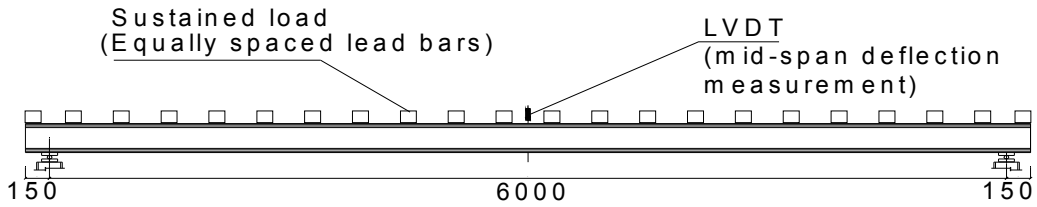

Figure 83: Long-term test set up and service loads

Figure 84: Timber composite beams in humidity chamber

These beams were exposed to similar environmental conditions as the TCC beams. The environmental condition was cyclically alternated between normal and very humid conditions whilst the temperature remained quasi constant (20±2 °C) – typical cycle duration was six to eight weeks.

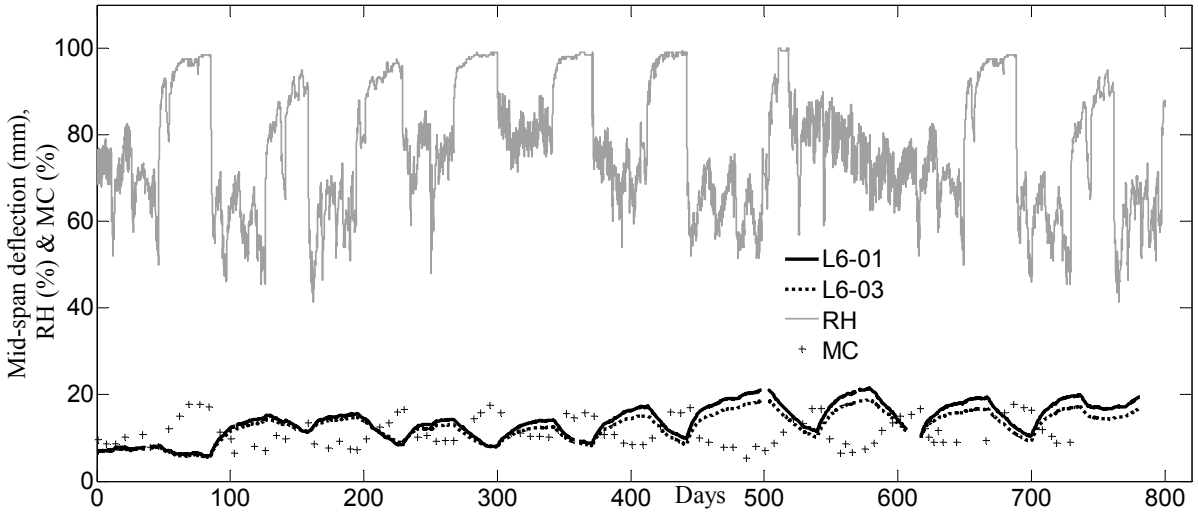

Figure 85: Relationship between the Mid-span deflection, moisture content and relative humidity of the chamber

A comprehensive plot of mid span deflection of the beams and relative humidity (RH) of the chamber is shown in Figure 85 (similar graph is also presented in large scale in Appendix H Figure 106). The experimental results to-date (800 days) show a general tendency towards flattening of the creep curves with slow rate of increase in creep for both beams with time with higher creep observed on beam L6-01. Slightly higher creep recorded for beam L6-01, could be due to variability in wood properties, or due to their differences in the stress levels.

When the specimens were loaded, the air humidity of the humidity chamber was not constant and was fluctuating between 55 to 75 %, and, moderate creep occurred in this period.

After approximately 50 days from loading, water was admitted in to the humidity chamber using a humidifier and the beams responded quickly by partially recovering the already attained deflections. This period may be considered as a subsequent adsorption period with the first adsorption being absorbed in the first 50 days without a significant notice, the unstable air humidity conditions in the chamber may have caused these phenomena in first few weeks of the test. In most literatures, however, the first adsorption period is characterized by increase in deflection (Epmeier 2007, Hausca and Bucar 1996, Bengtsson 2001). This period was followed by a dry period

and a sharp increase in creep was observed the usual response of beams in cyclic conditions in bending and the beams attained most of the creep during this period, similar finding was also reported by Lu and Erickson (1994), which explained that most of the mechano-sorptive creep was naturally produced during the first cycles.
The moisture content of the beams under load is cycled from dry to wet and back to dry again, the deformation also followed a cyclic pattern. However the recovery in each cycle is only partial and over six cycles the total amount of creep is very large as shown in Figure 85. The greater the moisture difference is in each cycle, the higher is the amount of creep. The air humidity cycled between about 50 % to 100 %, it should be noted that creep increased during drying (desorption) and decreased during the wetting cycle (adsorption) and this represents a typical creep behaviour of wood in bending and wood based materials (Armstrong and Kingston 1960, Toratti 1992).The changes in deflection during each complete cycle would have been much less if the range of change of air humidity was made narrower during moisture content cycling under load. Nevertheless, a decrease in deflection for each absorption and an increase for each desorption were still found for each cycle after the first cycle, which is similar to test results reported by Armstrong and Kingston (1960). The apparent creep recovery during subsequent humidification (wet periods), due to the size changes caused by difference in shrinkage coefficient between the tension and compression faces of the timber as explained by Gerhards (1985) and Hunt and Shelton (1987).That also explains the sinusoidal like deflection curves, with the amplitude of the curve increased with increase in the total deflection. If the shrinkage and swelling effect is subtracted from the creep strain, in approaching the stable state, appeared to be a monotonically increasing function of moisture changes regardless of the direction of the change. This mechano-sorptive effect continues to diminish with time as also was reported in Toratti (1992).

The cycling of the moisture seems to have induced a significant effect on the long-term deflection of the beams. The total deflection measured for L6-01, exceeded the limit (L/150 to L/300) given in Eurocode 5 for timber structures on two supports. The relative deflection referred j_2 is the ratio of the total deflection to the instantaneous deflection. The total deflections attained by the beams are expressed in

terms of the relative creep (total deflection divided by the instantaneous deflection) in Table 18.

Table 18 Relative creep values of the composite beams

Beam	Relative creep
L6-01	3.25
L6-03	2.98

The creep factors for timber beams are available in design codes, Eurocode 5, referred to as K_{def} and a value of 2.0 is recommended for LVL-timber for quasi-permanent load combinations, while in AS/NZS 1170.1:2008 a recommends a duration of load factor for creep deformation, $j_{2,}$ as a relative creep (relative deflection). The j_2 value for bending members with initial moisture content at time of load application less than or equal to 15 %, and for a load duration greater than or equal to one year is 2.0. This is lesser than the relative creep values obtained for the beams under investigation. The theoretical long-term deflection of the composite beams was also tried adopting a K_{def} value 2.0 for the LVL and assuming fully composite section. The total long-term deflection obtained for the end of service life of the beams was 18.5 mm and is about three times the instantaneous deflection calculated with the same approach. The details of the computations are given in Table 50: Appendix H. The findings from this experimental result show a creep factor 1.98 to 2.25 with an expected increase with increase in the deflection of the beams over time. These composite beams where initially loaded at MC less than 15 %, and during the course of the test period the beams were subjected to MC greater than 15 % for several times.

7.3 Concluding remarks

This chapter presented a long-term experimental investigation on timber composite beams. The creep rate and total creep were significantly affected by moisture changes, and that the observed response by the composite beams cannot be predicted from tests under constant conditions. The two beams were monitored under cyclic humidity conditions with the relative humidity varying from about 55 % in the dry period to about 100 % in the wet periods. The moisture content of the timber beams as well as the deflections followed cyclic patterns. These conditions induced a significant creep deflection reaching well above the limiting value of L/200 usually adopted in design codes. The humidity cycle was monitored using the moisture content samples and it was observed that the length and extent of the humidity change influenced the creep behaviour of the beams. The beams were observed to respond quicker when the humidity cycle was changed from wet to dry than vice versa. Additionally, during each subsequent cycle the total deflection and also the amplitude of the curves increased. And the total deflection actually reached more than three times their instantaneous deflections. There is no provisions for creep factor of a composite LVL beams in design codes, depending on the load and environment history, Eurocode 5, recommends a creep factor (K_{def}) values of 2.0 for LVL in environmental conditions characterized by service class 3. The results of this experimental result could suggest, a creep factor (K_{def}) of about 3 for the composite timber beams subjected to environmental conditions categorized as equivalent to or more severe than service class 3.

8 Conclusions

The main objective of this research was to experimentally investigate the long-term performance of timber-concrete composite beams. Four TCC beams with three different types of shear connectors (normal screws, concrete notches and SFS screws) were investigated and the amount of creep expected in the service life of TCC floor beams using these types of connectors were obtained based on the experimental data. Long-term behaviour of two timber only composite floor beams was also investigated under the same environmental conditions which complemented the finding on the TCC beams.

Following conclusions can be made based on this study.

Long-term test observations on TCC beams

The relative humidity monitored during the long-term test varied from 45 % to 100 % while the timber moisture content fluctuated in the range of 7 % to 20 %. During the long-term test the temperature remained quasi constant (21 °C±1). The environmental conditions can be described as equivalent as or more severe than service class 3 as defined in Eurocode 5, with the air humidity exceeded 85 % several occasions and kept approximately at 100 % for several weeks and repeated every four to six weeks. The environmental condition is also characterized by quasi-constant temperature and its effect on the long-term behaviour of the beams is little or insignificant.

The mid-span deflections for all the beams increased throughout the test and most of the deflection was attained in the first 700 days of the test. The mid-span deflection for B-NS (specimen with normal screw connector) increased continuously reaching above the limit value (L/200) with in the first 500 days.

As the moisture content of the loaded beams cycled from dry to wet and back to dry again, the deflection also followed a cyclic pattern. Increase in relative humidity and moisture content was followed by an increase in deflection in the first adsorption, and decrease of deflection (local recovery) in all subsequent absorptions. While, all desorption periods were accompanied by an increase in deflection throughout the test period. This behaviour is found to be a typical of wood under bending; however there

are hardly any available literatures on TCC beams under cyclic conditions to back up the findings. Most of the existing literatures on TCC structures are conducted on naturally varying environments and the beams behaved in contrary to this findings i.e. increase in deflection with increase in moisture content. A complementary study was also conducted on timber composite beams (chapter 7) under the same environmental conditions in bending. The timber only composite beams responded in similar manner to the TCC beams.

Creep factor for TCC beams

The total deflection of the two TCC beams with six bird-mouth notches (B-6N) and SFS screws (B-SFS) is in the range of 7- 8 times the instantaneous deflection; given that this environmental condition is very severe, the result is not surprising. The predicted end of life deflection i.e. 50 years using equations obtained from the fitted curves, overestimated the deflection. The gamma method was also employed to predict the end of life deflection. The estimate closely predicted the deflection for beam B-6N, while, it under-estimated the deflection for B-SFS. It is recommended that the beams will be monitored for more years for better predictions. However, from this experimental test an upper bound creep factor of seven is recommended for the TCC beams under investigation. This creep factor of the TCC beams can be reduced if high composite behaviour can be achieved by increasing the bending stiffness of the composite beams. Cecotti et al. 2006 and Yeoh et al. 2010 investigated TCC beams under normal conditions and the total creep deflections reported were about four times the instantaneous deflection. In this research the lower bound value of the creep (Figure 58) about 4.5 can be assumed conservatively as creep value for normal environmental conditions.

Residual strength and stiffness of TCC beams

The four-point bending test conducted on two TCC beams with four bird-mouth notches (B-4N) and normal wood screws (B-NS) before and after the long-term test (550 days), provided valuable information to understand the behavioural response of TCC to serviceability and ultimate failures. Significant deflections were observed in the specimens during the long-term tests, some of which was not recovered after removal of the load. Loss of stiffness and strength was also observed, as a

consequence of the long-term testing and both beams experienced reduction in their bending stiffness to a magnitude of up to 53 % for B-NS and 20 % for B-4N. During the ultimate test, B-NS showed poor composite behaviour while B-4N showed good composite behaviour throughout the test. The failure on both the beams was due to combined bending and tension failure in timber. The tests conducted on LVL cut from the timber joist revealed no noticeable loss of the stiffness of the LVL due to the long-term exposure.

Creep factor for Timber only composite beams

The timber only composite beams have been subjected to cyclic moisture conditions and induced large deflection both the beams. The moisture content cycled from dry to wet and back to dry again and the deflection also followed a cyclic pattern. During the test an increase in relative humidity and moisture content is followed by an increased in deflection and partial decrease in deflection (recovery) when RH increases. This behaviour is found to be a typical behaviour of wood in bending under cycling humidity conditions. The experimental result to-date (800 days) shows a general tendency towards flattening of the creep curves with slow rate of increase in creep for both beams with time. The beams exhibited good composite behaviour throughout the test period with no slip or gap at the interfaces. Both the beams deflected more than three times their instantaneous deflections. Based on the findings from this experimental result and considering the expected increase in defection over time, could suggest an overall creep factor of about 3 for the composite timber beams in environmental conditions categorized as equivalent to service class 3 according to Eurocode 5.

Similarity of behaviours between Timber-Concrete composite beams and Timber only composite beams

Both the TCC beams and timber only floor modules have shown similar behaviour in response to the moisture changes with generally increase in deflection during dry periods and recovery of deflection during wet period except the first humid cycles. Additionally both exhibited similar rate of creep and rate of recovery of creep during drying and wetting periods. The timber only beams had high composite efficiency as

compared to the timber-concrete beams and therefore had smaller creep factor compared to TCC beams.

9 Future works

Following recommendations for future studies are made based on the observations made during this experimental investigation.

1. In order to predict the long-term deflection of TCC beams, the long-term slip modulus is very important and hence an experimental investigation on the long-term slip behaviour and a corresponding creep factor is required. Hence, a long-term investigation on the following type of connectors are recommended for future works; normal screw connection, notch and SFS connections.

2. During the course of the long-term investigation under cyclic humidity conditions, it was observed that the extent and length of cycle play important role in the creep response of the TCC beams and hence an investigation on an optimum length of humidity cycle to induce the maximum deflection needs to be investigated.

3. The future works also include verifying the experimental results with the exiting FE models and make recommendations.

References

Ahmadi, B. H. & Saka, M. P. 1993, 'Behaviour of Composite Timber-Concrete Floors', Journal of Structural Engineering, vol. 119, no. 11, pp. 3111-30.

Amadio, C., Fragiacomo, M., Ceccotti, A. & Di Marco, R. 2001, 'Long-term behaviour of a timber-concrete connection system', paper presented to the RILEM Conference, Stuttgart, 12-14 Sept.

Andreas Monaridis, 2010, 'Evaluation of timber-concrete composite floors' Avdelningen for Konstruktionsteknik, Lunds Teknika Hogskola, Lund Universitet, Rapport TVBK-5187, ISSN 0349-4969.

Armstrong, L., Kingston, R. 1960, 'The effect of moisture changes on creep in wood', Nature 185:862-863.

Armstrong, L. 1972, 'Deformation of wood in compression during moisture movement', Wood Science 5:81-86.

Armstrong, L. D. and Christensen, G. N., 1961, 'influence of moisture changes on deformation of wood under stress', Nature, 191, 869-870.

Armstrong, L. D. and Grossman, P. U. A., 1972, 'The behaviour of Particle board and hard board beams during Moisture cycling', Wood Science and Technology, vol. 6, p. 9.

AS 1012.9 1999, Determination of the compressive strength of concrete specimens, Standards Australia Committee BD/42, Methods of Testing Concrete, Australia.

AS 1720.1-2010, Timber Structures, Design Methods, Standards Australia.

AS 1012.17 1997, Determination of the static chord modulus of elasticity and Poisson's ratio of concrete specimens, Standards Australia Committee BD/42, Methods of Testing Concrete, Australia.

AS/NZS 4063.1 2010, Characterization of structural timber - Test methods Australian Standards.

AS/NZS 4357.3 2006, Structural laminated veneer lumber (LVL) - Part 3: Determination of structural properties—Evaluation methods, Standards Australia/Standards New Zealand, Australia.

Balogh, J., Fragiacomo, M., Gutkowski, R. M. & Fast, R. S. 2008, 'Influence of Repeated and Sustained Loading on the Performance of Layered Wood-

Concrete Composite Beams', Journal of Structural Engineering, vol. 134, no. 3, pp. 430-9.

Bazan, I. M. M. 1980, 'Ultimate bending strength of timber beams', Nova Scotia Technical College, Canada, Halifax.

Bengtsson, C., 2001, 'Mechano-sorptive creep of timber influence of material parameters', HolzalsRoh- and Werkstoff, vol. 59, p. 236.

Bonamini, G., Uzielli, L. & Ceccotti, A. 1990, 'Short- and long-term experimental tests on antique larch and oak wood-concrete composite elements', paper presented to the C.T.E. Conference, Bologna.

Bodig, J. and Jayne, B. A. 1982 ‘Mechanics of wood and wood composites’ Chapter 5. Van Nostrand Reinhold Co. New York, 1982.

Bou Saïd, E., Jullien, J. F. & Ceccotti, A. 2004, 'Long term modelling of timber-concrete composite structures in variable climates', paper presented to the 8th World Conference on Timber Engineering (WCTE), Lahti, Finland, 14-17 June.

Bradford, M. A. & Gilbert, R. I. 1992, 'Composite beams with partial interaction under sustained loads', Journal of Structural Engineering, vol. 118, no. 7, pp. 1871-83.

Buchnan, A. , Deam, B. , Fragiacomo, M., Pampanin, S. and Palermo, A. 2008, ‘Multi-storey prestressed timber buildings in New Zealand, Structural Engineering International SEI, 18(2), 166-173.

Buell, T. W. & Saadatmanesh, H. 2005, 'Strengthening Timber Bridge beams using carbon fiber', Journal of Structural Engineering, vol. 131, no. 1, pp. 173-87.

Capretti, S. 1992, 'Time dependent analysis of timber and concrete composite (TCC) structures', paper presented to the RILEM Int. Symp. on Behaviour of Timber and Concrete Composite Load-Bearing Structures, Ravenna, Italy.

Capretti, S. & Ceccotti, A. 1996, 'Service behaviour of timber-concrete composite beams: A 5-year monitoring and testing experience', paper presented to the International Wood Engineering Conference, New Orleans, USA.

CEB-FIP 1993, CEB-FIP model code 1990: Design code, Thomas Telford, London.

Ceccotti, A., Fragiacomo, M. and Giordano, S., 2006, 'Long-term and collapse tests on a timber concrete composite beam with glued in connection', Materials and Structures, 2006, p. 10.

Ceccotti, A. 1995, 'Timber-Concrete Composite Structures', in, Timber Engineering, Step 2, 1st Edn. (Centrum Hout, The Netherlands) E13/1-E13/12, p. 16.

Ceccotti, A. 2002, 'Composite concrete–timber structures', Progress in structural engineering and materials, vol. 4, pp. 264-75.

Ceccotti, A. & Covan, C. 1990, 'Behaviour of timber and concrete composite load-bearing structures', paper presented to the The 1990 IUFRO S5.02 Timber Engineering, Saint John, New Brunswick, Canada.

Ceccotti, A., Fragiacomo, M. & Giordano, S. 2006a, 'Behaviour of a Timber-Concrete Composite Beam with Glued Connection at Strength Limit State', paper presented to the 9th World Conference on Timber Engineering (WCTE), Portland, Oregon, USA, 6-10 August.

Ceccotti, A., Fragiacomo, M. & Giordano, S. 2006b, 'Long-term and collapse tests on a timber-concrete composite beam with glued-in connection', Materials and Structures, vol. 40, no. 1, pp. 15-25.

CEN 1991, Timber Structures - Joints made with mechanical fasteners - General principles for the determination of strength and deformation characteristics. EN 26891, BSI, European Committee for Standardization, Brussels, Belgium.

CEN 2008, Eurocode 5: Design of timber structures - Part 1-1: General - Common rules and rules for buildings. EN 1995-1-1:2004+A1, BSI, European Committee for Standardization, Brussels, Belgium.

Clouston, P., Bathon, L. A. & Schreyer, A. 2005, 'Shear and bending performance of a novel wood-concrete composite system', Journal of Structural Engineering, vol. 131, no. 9, pp. 1404-12.

Clouston, P., Civjan, S. & Bathon, L. 2004, 'Experimental behavior of a continuous metal connector for a wood-concrete composite system', Forest Products Journal, vol. 54, no. 6, pp. 76-84.

Deam, B. L., Fragiacomo, M. & Buchanan, A. H. 2008a, 'Connections for composite concrete slab and LVL flooring systems', Materials and Structures, vol. 41, no. 3, pp. 495-507.

Deam, B. L., Fragiacomo, M. & Gross, L. S. 2008b, 'Experimental Behavior of Prestressed LVL-Concrete Composite Beams', Journal of Structural Engineering, vol. 134, no. 5, pp. 801-9.

Dias, A. M. P. G. 2005, 'Mechanical behaviour of timber-concrete joints', Ph.D. thesis, TechnischeUniversiteit Delft.

Dias, A. M. P. G., Cruz, H. M. P., Lopes, S. M. R. & Van de Kuilen, J. W. G. 2010, 'Stiffness of dowel-type fasteners in timber-concrete joints', Proceedings of the Institution of Civil Engineers: Structures and Buildings, vol. 163, no. 4, pp. 257-66.

Dias, A. M. P. G. & Jorge, L. F. C. 2011, 'The effect of ductile connectors on the behaviour of timber–concrete composite beams', Engineering Structures, vol. 33, no. 11, pp. 3033-42.

Dias, A. M. P. G., Lopes, S. M. R., Van de Kuilen, J. W. G. & Cruz, H. M. P. 2007a, 'Load-Carrying Capacity of Timber-Concrete Joints with Dowel-Type Fasteners', Journal of Structural Engineering, vol. 133, no. 5, pp. 720-7.

Dias, A. M. P. G., Van de Kuilen, J. W., Lopes, S. & Cruz, H. 2007b, 'A non-linear 3D FEM model to simulate timber-concrete joints', Advances in Engineering Software, vol. 38, no. 8-9, pp. 522-30.

Epmeier, H., Johonsson, M., Kliger, R. and Westin, M. 2007 ‘Bending creep performance of modified timber’, HolzRoh- Werkst.

Fragiacomo, M. 2005, 'A finite element model for long-term analysis of timber-concrete composite beams', Structural Engineering and Mechanics, vol. 20, no. 2, pp. 173-90.

Fragiacomo, M. 2006, 'Long-term behaviour of timber-concrete composite beams. II: numerical analysis and simplified evaluation', Journal of Structural Engineering, vol. 132, no. 1, pp. 23-33.

Fragiacomo, M. 2012, 'Experimental behaviour of a full-scale timber-concrete composite floor with mechanical connectors', Materials and Structures, pp. 1-19.

Fragiacomo, M., Amadio, C. & Macorini, L. 2007a, 'Short- and long-term performance of the “Tecnaria” stud connector for timber-concrete composite beams', Materials and Structures, vol. 40, no. 10, pp. 1013-26.

Fragiacomo M., 2006, 'Long-term behaviour of timber-concrete composite beams. I: finite element modelling and validation', StrucEng, vol. 132(1), pp. 13-22.

Fragiacomo, M. and Ceccotti, A., 2004, 'A simplified Approach for Long-Term Evaluation of Timber-Concrete Composite Beams', 8th WCTE, vol. 2, Lahti,Finland, pp. 537-42.

Fragiacomo, M., Balogh J. and Gutkowski, R., 2011, 'Long-term load test of a wood-concrete composite beam', Structures and Buildings ICE Volume 164 Issue SB2, p. 155-163.

Fragiacomo, M. & Ceccotti, A. 2006, 'Long-term behavior of timber-concrete composite beams. I: finite element modeling and validation', Journal of Structural Engineering, vol. 132, no. 1, pp. 13-22.

Fragiacomo, M., Gutkowski, R. M., Balogh, J. & Fast, R. S. 2007b, 'Long-Term behavior of wood-concrete composite floor/deck systems with shear key connection detail', Journal of Structural Engineering, vol. 133, no. 9, pp. 1307-15.

Fragiacomo, M. & Schänzlin, J. 2010, 'The effect of moisture and temperature variations on timber-concrete composite beams', paper presented to the 11th World Conference on Timber Engineering (WCTE), Riva del Garda, Trentino, Italy, 20-24 June.

Freedman G., Mettem C., Larsen P., Edwards S., 2002 ‘Timber Bridge and Foundations’ A report produced for the Forestry Commission.

Fridely, K. J., Tang, R. C., and Soltis, l. A. 1992 ‘Creep behaviour model for structural lumber’ J. of Structural Engineering 118(8): 2261-2277.

Gerber, C., Shrestha, R., Crews, K. 2012 ‘Design procedures for timber concrete composite floor systems in Australia and New Zealand’ STIC 2012-32 TCC Design Procedures ver2-3.

Gerhards, C. C. 1985 ‘Time-dependent bending deflection of Douglas-fir 2 by 4’s’, Journal of forest products, 35(4):18-26, 1985.

Gilbert, R. I. & Bradford, M. A. 1995, 'Time-dependent behavior of continuous composite beams at service loads', Journal of Structural Engineering, vol. 121, no. 2, pp. 319-27.

Gibson, E. J., 1965, 'Creep of wood:Role of water and effect of a changing moisture content', Nature, no. 4980.

Gowda, C., Kortesmaa, M., Ranta-Maunus, A., 1996, 'Long term creep tests on timber beams in heated and non-heated environment', Espoo, vol. VTT Publications 278, p. 35.

Grantham, R,, Fragiacomo M., Nogarol, C., Zidaric I. and Amadio, C., 2004, 'Potential upgrade of timber frame buildings in the UK using timber-concrete composites', In 8th World Conference on Timber Engineering WCTE 2004, vol. 2, WCTE 2004, Lahti, Finland, pp. 59-64.

Grossman, P. U. A. 1971, 'use of Leicester's "Rheological Model for Mechano-sorptive Deflection of Beams"', Wood Science and Technology ,Springer-Verlag 1971, vol. 5, p. 3.

Grossman, P. U. A., Clayton, T. and Nakai, 1987, 'Deflection of wood under intermittent loading', Wood Science and Technology, vol. 21, p. 9.

Gowda, S., Kortesmaa, M. &Ranta-Maunus, A. 1996, Long term creep tests on timber beams in heated and non-heated environments, VTT Publications 278, Espoo, Finland.

Grantham, R. & Fragiacomo, M. 2004, 'Potential Upgrade of Timber Frame Buildings in the UK Using Timber-Concrete Composites', paper presented to the 8th World Conference on Timber Engineering (WCTE), Lahti, Finland, 14-17 June.

Gurksnys, K., Kvedaras, A. & Kavaliauskas, S. 2005, 'Behaviour Evaluation Of 'Sleeved' Connectors In Composite Timber-Concrete Floors', Journal of Civil Engineering and Management, vol. 11, no. 4, pp. 277-82.

Gutkowski, R., Brown, K., Shigidi, A. & Natterer, J. 2008, 'Laboratory tests of composite wood-concrete beams', Construction and Building Materials, vol. 22, no. 6, pp. 1059-66.

Gutkowski, R. M., Brown, K., Shigidi, A. & Natterer, J. 2004, 'Investigation of Notched Composite Wood-Concrete Connections', Journal of Structural Engineering, vol. 130, no. 10, pp. 1553-61.

Hanhijärvi, A. & Hunt, D. 1998, 'Experimental indication of interaction between viscoelastic and mechano-sorptive creep', Wood Science and Technology, vol. 32, no. 1, pp. 57-70.

Harvey, C.H. 2007, New Zealand factory production data for LVL Truform recipe from January to May 2007, in CHH (ed.)Auckland, New Zealand.

Hansson, S. and Karlsson, K., 2007, 'Moisture-related creep of reinforced timber', Chalmers University of Technology, Goteborg.

Hearmon, R. F. S. and Paton, J. M. 1964 ‘Moisture content changes and creep of wood’, Forest Prod. J, 14(8):.357-379.

Hunt, D. G. 1989, 'Linearity and non-linearity in mechano-sorptive creep of softwood in compression and bending', Wood Science and Technology, vol. 23, p. 10.

Hunt, D. G. and Shelton, C. F. 1988, 'Longitudinal moisture-shrinkage coefficients of softwood at the mechano-sorptive creep limit', wood Science and Technology ,Springer-Verlag 1988, vol. 22, p. 11.

Hunt, D., Grs, j. 1988 ‘Comparison between juvenile and mature wood in the analysis of creep’. Proceedings of COST action E8 Mechanical performance of wood and wood products, Florence, Italy, 1988.

Hoffmeyer, P. and Davidson, R. W. 1989 ‘Mechano-sorptive creep mechanism of wood in compression and bending’. Wood Sci. Technol. 23:215-227.

Hoffmeyer, P. 1990 ‘Failure of wood as influenced by moisture and duration of load’. Doctoral Dissertation. College of Environmental Science and Forestry, SUNY, N.Y. USA.

Hoyle, R. J., Itani, J. K. & Eckard, J. J. 1986, 'Creep of douglas fir beams due to cyclic humidity fluctuations', Wood and Fiber Science, vol. 18, no. 3, pp. 468-77.

Hausca, M., Bucar, B. 1996 ‘Mechanos-sorptive creep in adult, juvenile and reaction wood’. Proceedings of the International COST 508 Wood Mechanics Conference Stuttrgart, Germany.

Jorge, L. F., Schänzlin, J., Lopes, S. M. R., Cruz, H. & Kuhlmann, U. 2010, 'Time-dependent behaviour of timber lightweight concrete composite floors', Engineering Structures, vol. 32, no. 12, pp. 3966-73.

Jorge L. F. C. 2005 ‘Timber-Concrete composite Structures using LWAC’. PhD thesis, University of Coimbra, Coimbra (in Portuguese).

Jorge, L. F., Lopes, S. & Cruz, H. 2011, ‘Interlayer influence on timber-LWAC composite structures with screw connections’. Journal of Structural Engineering, vol. 137, no. 5.p. 7.

Jan Willem, G. Van de Kuilen, Dias, Alfredo M. P. G. 2011, ‘Long-term load-deformation behaviour of timber-concrete joints’, Structure and Buildings, ICE proceedings, Volume 164 Issue SB2.

Kavaliauskas, S., Kvedaras, A. K. & Gurksnys, K. 2005, 'Evaluation of long-term behaviour of composite timber-concrete structures according to EC', Technological and Economic Development of Economy, vol. 11, no. 4, pp. 292-6.

Kenel, A. & Meierhofer, U. 1998, ‘Long-term performance of timber-concrete composite structural elements’, Report.No. 115/39, EMPA, Dübendorf, Switzerland, in German.

Kuhlmann, U., Aicher, S. & Michelfelder, B. 2004, ‘Trag- und Verformungsverhalten von KervenmitSchlüsselschraubenalsSchubverbindungbeiHolz-Beton-erbunddecken’, InstitutfürKonstruktion und Entwurf, Universität Stuttgart: Germany.

Kuhlmann, U. & Aldi, P. 2008, 'Simulation of grooved connections in timber-concrete composite beams considering the distribution of material properties', paper presented to the 10th World Conference on Timber Engineering (WCTE), Miyazak, JAPAN, 2-5 June.

Kuhlmann, U. & Michelfelder, B. 2004, 'Grooves as shear-connectors in timber-concrete composite structures', paper presented to the 8th World Conference on Timber Engineering (WCTE), Lahti, Finland, 14-17 June.

Kuhlmann, U. & Michelfelder, B. 2006, 'Optimised design of grooves in timber-concrete composite slabs', paper presented to the 9th World Conference on Timber Engineering (WCTE), Portland, Oregon, USA, 6-10 August.

Le Borgne, M. R. & Gutkowski, R. M. 2010, 'Effects of various admixtures and shear keys in wood-concrete composite beams', Construction and Building Materials, vol. 24, no. 9, pp. 1730-8.

Leicester, R. H. 1971 ‘A rheological model for mechano-sorptive deflection of beams’, Wood Sc. Technol. 5(3):211-220.

Leivo M. 1992 “Modelling the creep of wooden structures” Rakenteiden Mekaniikka: Vol. 25 No. 2 SS. 39-57.

Lu, JP. Leicester R.H.: Mechano-sorptive effects on timber creep, Wood Science Technol 31(5): 331-337, 1977.

Lu, W. and Erickson, R. W. 1994 ‘The effects of directed diffusion on the mechano-sorptive behaviour of small redwood beams’. Forest prod. J. 44(1):8-14.

Lukaszewska, E., 2009, 'Development of Prefabricated Timber-Concrete Composite Floors’ PHD Thesis, Lulea University of Technology, Sweden.

Lukaszewska, E., Fragiacomo, M. & Johnsson, H. 2010, 'Laboratory Tests and Numerical Analyses of Prefabricated Timber-Concrete Composite Floors', Journal of Structural Engineering, vol. 136, no. 1, pp. 46-55.

Lukaszewska, E., Johnsson, H. & Fragiacomo, M. 2008, 'Performance of connections for prefabricated timber–concrete composite floors', Materials and Structures, vol. 41, no. 9, pp. 1533-50.

Macorini, L., Fragiacomo, M., Amadio, C. &Izzuddin, B. A. 2006, 'Long-term analysis of steel-concrete composite beams: FE modelling for effective width evaluation', Engineering Structures, vol. 28, no. 8, pp. 1110-21.

Mario van der Linden. 1999, 'Timber-Concrete composite floor systems', Civil ingenieur, Technisch University Delft, HEBRON ED, VOL. 44, NO. 3, P. 26..

Mårtensson, A. 1992, 'Mechanical behaviour of wood exposed to humidity variations', Ph.D thesis, LundsUniversitet (Sweden), Sweden.

Meierhofer A.U. 1993 ‘Tests on Timber Concrete Composite Structural Elements’ CIB W18, Meeting Twenty-Six, Athens, Georgia, USA.

Mueller, J., Haedicke, W., Simon, A. & Rautenstrauch, K. 2008, 'Long-term performance of hybrid timber bridges – experimental and numerical investigations', paper presented to the 10th World Conference on Timber Engineering (WCTE), Miyazak,JAPAN, 2-5 June.

Martensson, A. 1994, 'Mechano-sorptive effect in wood material', Wood Science and Technology, Springer-Verlag 1994, vol. 28, no. 28, p. 12.

Mohager, M.T., 1993, 'Long ter, bending creep of wood in cyclic relative humidity', Wood Science and Technology, vol. 27, p. 49.

Morlier, P. and Palka, P. 1994 ‘Creep in Timber Structures, Chapter 2, basic knowledge’ Report of RILEM Technical Committee 112-TSC. London: E & FN Span. Pp. 43-60.. In

Mungwa, M. & Kenmou, D. 1993, 'Instantaneous and time-dependent analysis of composite wood-concrete cross-sections using Dischinger‟s equations of state: Part 1-Instantaneous analyses, Materials and Structures, vol. 26, no. 2, pp. 98-102.

Nima Khorsandnia: Finite Element Analysis for predicting the short-term and long-term behaviour of Timber Concrete Composite structures; PHD Thesis, University of Technology, Sydney, 2013.

Nima Khorsandnia, Hamid R. Valipour, Keith Crew, 2012' Experimental and analytical investigation of short-term behaviour of LVL-concrete composite connections and beams', Journal of Construction and Building Materials, 37(2012) 229-238.

Pham, V. L. 2010, Testing analyses and discussion for TCC beams, Faculty of Engineering and Information Technology, University of Technology, Sydney (UTS), Australia.

Piter, J. C., Calvo, C. F. and Cuffre, A. G. 2007, 'Creep in structural sized beams of Argentinean eucalyptus grandis', p. 9.

Ranta-Maunus, A. 1975, 'The viscoelasticity of wood at varying moisture content', Wood Science and Technology, vol. 9, no. 3, pp. 189-205.

Ranta-Maunus, A. & Kortesmaa, M. 2000, 'Creep of timber during eight years in natural environments', paper presented to the 6th World Conference on Timber Engineering (WCTE), Whistler Resort, British Columbia, Canada, 31 July-3August.

Rijal, R. 2013, 'Dynamic performance of timber and timber-concrete composite flooring systems', Ph.D. thesis, University of Technology, Sydney, Australia.

Schniewind, A.P. and Richmond, C., 1968, 'Recent Progress in the study of the Rheology of Wood', Wood Science and Technology, vol. 2, p. 18.

Schänzlin, J. 2010, 'Modeling the long-term behavior of structural timber for typical serviceclass-II-conditions in South-West Germany', Habilitation thesis, University of Stuttgart, Germany.

Schänzlin, J. & Fragiacomo, M. 2007, Extension of Eurocode5 Annex B formulas for the design of timber-concrete composite structures, In: Meeting forty of the Working Commission W18- Timber Structures, CIB, International Council for Research and Innovation, Bled (Slovenia).

Schänzlin, J. & Fragiacomo, M. 2008, 'Modelling and design of timber-concrete-composite structures in the long-term', paper presented to the 10th World Conference on Timber Engineering (WCTE), Miyazak,JAPAN, 2-5 June.

Shen, Y. Gupta, R. 1997 ‘Evaluation of creep behaviour of structural lumber in a natural environment’. Journal of forest products, 47(1).

Steinberg, E., Selle, R. & Faust, T. 2003, 'Connectors for Timber-Lightweight Concrete Composite Structures', Journal of Structural Engineering, vol. 129, no. 11, pp. 1538-45.

Szabo, T. and G. Ifju 1977 ‘Influence of stress on creep and moisture distribution in wooden beams under sorption conditions’. Journal of Wood Sci., 2(3):159-167.

Thelandersson, S. & Larsen, H. J. 2003, Timber Engineering, John Wiley, Chichester.

Toratti, T. 1992, 'Creep of timber beams in variable environment', Ph.D. thesis, Helsinki University of Technology, Laboratory of Structural Engineering and Building Physics.

Toratti, T. 1993, 'Long-term deflection of timber beams', Rakenteiden Mekaniikka: Vol. 26 No. 3 PP. 19 - 28.

Toratti, T. 2004, 'Service limit states: effects of duration of load and moisture on deformationse', paper presented to the Cost E24 Reliability of Timber structures, Florence, 27-28 May.

Unnikrishna Pillai, S. and Ramakrishnan, P, 1977 ‘Nail shear connectors in timber-concrete composites ’. Journal of Institution of Engineers (India), 58(1), pp. 34-39.

Yeoh, D. F.,and Deam, B., 2010, 'Long-term behaviour of LVL-concrete composite connection and beams under sustained loads', unpublished, University of Canterbury.

Yeoh, D. 2010, 'Behaviour and design of timber-concrete composite floor system', Ph.D. thesis, University of Canterbury, Christchurch, New Zealand.

Yeoh, D., Fragiacomo, M., Aldi, P., Mazzilli, M. & Kuhlmann, U. 2008, 'Performance of notched coach screw connection for timber-concrete composite floor system', paper presented to the 10th World Conference on Timber Engineering (WCTE), Miyazak, JAPAN, 2-5 June.

Yeoh, D., Fragiacomo, M., Buchanan, A. & Gerber, C. 2009, 'Preliminary research towards a semi-prefabricated LVL-concrete composite floor system for the Australasian market', Australian Journal of Structural Engineering, vol. 9, no. 3, pp. 225-40.

Yeoh, D., Fragiacomo, M., De Franceschi, M. & Buchanan, A.H. 2011a, 'Experimental tests of notched and plate connectors for LVL-concrete composite beams', Journal of Structural Engineering, vol. 137, no. 2, pp. 261-9.

Yeoh, D., Fragiacomo, M. & Deam, B. 2010, 'Long-term behaviour of LVL-concrete composite connections and beams under sustained load', unpublished.

Yeoh, D., Fragiacomo, M. & Deam, B. 2011b, 'Experimental behaviour of LVL-concrete composite floor beams at strength limit state', Engineering Structures, vol. 33, no. 9, pp. 2697-707.

Yeoh, D., Fragiacomo, M. & Deam, B. 2012, 'Long-term performance of LVL-concrete composite beams under service load', paper presented to the 12th World Conference on Timber Engineering (WCTE), Auckland, New Zealand.

Yttrup, P., 1996, 'Concrete enhanced timber', Proc., International Wood Engineering Conference (IWEC), New Orleans, USA, 3, pp. 304-308.

Zabihi, Z., Samali, B., Shrestha, R., Gerber, C. & Crews, K. 2012, 'Serviceability and ultimate performance of long span timber floor modules', paper presented to the 12th World Conference on Timber Engineering (WCTE), Auckland, New Zealand.

Zabihi, Z.: Performance of long-span timber floor modulus; PHD Thesis, University of Technology, Sydney, 2014.

Appendix A

Graphs from literature reviews

This annex presents typical curves from the literature reviews which have more relevant information for this experimental investigation

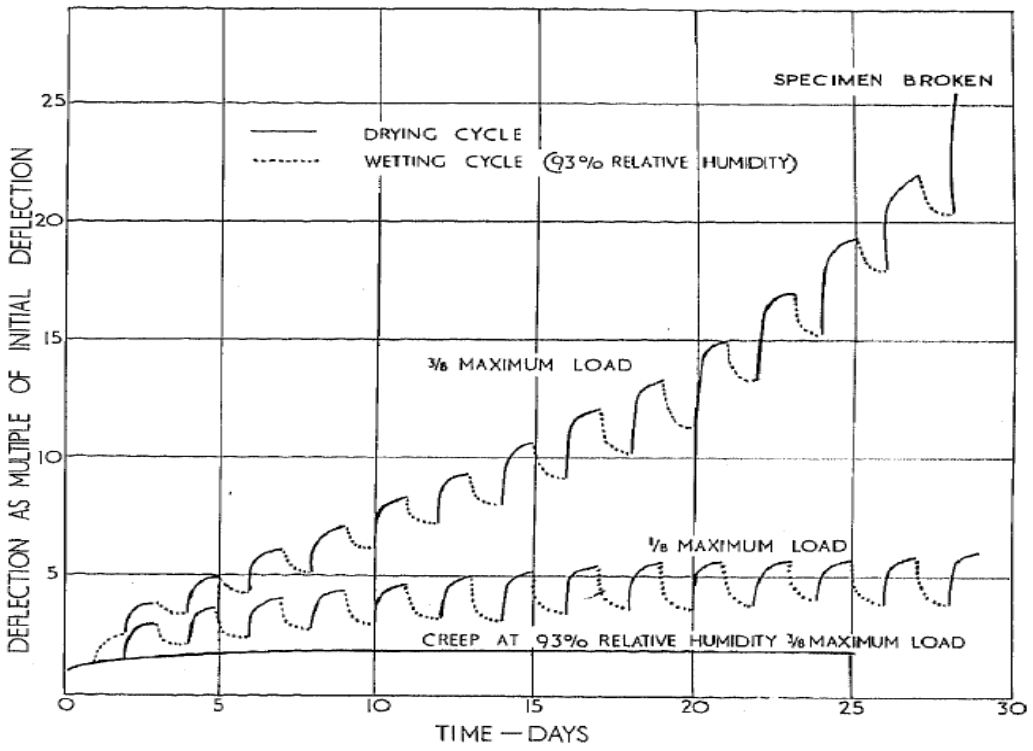

Figure 86 Relationship between deflection and length of exposure cycle (Hearmon and Paton 1964)

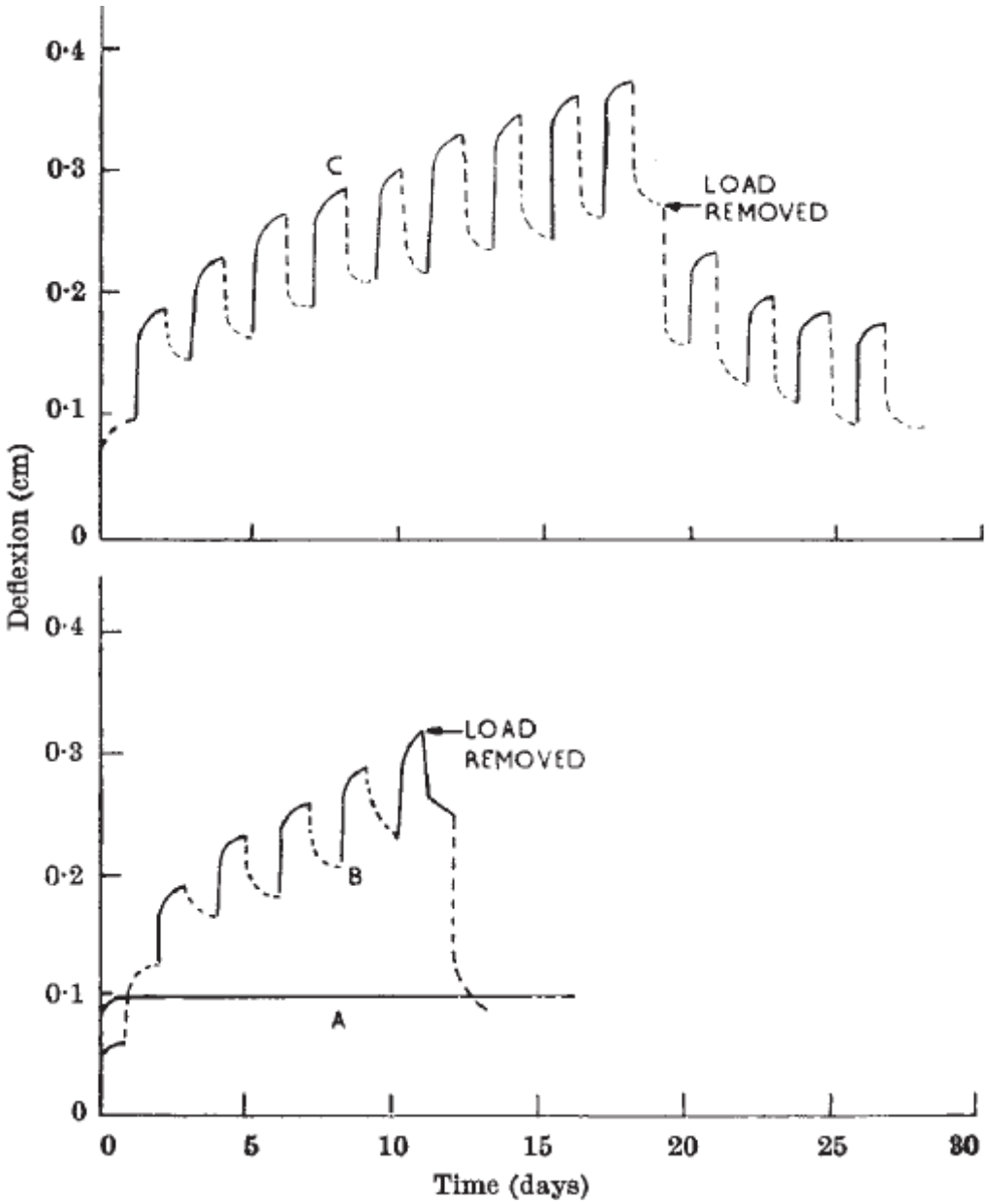

Figure 87 Deflection of loaded beech beams, Curve A, specimen maintained at R.H. 93%;Curve B, specimen, specimen loaded dry and then 'cycled'; curve, specimen loaded at R.H.93% and then 'cycled'. Solid line. R.H. zero; broken line, R.H.93%.(Gibson, 1965)

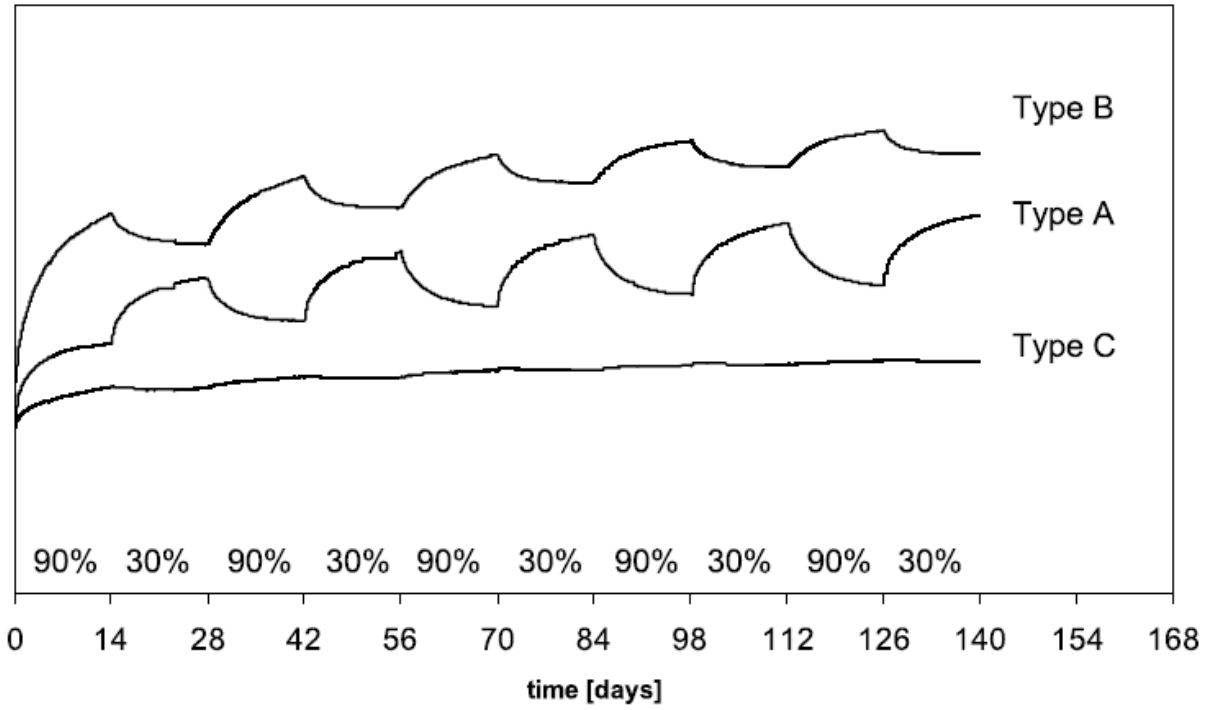

Figure 88 Typical creep curves A, B and C, due to cycling of relative humidity between 90% and 30%, adopted from Epmeier (2007)

Appendix B

This annex presents the properties of the LVL from the supplier and also the relevant properties of the connections used.

Table 19 LVL properties (Carter Holt Harvey)

Property		Characteristic value
Strength	Bending, f'_b	48 N/mm^2
	Tension, f'_t	33 N/mm^2
	Compression parallel to grain f'_c	45 N/mm^2
	Compression perpendicular to grain f'_p	12 N/mm^2
	Shear in beams, f'_s	5.3 N/mm^2
	Shear at joint details, f'_{sj}	5.3 N/mm^2
Stiffness	Modulus of elasticity, E	13200 N/mm^2
	Shear modulus, G	660 N/mm^2
Density	At 12% moisture content, ρk	620 Kg/m^3

Figure 89 the lengths of the coach screw, SFS and normal screw used in the connectors

Table 20 Shear strength of the connectors used (Khorsandnia et al 2012)

Type of connector		Normal screw	SFS screw	Notch
Shear strength, F_{max} (kN)	Range	9.4-12.3	47.0-66.2	30.8-34.5
	Average	10.9	59.5	32.6
F_{max} (5%)		9.5	46.5	30.6
std		0.9	8.0	1.1
Cov		7.9	13.4	3.5

Table 21 Slip moduli of the connectors used (Khorsandnia et al. 2012)

	Type of connector	Range	Average	std	cov
Normal screw	Slip moduli (kN/mm), K_i	5.8-29.1	14.7	9.8	66.9
	Ks,0.4	32.5-62.4	45.0	12.9	28.8
	Ks,0.6	5.8-8.0	7.1	0.8	12
	Ks,0.8	1.7-2.7	2.2	0.4	17.8
Notch	Slip moduli (kN/mm), K_i	20.2-30	26.2	4.1	15.5
	Ks,0.4	31.7-42.5	36.9	4.9	13.2
	Ks,0.6	29.1-42.0	35.1	5.4	15.4
	Ks,0.8	25.4-38.3	31.6	6.0	19
SFS screw	Slip moduli (kN/mm), K_i	21-43.5	25	7	28.1
	Ks,0.4	38.4-77.7	54.9	11.9	21.7
	Ks,0.6	28.8-42.8	34.4	4.8	13.8
	Ks,0.8	19.1-31.2	24.4	3.4	14

Table 22 Slip moduli of the connectors used (Gerber et al. 2011)

Connection Description	**Strength Q_k (kN)**	**K_{ser} (kN/mm)**	**K_u (kN/mm)**
T1 – 48mm LVL, 16mm coach screw	46 – 8.7%	87 – 20.5%	60 – 13.0%
T2 – 48mm LVL, 12mm coach screw	46 – 6.6%	106 – 15.0%	87 – 17.9%
T3 – 63mm LVL, 16mm coach screw	78 – 6.4%	109 – 19.3%	81 – 24.7%
T4 – 96mm LVL, 12mm coach screw	89 – 10.0%	110 – 34.8%	93 – 39.3%
T5 – 126mm LVL, 16mm coach screw	134 – 4.8%	124 – 41.3%	103 – 30.2%
B1 – 48mm LVL, 16mm coach screw	55 – 8.1%	37 – 12.4%	36 – 15.2%
B2 – 48mm LVL, 12mm coach screw	51 – 8.4%	115 – 48.4%	46 – 54.0%
B3 – 63mm LVL, 16mm coach screw	66 – 7.7%	98 – 12.9%	74 – 27.7%
B4 – 96mm LVL, 12mm coach screw	91 – 5.5%	156 – 19.8%	119 – 20.8%
B5 – 126mm LVL, 16mm coach screw	120 – 11.6%	213 – 34.2%	150 – 22.7%

Notes:

a) *integer = capacity; % = CV*
b) *Strength – 5th percentile based on a log normal distribution*
c) *Stiffness – 50th percentile*

Appendix C

This appendix presents the materials properties and the calculated serviceability bending stiffness's for the TCC.

Table 23: Geometric properties of concrete and timber for all the TCC beams

Concrete Topping:	B_NS
Length (mm) - Lc = Lt	6000.00
Width (mm) - Bc	600.00
Tributary width of concrete- Bc =Bt+0.2*L <= Bc	1248.00
Depth (mm) - Hc	75.00
plywood thick af =	0.00
H = hc/2 +af + ht/2	162.50
Area (mm^2) - Ac	45000.00
MoI (mm^4) - Ic	2.11E+07
LVL Timber Joists:	
Width (mm) - Bt	48
Depth (mm) - Ht	250.000
Area (mm^2) - At	12000
MoI (mm^4) - It	6.25E+07
$Zt = b_t h_t^2/6$	5.00E+05
Where, af = Plywood thickness	

Table 24: Properties of concrete used

Concrete	
Density (kg/m^3) - ρc	2390.86
Compression strength (f'c,c) at 28 days	39.54
Tensile stength (f't,c) = 0.4 * sqrt(f'c) at 28 days	2.52
Compression strength (f_{cu},91), (N/mm^2)	50.33
MoE (N/mm^2), $E_{c,j} = (\rho_c)^{1.5} \times (0.043*\sqrt{f_{cm}})$ for fcmi <40MPa	
MoE (N/mm^2), $E_{c,j} = (\rho_c)^{1.5} \times (0.043*\sqrt{f_{cm}}+0.12)$ for fcmi >40MPa	33933
the above values have a range of +-20%	

Table 25 Theoretical effective serviceability bending stiffness for B-NS

Geometric Input

Joist Span	L = 5.8 m (Total length 6.0 m)
Spacing	S = 600 mm
Beam Depth	h_t = 250 mm
Beam width	b_t = 48 mm
Concrete Thickness	h_c = 75 mm
Concrete Width	b_c = 600 mm
Concrete tributary width	$B_c = b_t+0.2L <= b_c$ ok.
Section Properties	
Area of timber	A_t = 12000 mm^2
$I_t = b_t h_t^3/12$	I_t = 62.5E+06
Area of concrete	A_c = 45000 mm^2
$I_c = b_c h_c^3/12$	I_c = 21.1E+06
Materials Properties	
Density of concrete	ρ_c = 2390.9 kg/m^3
Compressive strength at 28 days	$f'_{c,c.}$ = 39.5 MPa
Compressive strength at 91 days	$f'_{c,}$ = 50.33 MPa
MOE of concrete	E_c = 33933 MPa (AS3600-3.1.2)
Tensile strength of concrete	$f'_{t,c}$ = 2.52 MPa
Density of timber	ρ_t = 620.0 kg/m^3
Compressive strength	$f'_{c,t.}$ = 45 MPa
Bending strength	$f'_{b,t}$ = 48 MPa
Tensile strength	$f'_{t,t}$ = 33 MPa
Shear strength	$f'_{s,t.}$ = 5.3 MPa
Bearing strength	$f'_{p,t.}$ = 12 MPa
MOE of timber	E_t = 12402 MPa (this is the MOE of the LVL obtained from tests done after carved)
Connection Properties	
Stiffness of connection from push out tests	

Serviceability $K_{SLS,0.4}$ = 45000 N/mm

Ultimate at 60 % (average) $K_{ULS,0.6}$ = 7100 N/mm

Spacing of the connections

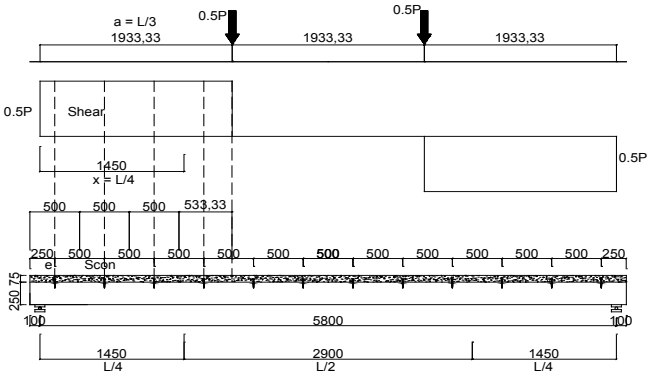

n = number of connectors along half span (from support to mid length) = 6

e = 250

s_{con} = (L/4-e)/ (n-1), S_{con} = 500 mm already given

$S_{end} = S_{con}/2 + e = 500/2+250 = 500$ mm

S_{min} = min (S_{con}, S_{end}) = 500 mm

S_{max} = L/4 + $S_{con}/2$, but for equally spaced connectors case 2($S_{con}/2$) = 500 /2 + 500 /2 = 500 mm

$S_{eff} = 0.75\ S_{min} + 0.25\ S_{max}$ = 500 mm

Gamma coefficient

$\gamma_c = \frac{1}{1+\pi^2 * E_c * A_c * \frac{S_{eff}}{(K_{SLS} * L^2)}}$,γ_c = 0.17 and γ_t = 1.0

$H = h_c/2+a_f+h_t/2$ H = 162.5 mm

$a_c = \frac{\gamma t\ Et\ AtH}{\gamma c\ Ec\ Ac + \gamma t\ Et\ At}$ a_c = 59.8 mm

$a_t = \frac{\gamma c\ Ec\ AcH}{\gamma c\ Ec\ Ac + \gamma t\ Et\ At}$ a_t = 102.7 mm

Effective bending stiffness

$EI_{eff} = E_c I_c + E_t I_t + \gamma_c E_c A_c a_c^2 + \gamma_t E_t A_t a_t^2$ EI_{eff} = 3.97E+12 Nmm^2

Table 26 Theoretical effective serviceability bending stiffness for B-4N

Geometric Input

Joist Span	L = 5.8 m (Total length 6.0 m)
Spacing	S = 600 mm
Beam Depth	h_t = 250 mm
Beam width	b_t = 48 mm
Concrete Thickness	h_c = 75 mm
Concrete Width	b_c = 600 mm
Concrete tributary width	$B_c = b_t+0.2L <= b_c$ ok.
Section Properties	
Area of timber	A_t = 12000 mm^2
$I_t = b_t h_t^3/12$	I_t = 62.5E+06
Area of concrete	A_c = 45000 mm^2
$I_c = b_c h_c^3/12$	I_c = 21.1E+06
Materials Properties	
Density of concrete	ρ_c = 2390.9 kg/m^3
Compressive strength at 28 days	$f'_{c,c.}$ = 39.5 MPa
Compressive strength at 91 days	$f'_{c,}$ = 50.33 MPa
MOE of concrete	E_c = 33933 MPa (AS3600-3.1.2)
Tensile strength of concrete	$f'_{t,c}$ = 2.52 MPa
Density of timber	ρ_t = 620.0 kg/m^3
Compressive strength	$f'_{c,t.}$ = 45 MPa
Bending strength	$f'_{b,t}$ = 48 MPa
Tensile strength	$f'_{t,t}$ = 33 MPa
Shear strength	$f'_{s,t.}$ = 5.3 MPa
Bearing strength	$f'_{p,t.}$ = 12 MPa
MOE of timber	E_t = 13153 MPa (this is the MOE of the LVL obtained from tests done after carved)
Connection Properties	
Stiffness of connection from push out tests	

Serviceability (average)	$K_{SLS,0.4}$ = 36900 N/mm
Serviceability (fifth percentile)	$K_{SLS,0.4}$ = 31700 N/mm
Ultimate (average)	$K_{ULS,0.6}$ = 35100 N/mm
Ultimate (fifth percentile)	$K_{ULS,0.6}$ = 29100 N/mm

Spacing of the connections

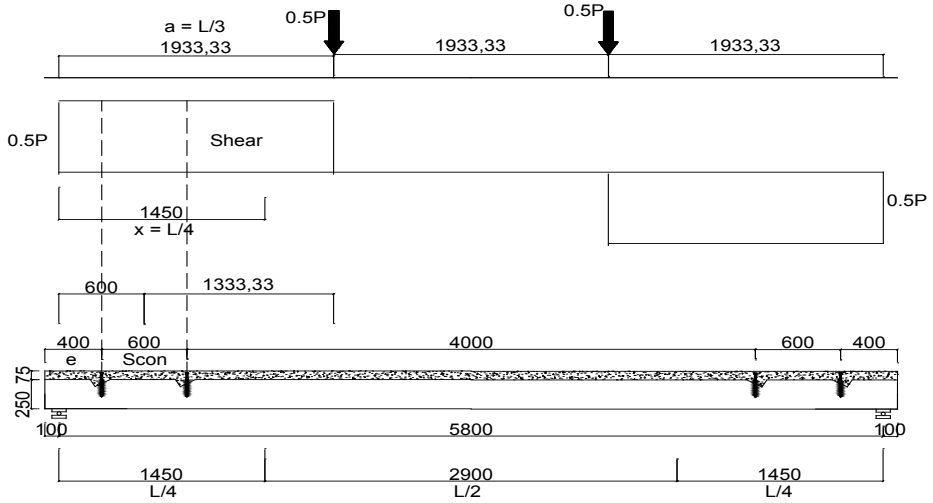

n = number of connectors along half span (from support to mid length) = 2

e = 400

s_{con} = (L/4-e)/ (n-1), S_{con} = 600 mm already given

$S_{end} = S_{con}/2 + e = 600/2+400 = 700$ mm

S_{min} = min (S_{con}, S_{end}) = 600 mm

S_{max} = 4000/2 + 600 /2 = 2300 mm

$S_{eff} = 0.75\ S_{min} + 0.25\ S_{max} = 1025$ mm

<u>Gamma coefficient</u>

$\gamma_c = \frac{1}{1+\pi^2 * E_c * A_c * \frac{S_{eff}}{(K_{sls} * L^2)}}$, γ_c = 0.074 and γ_t = 1.0

$H = h_c/2 + a_f + h_t/2$ H = 162.5 mm

$a_c = \frac{\gamma t\ Et\ At H}{\gamma c\ Ec\ Ac + \gamma t\ Et\ At}$ a_c = 94.7 mm

$a_t = \frac{\gamma c\ Ec\ Ac H}{\gamma c\ Ec\ Ac + \gamma t\ Et\ At}$ a_t = 67.79 mm

<u>Effective bending stiffness</u>

$EI_{eff} = E_c I_c + E_t I_t + \gamma_c E_c A_c a_c^2 + \gamma_t E_t A_t a_t^2$ $EI_{eff} = 3.28E+12$ Nmm^2

Table 27 Theoretical effective serviceability bending stiffness for B-6N

Geometric Input

Joist Span	L = 5.8 m (Total length 6.0 m)
Spacing	S = 600 mm
Beam Depth	h_t = 250 mm
Beam width	b_t = 48 mm
Concrete Thickness	h_c = 75 mm
Concrete Width	b_c = 600 mm
Concrete tributary width	$B_c = b_t+0.2L <= b_c$ ok.
Section Properties	
Area of timber	A_t = 12000 mm^2
$I_t = b_t h_t^3/12$	I_t = 62.5E+06
Area of concrete	A_c = 45000 mm^2
$I_c = b_c h_c^3/12$	I_c = 21.1E+06
Materials Properties	
Density of concrete	ρ_c = 2390.9 kg/m^3
Compressive strength at 28 days	$f'_{c,c.}$ = 39.5 MPa
Compressive strength at 91 days	$f'_{c,}$ = 50.33 MPa
MOE of concrete	E_c = 33933 MPa (AS3600-3.1.2)
Tensile strength of concrete	$f'_{t,c}$ = 2.52 MPa
Density of timber	ρ_t = 620.0 kg/m^3
Compressive strength	$f'_{c,t.}$ = 45 MPa
Bending strength	$f'_{b,t}$ = 48 MPa
Tensile strength	$f'_{t,t}$ = 33 MPa
Shear strength	$f'_{s,t.}$ = 5.3 MPa
Bearing strength	$f'_{p,t.}$ = 12 MPa

MOE of timber E_t = 13482 MPa (this is the MOE of the LVL obtained from tests done after carved)

Connection Properties

Stiffness of connection from push out tests

Serviceability (average) $K_{SLS,0.4}$ = 36900 N/mm

Serviceability (fifth percentile) $K_{SLS,0.4}$ = 31700 N/mm

Ultimate (average) $K_{ULS,0.6}$ = 35100 N/mm

Ultimate (fifth percentile) $K_{ULS,0.6}$ = 29100 N/mm

Spacing of the connections

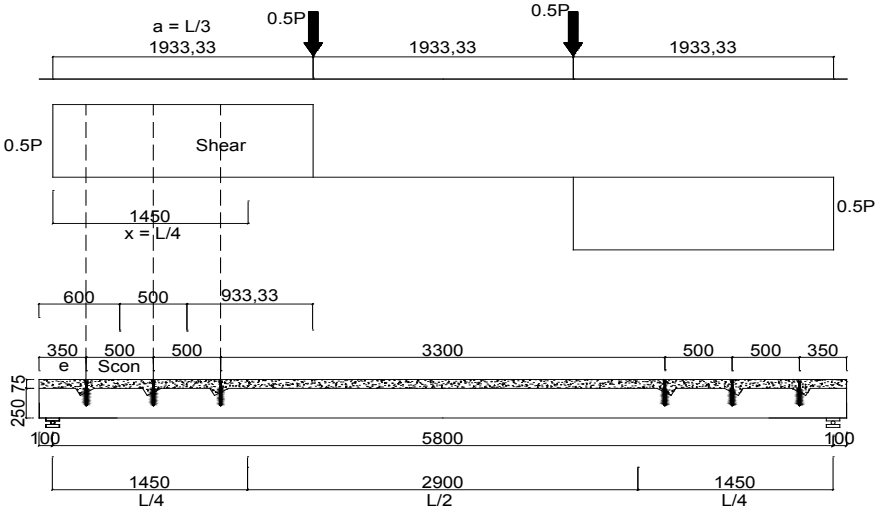

n = number of connectors along half span (from support to mid length) = 3

e = 400

s_{con} = (L/4-e)/ (n-1), S_{con} = 500 mm already given

$S_{end} = S_{con}/2 + e = 500/2+350 = 600$ mm

$S_{min} = \min(S_{con}, S_{end}) = 500$ mm

$S_{max} = 3300/2 + 500/2 = 1900$ mm

$S_{eff} = 0.75\, S_{min} + 0.25\, S_{max} = 850$ mm

Gamma coefficient

$\gamma_c = \frac{1}{1+\pi^2 * E_c * A_c * \frac{S_{ef}}{(K_{sls} * L^2)}}$, $\gamma_c = 0.088$ and $\gamma_t = 1.0$

$H = h_c/2 + a_f + h_t/2$ H = 162.5 mm

$$a_c = \frac{\gamma t\ Et\ AtH}{\gamma c\ Ec\ Ac + \gamma t\ Et\ At}$$ $a_c = 88.6$ mm

$$a_t = \frac{\gamma c\ Ec\ AcH}{\gamma c\ Ec\ Ac + \gamma t\ Et\ At}$$ $a_t = 73.9$ mm

Effective bending stiffness

$EI_{eff} = E_c I_c + E_t I_t + \gamma_c E_c A_c a_c^2 + \gamma_t E_t A_t a_t^2$ $EI_{eff} = 3.50E+12$ Nmm^2

Table 28 Theoretical effective serviceability bending stiffness for B-SFS

Geometric Input

Joist Span	L = 5.8 m (Total length 6.0 m)
Spacing	S = 600 mm
Beam Depth	h_t = 250 mm
Beam width	b_t = 48 mm
Concrete Thickness	h_c = 75 mm
Concrete Width	b_c = 600 mm
Concrete tributary width	$B_c = b_t + 0.2L <= b_c$ ok.
Section Properties	
Area of timber	$A_t = 12000\ mm^2$
$I_t = b_t h_t^3/12$	I_t = 62.5E+06
Area of concrete	$A_c = 45000\ mm^2$
$I_c = b_c h_c^3/12$	I_c = 21.1E+06
Materials Properties	
Density of concrete	$\rho_c = 2390.9\ kg/m^3$
Compressive strength at 28 days	$f'_{c,c.}$ = 39.5 MPa
Compressive strength at 91 days	$f'_{c,}$ = 50.33 MPa
MOE of concrete	E_c = 33933 MPa (AS3600-3.1.2)
Tensile strength of concrete	$f'_{t,c}$ = 2.52 MPa

Density of timber $\rho_t = 620.0$ kg/m^3

Compressive strength $f'_{c,t.} = 45$ MPa

Bending strength $f'_{b,t} = 48$ MPa

Tensile strength $f'_{t,t} = 33$ MPa

Shear strength $f'_{s,t.} = 5.3$ MPa

Bearing strength $f'_{p,t.} = 12$ MPa

MOE of timber $E_t = 12312$ MPa (this is the MOE of the LVL obtained from tests done after carved)

Connection Properties

Stiffness of connection from push out tests

Serviceability (average) $K_{SLS,0.4} = 54900$ N/mm

Serviceability (fifth percentile) $K_{SLS,0.4} = 38400$ N/mm

Ultimate (average) $K_{ULS,0.6} = 34400$ N/mm

Ultimate (fifth percentile) $K_{ULS,0.6} = 28800$ N/mm

Spacing of the connections

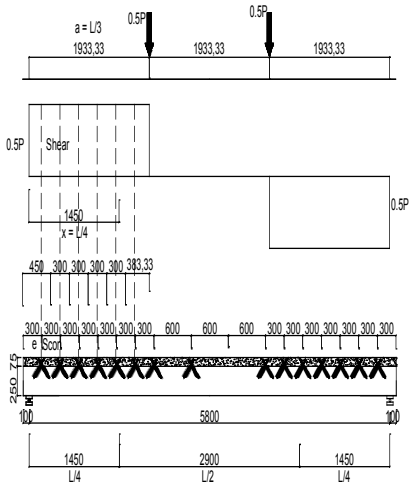

n = number of connectors along half span (from support to mid length) = 8

e = 300

$s_{con} = (L/4\text{-}e)/(n\text{-}1)$, $S_{con} = 300$ mm already given

$S_{end} = S_{con}/2 + e = 300/2 + 300 = 450$ mm

$S_{min} = \min(S_{con}, S_{end}) = 300$ mm

$S_{max} = 600/2 + 600/2 = 600$ mm

$S_{eff} = 0.75\, S_{min} + 0.25\, S_{max} = 375$ mm

Gamma coefficient

$\gamma_c = \frac{1}{1+\pi^2 * E_c * A_c * \frac{S_{cr}}{(K_{ns} * L^2)}}$,γ_c = 0.25 and γ_t = 1.0

$H = h_c/2+a_f+h_t/2$ H = 162.5 mm

$a_c = \frac{\gamma t\ Et\ AtH}{\gamma c\ Ec\ Ac + \gamma t\ Et\ At}$ a_c = 45.8 mm

$a_t = \frac{\gamma c\ Ec\ AcH}{\gamma c\ Ec\ Ac + \gamma t\ Et\ At}$ a_t = 116.7 mm

Effective bending stiffness

$EI_{eff} = E_c I_c + E_t I_t + \gamma_c E_c A_c a_c^2 + \gamma_t E_t A_t a_t^2$ EI_{eff} = 4.29E+12 Nmm^2

Appendix D

Location of the TCC beams *and the moisture content samples* in the humidity chamber.

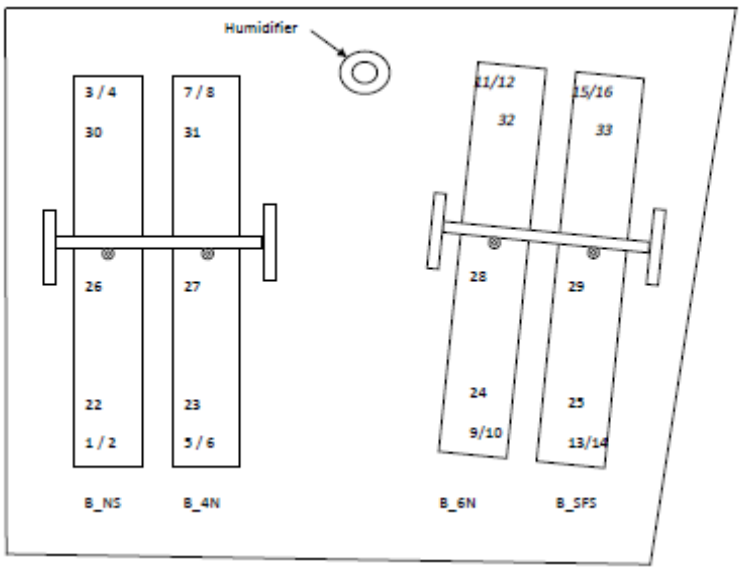

Figure 90 Location of MC samples in the fog-room

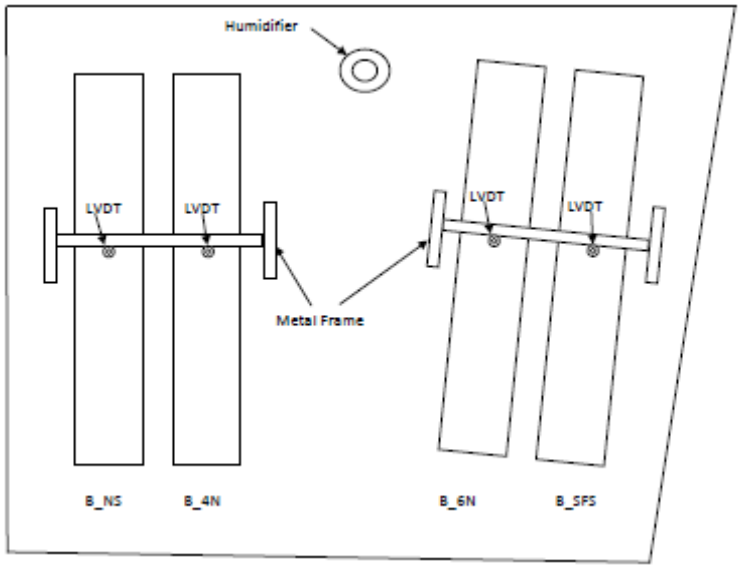

Figure 91 General layout of TCC beams in fog-room

Design load for TCC beams

Table 29 Serviceability design load for TCC beam

Actions	Material	Depth	Width	Density		
		mm	mm	kN/m^3	kN/m^2	kN/m
Dead load	Concrete	75	600	24		1.1
	finishing		600		1	0.6
	LVL	250	45	6.2		0.1
G						**1.7**
Live loads (Imposed loads)		AS/NZS 1170.1.2002				
Q			600		3	**1.8**
Design service load, W_{SLS}		$G+\Psi_\ell Q$	where:	Ψ_ℓ	0.4	**2.5**
Quasi-permannet load on the TCC beams, q						**1.05**
	Hence,			**q=**	**43%**	**W_{SLS}**

Table 30 Weights (lead bars) on the TCC beams

Beam	lead bars	Total weight	Equivalent uniform distributed load	
	pcs	kg	kN/m^2	kN/m
B-NS	26	613	1.67	1.05
B-4N	26	625	1.70	1.05
B-6N	26	638	1.74	1.05
B-SFS	26	639	1.74	1.05

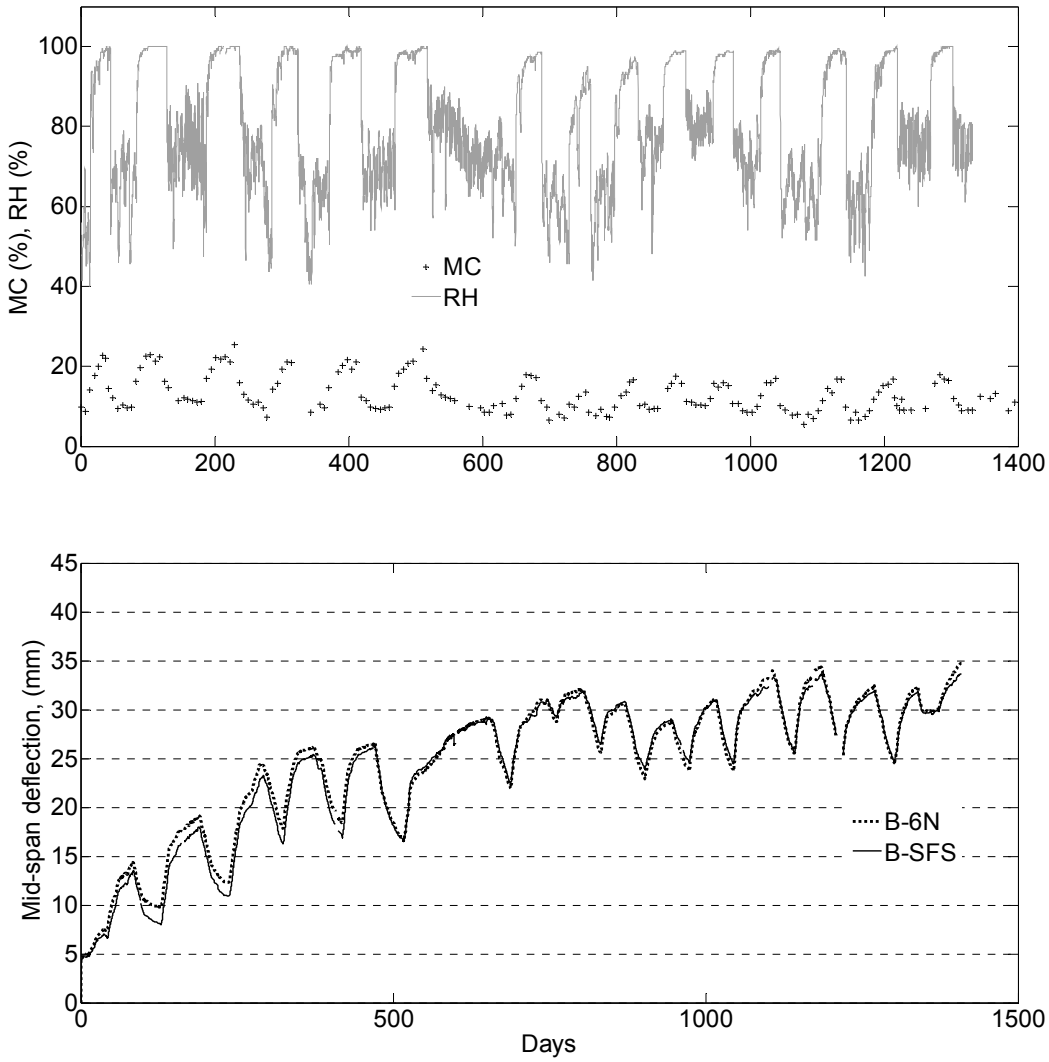

Figure 92 Relationship between air humidity and moisture content (top) and deflection (bottom) with time

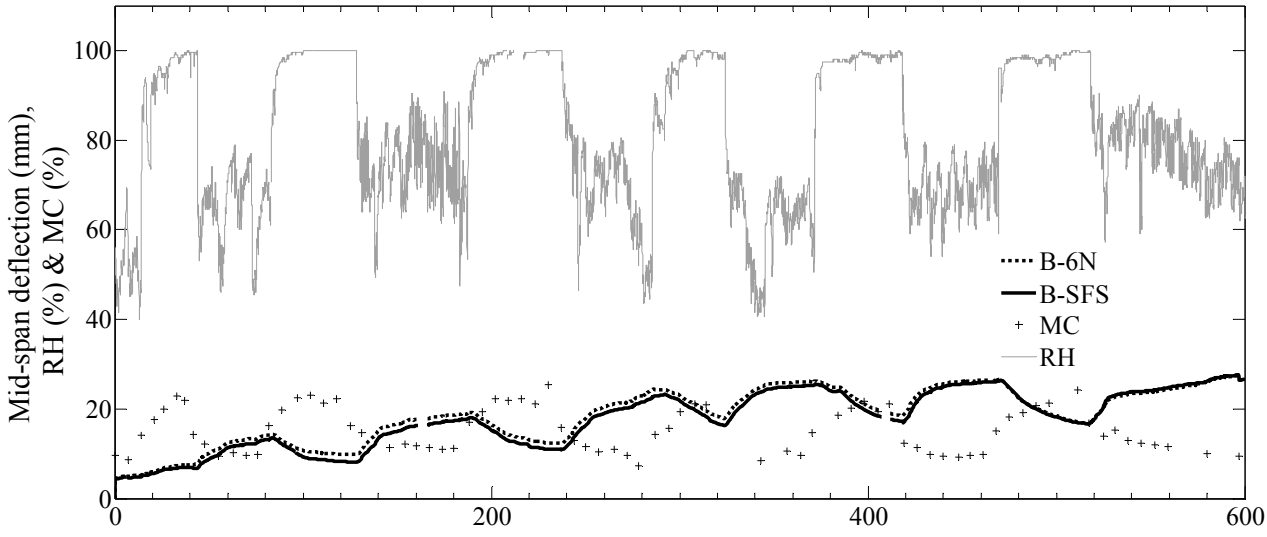

Figure 93 Relationship between deflection, moisture content and air humidity

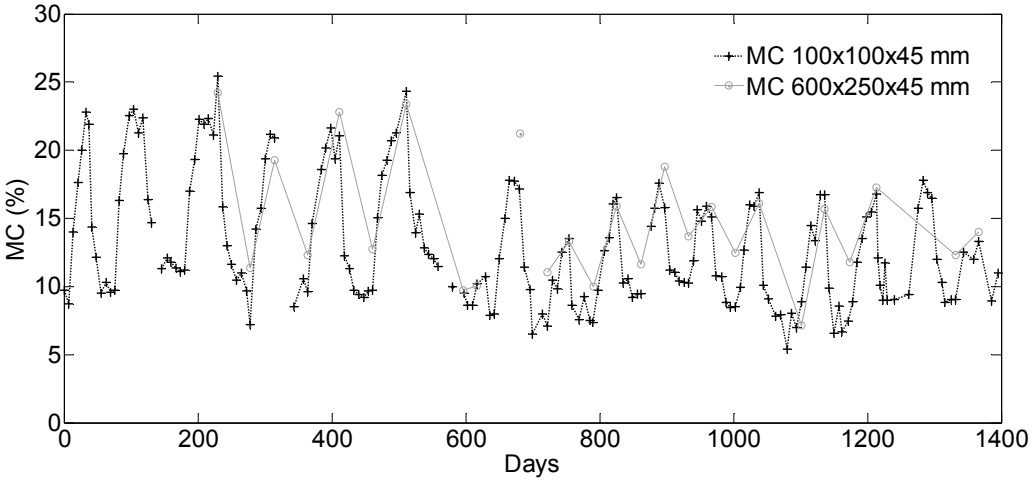

Figure 94 Comparison of the MC measurement between small and large samples.

Appendix E

This appendix presents the properties of the transformed section, composite efficiency and the creep and shrinkage factors used in analysing the long-term deflection of the TCC beams.

Table 31: Transformed section properties for B_NS (typical)

Simply Supported beam subjected to 4 point bending load (P)							
						L1 (mm)	L2 (mm)
Span	5.8	m	5800		mm	1933	1933
Section Properties							
Timber			Concrete				
Et	12.402	Gpa	Ec		50	Gpa	
b	48		b		600		
d	250		d		75		
No. of section	1		No. of section		1		
			Equivalent width		2418.96		
Calculation for fully composite action							
Modular ratio, n		4.03					
Calculation of centroid from the base							
Ref	No. of section	Area, A	Y, from the base		AxY		
Timber	1	12000	125		1500000		
Concrete	1	181422.35	287.5		52158925.98		
Sum		193422.35			53658925.98		
Y	**277.42**	**mm**					
Calculation of moment of inertia about the plane of bending							
Ref	No. of section	Ixx (mm^4)	A (mm^2)		h (mm)	Icentroid	
Timber	1	62500000.00	12000.00		152.42	341276552.06	
Concrete	1	85041727.14	181422.35		-10.08	103481123.4	
Sum					**Icentroid**	444757675.46	
		Fully composite stiffness			**EI=**	**5.51588E+12**	**Nmm^2**

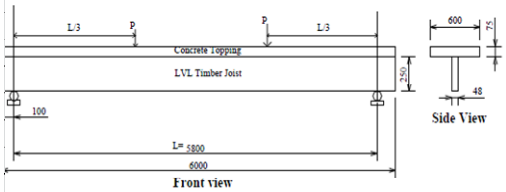

Figure: TCC beam's Geometry

Calculation for fully non-composite action				
Ref	I	E	EI	
	mm4	Mpa		
Timber	62500000	12402	7.75125E+11	
Concrete	85041727.14	12402	1.05469E+12	
		EI=	**1.82981E+12**	Nmm^2

Table 32: Bending stiffness theoretical and experimental

Beam	EI (Nmm^2)		
	non-composite	fully-composite	experimental
B-NS	1.8E+12	5.5E+12	2.8E+12
B-4N	1.9E+12	5.8E+12	4.1E+12
B-6N	1.9E+12	5.9E+12	4.3E+12
B-SFS	1.8E+12	5.5E+12	4.6E+12

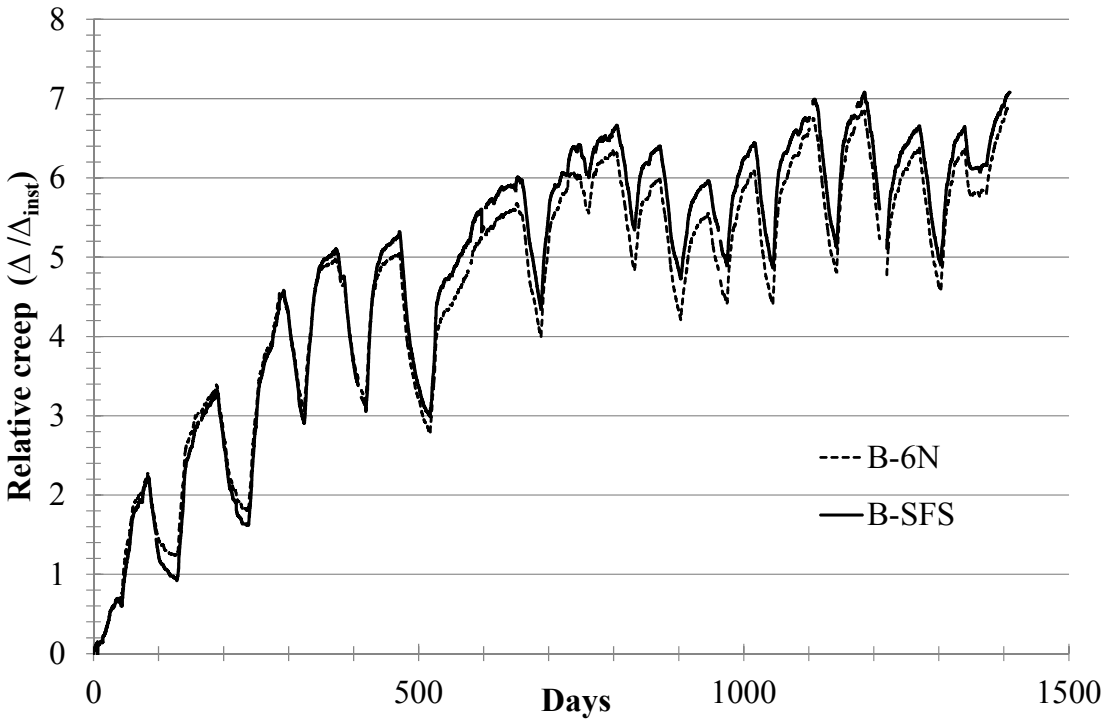

Figure 95 Relative creep of TCC beams with time

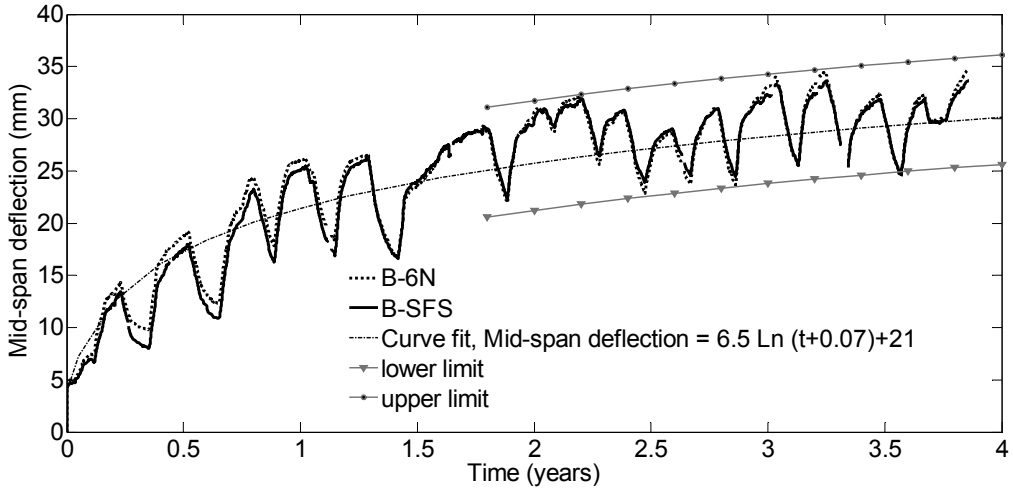

Figure 96 Logarithmic curve fitting

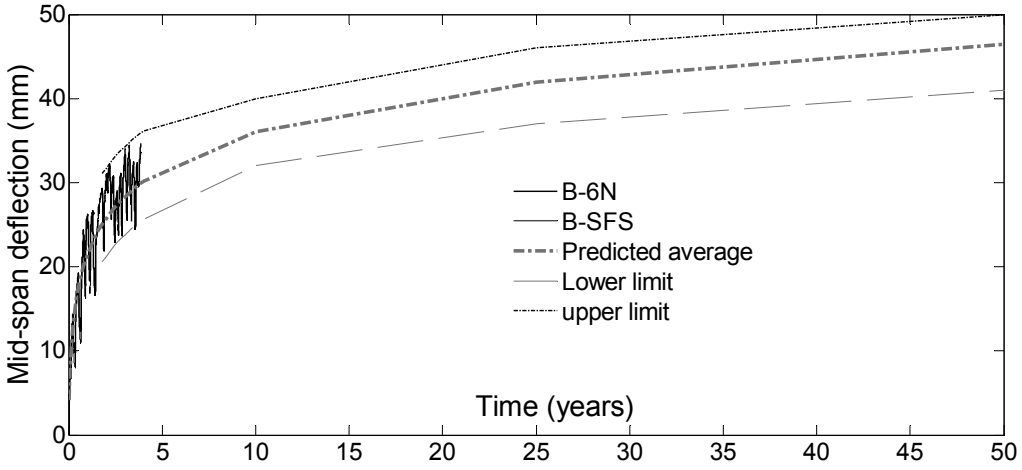

Figure 97 Logarithmic curve fitting

Creep and Shrinkage coefficients of concrete

Table 33: Concrete design creep coefficient (t=3years after loading)

Concrete Creep coeff										
AS3600-2009 (Clause 3.1.8)										
B_c	600		h_c	75						
f'c (MPa)	39.54	at t_o days								
t_o	200		t	3650	days					
Table 3.1.8.2		Basic creep coefficient								
f'c (MPa)		20	25	32		40	>50			
Creep factor,$\varphi_{cc\,b}$		5.2	4.2	3.4		2.8	2			
Design creep factor,	$K_2 K_3 K_4 K_5 \varnothing_{ccb} = \varnothing cc$			t_h =2Ag/exposed perimeter						
t_h = hypotetical thickness		.= 2Ag/Ue		Ag =2*B_c*h_c /(2*(B_c+h_c)-48)			69.12			
time "t" after loading		3 years								
k_2	1.6	Figure 3.1.8.3A, interior environments and time after t days of loading								
k_3 = 2.7 /	0.817926527	Figure 3.1.8.3B, age of concrete at time of loading				200	days			
k_4	0.65	for interior environment according to 3.1.8.3								
k_5	1	for f'c < 50MPa according to 3.1.8.3								
$\varnothing_{ccb}$ =	2.8	for f'_c	40	according to Table 3.1.8.2 AS 3600 -2009						
Design creep factor,										
$K_2 K_3 K_4 K_5 \varnothing_{ccb} = \varnothing cc$	2.3818									

Table 34: Concrete design creep coefficient (t=0, instant of loading)

Concrete Creep coeff										
AS3600-2009 (Clause 3.1.8)										
B_c	600		h_c	75						
f'c (MPa)	39.54	at t_o days								
t_o	200		t	3650	days					
Table 3.1.8.2		Basic creep coefficient								
f'c (MPa)		20	25	32		40	>50			
Creep factor,$\varphi_{cc\,b}$		5.2	4.2	3.4		2.8	2			
Design creep factor,	$K_2 K_3 K_4 K_5 \varnothing_{ccb} = \varnothing cc$			t_h =2Ag/exposed perimeter						
t_h = hypotetical thickness		.= 2Ag/Ue		Ag =2*B_c*h_c /(2*(B_c+h_c)-48)			69.12			
time "t" after loading		1 days								
k_2	0.15	Figure 3.1.8.3A, interior environments and time after t days of loading								
k_3 = 2.7 /(1+log(t))	0.818	Figure 3.1.8.3B, age of concrete at time of loading				200	days			
k_4	0.65	for interior environment according to 3.1.8.3								
k_5	1	for f'c < 50MPa according to 3.1.8.3								
$\varnothing_{ccb}$ =	2.8	for f'_c	40	according to Table 3.1.8.2 AS 3600 -2009						
Design creep factor,										
$K_2 K_3 K_4 K_5 \varnothing_{ccb} = \varnothing cc$	0.2233									

Table 35: Concrete design shrinkage coefficient

Concrete shrinkage					
AS 3600 - 2009 (Clause 3.1.7)					
B_c	600	h_c	75		
f'c (MPa)	39.54	at t_o days			
t_o	200	t	1095	days	time after loading
3.1.7. Shrinkage					
3.1.7.1 calculation of design shrinkage strain					
a) from measurement on similar local concrete					
b) by tests after eight weeks of drying modified for long-term value,in accordance with AS1012.13;					
c) by calculation in accordance with clause 3.1.7.2					
3.1.7.2 Design shrinkage strain					
it is the sum of chemical (autogenous) shrinkage strain and drying shrinkage strain					
$\varepsilon_{cs} = \varepsilon_{cse} + \varepsilon_{csd}$		$\varepsilon_{cse} = \varepsilon^*_{cse}\ (1-e^{-0.1t})$		autogenous shrinkage strain	
ε^*_{cse} = (0.06f'c-1)(50/100000(		6.86E-05		final autogenous shrinkage strain	
$\varepsilon_{cse} = \varepsilon^*_{cse}\ (1-e^{-0.1t})$		6.86E-05		e =	2.7183
At any time t (in days) after the commencement of drying, the drying shrinkage strain shall be taken as-					
$\varepsilon_{csd} = k_1 k_4 \varepsilon_{csd,b}$					
K_1	1.58	Figure 3.1.7.2 , AS 3600 -2900			
at time " t " since commencement of drying			3	years	and with t_h
t_h = hypotetical thickness	.= 2Ag/Ue		Ag =2*B_c*h_c /(2*(B_c+h_c)-48)		69.12
K_4	0.65	for interior environment, AS 3600 - 2009			
$\varepsilon_{csd,b}$ = (1.0 - 0.008 f'c) * $\varepsilon^*_{csd,b}$		1.05E-03	$\varepsilon^*_{csd,b}$ =	8.00E-04	for Sydney
$\varepsilon_{csd} = k_1 k_4 \varepsilon_{csd,b}$		0.001081			
$\varepsilon_{cs} = \varepsilon_{cse} + \varepsilon_{csd}$		0.00115			
The Design shrinkage coefficient for concrete		0.0012			

Table 36: Long-term bending stiffness of B-6N

Geometric Input

Joist Span	L = 5.8 m (Total length 6.0 m)
Spacing	S = 600 mm
Beam Depth	h_t = 250 mm
Beam width	b_t = 48 mm
Concrete Thickness	h_c = 75 mm
Concrete Width	b_c = 600 mm
Concrete tributary width	$B_c = b_t+0.2L <= b_c$ ok.
Section Properties	
Area of timber	A_t = 12000 mm^2
$I_t = b_t h_t^3/12$	I_t = 62.5E+06
Area of concrete	A_c = 45000 mm^2

$I_c = b_c h_c^3/12$ $I_c = 21.1E+06$

Materials Properties

Density of concrete $\rho_c = 2390.9$ kg/m^3

Compressive strength at 28 days $f'_{c,c.} = 39.5$ MPa

Compressive strength at 91 days $f'_{c,} = 50.33$ MPa

MOE of concrete $E_c = 33933$ MPa (AS3600-3.1.2)

Tensile strength of concrete $f'_{t,c} = 2.52$ MPa

Density of timber $\rho_t = 620.0$ kg/m^3

Compressive strength $f'_{c,t.} = 45$ MPa

Bending strength $f'_{b,t} = 48$ MPa

Tensile strength $f'_{t,t} = 33$ MPa

Shear strength $f'_{s,t.} = 5.3$ MPa

Bearing strength $f'_{p,t.} = 12$ MPa

MOE of timber $E_t = 13482$ MPa (this is the MOE of the LVL obtained from tests done after carved)

Connection Properties

Stiffness of connection from push out tests

Serviceability (average) $K_{SLS,0.4} = 36900$ N/mm

Serviceability (fifth percentile) $K_{SLS,0.4} = 31700$ N/mm

Ultimate (average) $K_{ULS,0.6} = 35100$ N/mm

Ultimate (fifth percentile) $K_{ULS,0.6} = 29100$ N/mm

$S_{min} = \min(S_{con}, S_{end}) = 500$ mm

$S_{max} = 3300/2 + 500/2 = 1900$ mm

$S_{eff} = 0.75\, S_{min} + 0.25\, S_{max} = 850$ mm

Effective modulus

Concrete: $Ec = \frac{Ec}{(1+ecs)+(1+\emptyset cc)}$, = 27705.9 MPa

Gamma coefficient

$\gamma_c = \frac{1}{1+\pi^2 * E_c * A_c * \frac{S_{eff}}{(K_{SLS} * L^2)}}$, $\gamma_c = 0.109$ and $\gamma_t = 1.0$

$H = h_c/2+a_f+h_t/2$ $H = 162.5$ mm

$$a_c = \frac{\gamma t\ Et\ AtH}{\gamma c\ Ec\ Ac + \gamma t\ Et\ At}$$ $a_c = 88.33$ mm

$$a_t = \frac{\gamma c\ Ec\ AcH}{\gamma c\ Ec\ Ac + \gamma t\ Et\ At}$$ $a_t = 74.2$ mm

Effective bending stiffness

$EI_{eff} = E_c I_c + E_t I_t + \gamma_c E_c A_c a_c^2 + \gamma_t E_t A_t a_t^2$ $EI_{eff} = 3.38E+12$ Nmm^2

At time t= ∞

Effective modulus

Concrete: $E_{c,fin} = \frac{E_{cm}(t)}{(1+\varphi(\infty,t_0))} = 10027$ MPa

Timber: $E_{t,fin} = \frac{E_{0,mean}}{(1+k_{def})} = 4494$ MPa

$K_{fin} = \frac{K}{(1+2k_{def})} = 7380$ kN/mm

Gamma coefficient

$\gamma_c = \frac{1}{1+\pi^2 * E_c * A_c * \frac{S_{ef}}{(K_{ins} * L^2)}}$, $\gamma_c = 0.063$ and $\gamma_t = 1.0$

$H = h_c/2+a_f+h_t/2$ $H = 162.5$ mm

$$a_c = \frac{\gamma t\ Et\ AtH}{\gamma c\ Ec\ Ac + \gamma t\ Et\ At}$$ $a_c = 106.24$ mm

$$a_t = \frac{\gamma c\ Ec\ AcH}{\gamma c\ Ec\ Ac + \gamma t\ Et\ At}$$ $a_t = 56.26$ mm

Effective bending stiffness

$EI_{eff} = E_c I_c + E_t I_t + \gamma_c E_c A_c a_c^2 + \gamma_t E_t A_t a_t^2$ $EI_{eff} = 9.85E+11$ Nmm^2

Table 37: Long-term bending stiffness of B-SFS

Geometric Input	
Joist Span	L = 5.8 m (Total length 6.0 m)
Spacing	S = 600 mm
Beam Depth	h_t = 250 mm
Beam width	b_t = 48 mm
Concrete Thickness	h_c = 75 mm
Concrete Width	b_c = 600 mm
Concrete tributary width	$B_c = b_t+0.2L <= b_c$ ok.
Section Properties	
Area of timber	A_t = 12000 mm^2
$I_t = b_t h_t^3/12$	I_t = 62.5E+06
Area of concrete	A_c = 45000 mm^2
$I_c = b_c h_c^3/12$	I_c = 21.1E+06
Materials Properties	
Density of concrete	ρ_c = 2390.9 kg/m^3
Compressive strength at 28 days	$f'_{c,c.}$ = 39.5 MPa
Compressive strength at 91 days	$f'_{c,}$ = 50.33 MPa
MOE of concrete	E_c = 33933 MPa (AS3600-3.1.2)
Tensile strength of concrete	$f'_{t,c}$ = 2.52 MPa
Density of timber	ρ_t = 620.0 kg/m^3
Compressive strength	$f'_{c,t.}$ = 45 MPa
Bending strength	$f'_{b,t}$ = 48 MPa
Tensile strength	$f'_{t,t}$ = 33 MPa
Shear strength	$f'_{s,t.}$ = 5.3 MPa
Bearing strength	$f'_{p,t.}$ = 12 MPa
MOE of timber	E_t = 12312 MPa (this is the MOE of the LVL obtained from tests done after carved)
Connection Properties	

Stiffness of connection from push out tests

Serviceability (average)	$K_{SLS,0.4}$ = 54900 N/mm
Serviceability (fifth percentile)	$K_{SLS,0.4}$ = 38400 N/mm
Ultimate (average)	$K_{ULS,0.6}$ = 34400 N/mm
Ultimate (fifth percentile)	$K_{ULS,0.6}$ = 28800 N/mm

Spacing of the connections

S_{min} = min (S_{con}, S_{end}) = 300 mm

S_{max} = 600 /2 + 600 /2 = 600 mm

S_{eff} = 0.75 S_{min} + 0.25 S_{max} = 375 mm

Effective modulus

Concrete: $Ec = \frac{Ec}{(1+\varepsilon cs)+(1+\emptyset cc)}$ = 27705.9 MPa

Gamma coefficient

$\gamma_c = \frac{1}{1+\pi^2 * E_c * A_c * \frac{S_{ef}}{(K_{ns} * L^2)}}$, γ_c = 0.29 and γ_t = 1.0

$H = h_c/2+a_f+h_t/2$	H = 162.5 mm
$a_c = \frac{\gamma t\ Et\ AtH}{\gamma c\ Ec\ Ac + \gamma t\ Et\ At}$	a_c = 47.6 mm
$a_t = \frac{\gamma c\ Ec\ AcH}{\gamma c\ Ec\ Ac + \gamma t\ Et\ At}$	a_t = 114.9 mm

Effective bending stiffness

$EI_{eff} = E_c I_c + E_t I_t + \gamma_c E_c A_c a_c^2 + \gamma_t E_t A_t a_t^2$ EI_{eff} = 4.11E+12 Nmm^2

At time t= ∞

Effective modulus

Concrete: $E_{c,fin} = \frac{E_{cm}(t_o)}{(1+\varphi(t,t_o))}$ = 10027 MPa

Timber: $E_{t,fin} = \frac{E_{o,mean}}{(1+k_{def})}$ = 4104 MPa

$$K_{fin} = \frac{K}{(1 + 2k_{def})} = 10980 \text{ kN/mm}$$

Gamma coefficient

$$\gamma_c = \frac{1}{1 + \pi^2 * E_c * A_c * \frac{S_{cr}}{(K_{ns} * L^2)}}$$, $\gamma_c = 0.18$ and $\gamma_t = 1.0$

$H = h_c/2 + a_f + h_t/2$ $H = 162.5$ mm

$$a_c = \frac{\gamma t \, Et \, AtH}{\gamma c \, Ec \, Ac + \gamma t \, Et \, At}$$ $a_c = 61.1$ mm

$$a_t = \frac{\gamma c \, Ec \, AcH}{\gamma c \, Ec \, Ac + \gamma t \, Et \, At}$$ $a_t = 101.4$ mm

Effective bending stiffness

$EI_{eff} = E_c I_c + E_t I_t + \gamma_c E_c A_c a_c^2 + \gamma_t E_t A_t a_t^2$ $EI_{eff} = 1.28E+12$ Nmm^2

Table 38: Predicted immediate mid span deflection of the TCC beam during loading (Euro code 5)

Beam	B-NS	B-4N	B-6N	B-SFS
Loads and Load combinations				
q = quasi-permanent (lead bars), kN/m	1.05			
Self weight (G), kN/m	0.00			
Q, kN/m	0.00			
$G + \psi Q$, kN/m ($\psi = 0.4$)	1.05			
Effective bending stiffness				
EI_{eff} (Nmm^2)	3.84.E+12	3.29.E+12	3.38.E+12	4.11.E+12
Mid-span deflection (mm)				
$\Delta = 5 (G + \psi Q) L^4/384EI_{eff}$	4.0	4.7	4.6	3.8

Table 39: Predicted mid span deflection of the TCC beam at the end of life (Euro code 5)

Beam	B-6N	B-SFS
Loads and Load combinations		
q = quasi-permanent (lead bars), kN/m	1.05	
Self weight (G), kN/m	1.20	
Q, kN/m	0.00	
$G + \psi Q$, kN/m ($\psi = 4$)	2.25	
Effective bending stiffness		
EI_{eff} (Nmm^2)	9.90.E+11	1.28.E+12
Mid-span deflection (mm)		
$\Delta = 5 (G + \psi Q) L^4/384EI_{eff}$	33.5	25.9

Appendix F

This annex presents the short term results in order to compare those tests conducted before the long-term test and after the long-term test.

Table 40 Magnitude of strain along mid span cross section during serviceability test (Pham, 2010)

			Strain (με) at a total load of 2P						
		Load 2P (kN)	2kN	4kN	6kN	8kN			
	Strain gauge locations from bottom of LVL	325	0.00	0.00	0.00	0.00			
		325	-28.67	-59.33	-91.00	-118.67			
		250	12.33	33.33	52.75	73.50			
		249.9	**-6.25**	**-55.00**	**-80.00**	**-120.00**			
		240	-6.25	-43.00	-71.75	-97.00			
		125	49.67	83.33	121.67	157.67			
		0	115.67	239.00	360.33	492.67			
		0	0.00	0.00	0.00	0.00			
		Timber N.A.	0	0	0	0			

Table 41 Magnitude of strain along mid span cross section during ultimate

			Strain (με) at a total load of 2P						
		Load 2P (kN)	2kn	4kN	6kN	8kN	10kN	20kN	22.8kN
		325	0	0	0	0	0	0	0
	Strain gauge locations from bottom of LVL	325	-23.358	-46.716	-72.669	-92.782	-123.926	-195.297	-208.922
		250	27.9	54.503	92.136	140.151	232.287	485.986	581.367
		249.99	**-250.00**	**-411.47**	**-641.71**	**-896.43**	**-1161.77**	**-2942.36**	**-3680.27**
		240	-217.312	-382.729	-597.446	-835.516	-1084.61	-2760.18	-3460.11
		125	1.946	11.03	15.571	18.166	15.571	-53.85	-112.891
		20	198.47	370.351	568.823	779.62	980.037	2223.41	2639.116
		0	200	430	690	890	1150	2550	3100

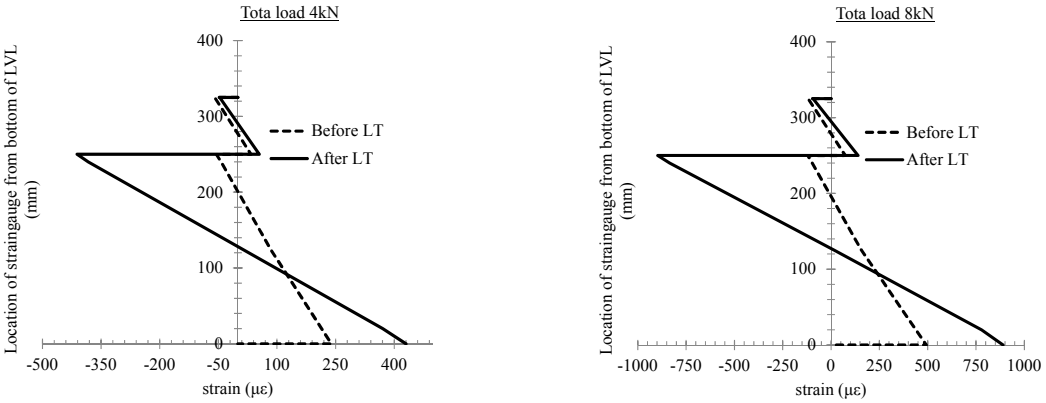

Figure 98 Magnitude of the Strain measured on tests conducted before and after long-term test for B-NS (LT= long-term test)

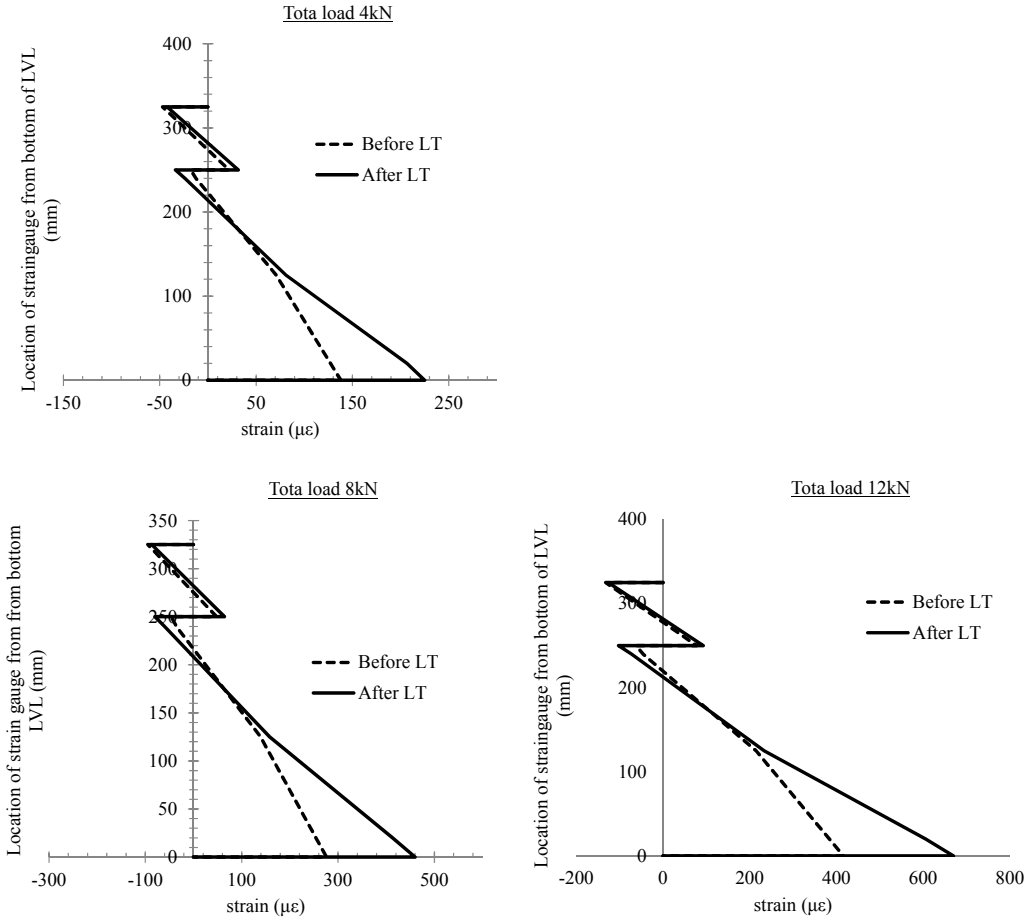

Figure 99 Magnitude of the Strain measured on tests conducted before and after long-term test for B-4N (LT= long-term test)

Appendix G

This annex presents a calculation example of timber composite beams, based on the theoretical method for composite section suggested in chapter 5. The main purpose of this appendix is to obtain the maximum failure loads and compare them with the failure loads obtained from the experiment.

Table 42: ULS analysis of beam B-NS

Geometric Input

Joist Span	L = 5.8 m (Total length 6.0 m)
Spacing	S = 600 mm
Beam Depth	h_t = 250 mm
Beam width	b_t = 48 mm
Concrete Thickness	h_c = 75 mm
Concrete Width	b_c = 600 mm
Concrete tributary width	$B_c = b_t+0.2L <= b_c$ ok.
Section Properties	
Area of timber	A_t = 12000 mm^2
$I_t = b_t h_t^3/12$	I_t = 62.5E+06
Area of concrete	A_c = 45000 mm^2
$I_c = b_c h_c^3/12$	I_c = 21.1E+06
Materials Properties	
Density of concrete	ρ_c = 2390.9 kg/m^3
Compressive strength at 28 days	$f'_{c,c.}$ = 39.5 MPa
Compressive strength at 91 days	$f'_{c,}$ = 50.33 MPa
MOE of concrete	E_c = 33933 MPa (AS3600-3.1.2)
Tensile strength of concrete	$f'_{t,c}$ = 2.52 MPa
Density of timber	ρ_t = 620.0 kg/m^3
Compressive strength	$f'_{c,t.}$ = 45 MPa
Bending strength	$f'_{b,t}$ = 48 MPa
Tensile strength	$f'_{t,t}$ = 33 MPa

Shear strength $f'_{s,t.}$ = 5.3 MPa

Bearing strength $f'_{p,t.}$ = 12 MPa

MOE of timber E_t = 12402 MPa (this is the MOE of the LVL obtained from tests done after carved)

Connection Properties

Stiffness of connection from push out tests

Serviceability $K_{SLS,0.4}$ = 45000 N/mm

Ultimate at 60 % (average) $K_{ULS,0.6}$ = 7100 N/mm

Spacing of the connections

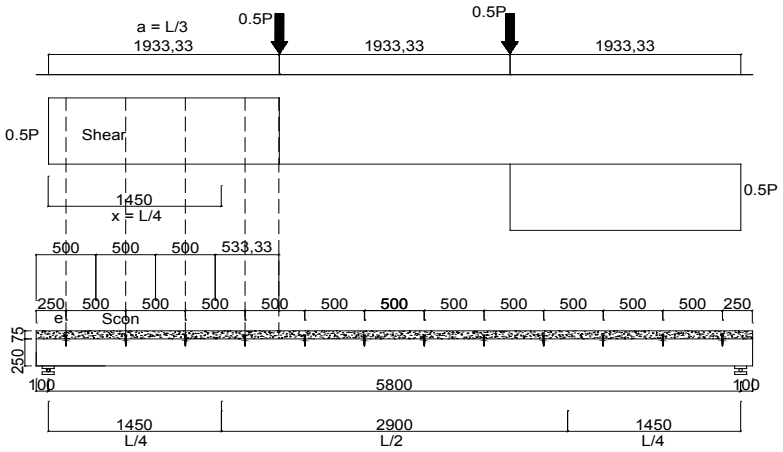

n = number of connectors along half span (from support to mid length) = 6

e = 250

s_{con} = (L/4-e)/ (n-1), S_{con} = 500 mm already given

$S_{end} = S_{con}/2 + e = 500/2+250 = 500$ mm

S_{min} = min (S_{con}, S_{end}) = 500 mm

S_{max} = L/4 + $S_{con}/2$, but for equally spaced connectors case 2($S_{con}/2$) = 500 /2 + 500 /2 = 500 mm

S_{eff} = 0.75 S_{min} + 0.25 S_{max} = 500 mm

Gamma coefficient

$$\gamma_c = \frac{1}{1+\pi^2 * E_c * A_c * \frac{S_{eff}}{(K_{uls} * L^2)}}$$,γ_c = 0.03 and γ_t = 1.0

$H = h_c/2+a_f+h_t/2$ H = 162.5 mm

$a_c = \frac{\gamma t\ Et\ AtH}{\gamma c\ Ec\ Ac + \gamma t\ Et\ At}$ a_c = 123.6 mm

$a_t = \frac{\gamma c\ Ec\ AcH}{\gamma c\ Ec\ Ac + \gamma t\ Et\ At}$ a_t = 38.9 mm

Effective bending stiffness

$EI_{eff} = E_c I_c + E_t I_t + \gamma_c E_c A_c a_c^2 + \gamma_t E_t A_t a_t^2$ EI_{eff} = 2.43E+12 Nmm^2

Analysis of the beam (strength limitations of the sections)

Concrete:

Bending strength limited by concrete capacity

$\phi M_u = \phi f'_c \frac{2(EI)_{eff}}{\gamma_c E_c h_c}$, Where (ϕ =0.6) ϕM_u =

1922.25E+06 Nmm

and the applied bending stress is $\sigma_{b,c} = \frac{E_c h_c M^*}{2(EI)_{eff}.}$, $\sigma_{b,c} = (52.4E-08)M^*$

Concrete axial capacity, $\phi N_u = \phi f'_c A_c = 1358.9E+03\ N$, and the applied axial stress is

$\sigma_{c,c} = \frac{\gamma_c E_c a_c M^*}{(EI)_{eff}.}$, $\sigma_{c,c} = (5.18E-08)M^*$, $N^*_c\ \sigma_{c,c} A_c = 0.23E-03M^*$ and the

Check compressive strength

$f'_{c,c} \geq \sigma_{c,c} + \sigma_{b,c}$ and $f'_{c,c} \geq (5.18E-08) + (52.4E-08)$, $f'_{c,c} \geq f'_{c,c}$

Hence, M* < (50.33) / 57.58E-08 < 87408.8 kNmm

The equivalent load at four point loading test should not exceed; M* = (P_{tot}/2) a (where: a = L/3) and P_{tot} < 90.4 kN

Check tensile strength

$f'_{c,t} \geq \sigma_{c,c} - \sigma_{b,c}$ and $f'_{c,t} \geq (5.18E-08)$ $(52.4E-08)$, $f'_{c,t} \geq f'_{c,t}$

Hence, M* < (2.52) / 47.22E-08 < 5336.7 kNmm

The equivalent load at four point loading test should not exceed; M* = (P_{tot}/2) a (where: a = L/3)

P_{tot} < 5.5 kN , Note that steel mesh are provided to resist the tensile stresses on the concrete.

Timber:

Bending strength limited by timber capacity

Φ = 0.85 (capacity factor)

K_1 = 1.0 (standard test)

K_4 = 1.0 (moisture content < 15 %)

K_6 = 1.0 (normal temperature)

K_9 = 1.0

K_{11} = 1.0 (size factor for bending)

K_{12} = 1.0 (stability factor)

$$\phi M_u = \phi K_1 K_4 K_6 K_9 K_{11} K_{12} f'_b \frac{2(\mathrm{EI})_{eff}}{\gamma_t E_t h_t} \qquad \phi M_u = \qquad 60.3$$

E+6Nmm

K_{11} = 0.958 (size factor for tension)

and the applied bending stress is $\sigma_{b,t} = \dfrac{E_t h_t M^*}{2(\mathrm{EI})_{eff}.}$, $\sigma_{b,t} = (63.8E-08)M^*$

Timber axial capacity

and $\phi N_u = \phi K_1 K_4 K_6 K_9 K_{11} K_{12} f'_t A_t$,

, $\phi N_u = 0.322\ E+06\ N$, and the applied axial stress is;

$\sigma_{t,t} = \dfrac{\gamma_t E_t a_t M^*}{(\mathrm{EI})_{eff}.}$, $\sigma_{t,t} = (19.8E-08)M^*$, $N^*_t = \sigma_{t,t} A_t = 2.38E-03M^*$ and the

Check combined stresses

$\dfrac{N^*_t}{\varphi N_u.} + \dfrac{M^*}{\varphi M_u}$

, Substituting the above values in the equation; 7.4E-09M*+16.6E-

09M* < 1.0,

Hence, M* < 1/ 23.98E-09 < 41701.4 kNmm

The equivalent load at four point loading test should not exceed; M* = (P_{tot}/2) a (where: a = L/3) and P_{tot} < 43.14 kN

Shear connector strength

Φ = 0.8 (capacity factor for nails)

K_1 = 0.86 (short term test 5 hours for connection)

$\phi N_j = \phi K_1 K_4 K_6 Q_k$

Q_k = 10.9 kN (average strength) , $\phi N_j = 7.5 kN$

At the support (x=0) ,

V* = P_{tot}/2 (four point loading)

$Q^* = \gamma_c E_c A_c a_c S_{\min} V^* / (EI)_{eff}$, = 1.17V*, and $\varphi N_j \geq Q^*$, hence,

$7.5E+03 \geq 1.17V^*$

, P_{tot} = 13 kN

Table 43: ULS analysis of the beam B-4N

Geometric Input

Joist Span	L = 5.8 m (Total length 6.0 m)
Spacing	S = 600 mm
Beam Depth	h_t = 250 mm
Beam width	b_t = 48 mm
Concrete Thickness	h_c = 75 mm
Concrete Width	b_c = 600 mm
Concrete tributary width	$B_c = b_t+0.2L <= b_c$ ok.
Section Properties	
Area of timber	A_t = 12000 mm^2
$I_t = b_t h_t^3/12$	I_t = 62.5E+06
Area of concrete	A_c = 45000 mm^2
$I_c = b_c h_c^3/12$	I_c = 21.1E+06
Materials Properties	
Density of concrete	ρ_c = 2390.9 kg/m^3
Compressive strength at 28 days	$f'_{c,c.}$ = 39.5 MPa

Compressive strength at 91 days	$f'_{c,}$ = 50.33 MPa
MOE of concrete	E_c = 33933 MPa (AS3600-3.1.2)
Tensile strength of concrete	$f'_{t,c}$ = 2.52 MPa
Density of timber	ρ_t = 620.0 kg/m^3
Compressive strength	$f'_{c,t.}$ = 45 MPa
Bending strength	$f'_{b,t}$ = 48 MPa
Tensile strength	$f'_{t,t}$ = 33 MPa
Shear strength	$f'_{s,t.}$ = 5.3 MPa
Bearing strength	$f'_{p,t.}$ = 12 MPa
MOE of timber	E_t = 12402 MPa (this is the MOE of the LVL obtained from tests done after carved)

Connection Properties

Stiffness of connection from push out tests

Serviceability (average)	$K_{SLS,0.4}$ = 36900 N/mm
Serviceability (fifth percentile)	$K_{SLS,0.4}$ = 31700 N/mm
Ultimate (average)	$K_{ULS,0.6}$ = 35100 N/mm
Ultimate (fifth percentile)	$K_{ULS,0.6}$ = 29100 N/mm

Spacing of the connections

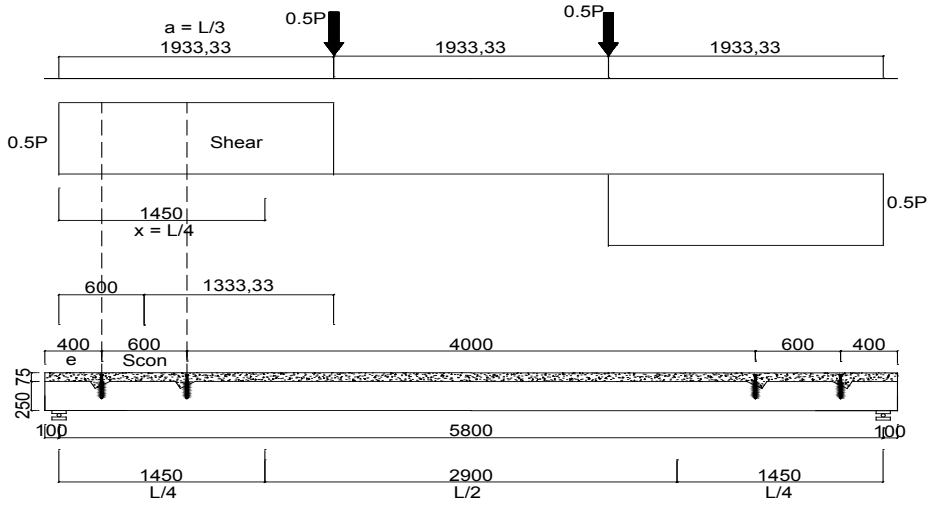

n = number of connectors along half span (from support to mid length) = 2

e = 400

s_{con} = (L/4-e)/ (n-1), S_{con} = 600 mm already given

S_{end} = S_{con}/2 +e =600/2+400 = 700 mm

S_{min} = min (S_{con}, S_{end}) = 600 mm

S_{max} = 4000/2 + 600 /2 = 2300 mm

S_{eff} = 0.75 S_{min} + 0.25 S_{max} = 1025 mm

Gamma coefficient

$$\gamma_c = \frac{1}{1+\pi^2 * E_c * A_c * \frac{S_{eff}}{(K_{ties} * L^2)}}$$,γ_c = 0.07 and γ_t = 1.0

H = $h_c/2+a_f+h_t/2$ H = 162.5 mm

$$a_c = \frac{\gamma t\ Et\ AtH}{\gamma c\ Ec\ Ac + \gamma t\ Et\ At}$$ a_c = 96.33 mm

$$a_t = \frac{\gamma c\ Ec\ AcH}{\gamma c\ Ec\ Ac + \gamma t\ Et\ At}$$ a_t = 66.17 mm

Effective bending stiffness

$EI_{eff} = E_c I_c + E_t I_t + \gamma_c E_c A_c a_c^2 + \gamma_t E_t A_t a_t^2$ EI_{eff} = 3.24E+12 Nmm^2

Analysis of the beam (strength limitations of the sections)

Concrete:

Bending strength limited by concrete capacity

$\phi M_u = \phi f'_c \frac{2(EI)_{eff}}{\gamma_c E_c h_c}$, Where (ϕ =0.6), and the applied bending stress is

$\sigma_{b,c} = \frac{E_c h_c M^*}{2(EI)_{eff}}$, $\sigma_{b,c} = (39.27E-08)M^*$

Concrete axial capacity, $\phi N_u = \phi f'_c A_c$, and the applied axial stress is

$\sigma_{c,c} = \frac{\gamma_c E_c a_c M^*}{(EI)_{eff}}$, $\sigma_{c,c} = (7.16E-08)M^*$, $N^*_c\ \sigma_{c,c} A_c = 3.33E-03M^*$ and the

Check compressive strength

$f'_{c,c} \geq \sigma_{c,c} + \sigma_{b,c}$ and $f'_{c,c} \geq (7.41E-08)+(39.27E-08)$,

Hence, M* < (50.33) / 46.4E-08 < 108329.72 kNmm

The equivalent load at four point loading test should not exceed; M* = (P_{tot}/2) a (where: a = L/3), P_{tot} < 112.1 kN

Check tensile strength

$f'_{c,t} \geq \sigma_{c,c} - \sigma_{b,c}$ and $f'_{c,t} \geq (7.16E-08)$ $(39.27E-08)$,

Hence, M* < (2.52) / 32.11E-08 < 7848 kNmm

The equivalent load at four point loading test should not exceed; M* = (P_{tot}/2) a (where: a = L/3), P_{tot} < 8.1 kN , Note that steel mesh are provided to resist the tensile stresses on the concrete.

Timber:

Bending strength limited by timber capacity

Φ = 0.85 (capacity factor)

K_1 = 1.0 (standard test)

K_4 = 1.0 (moisture content < 15 %)

K_6 = 1.0 (normal temperature)

K_9 = 1.0

K_{11} = 1.0 (size factor for bending)

K_{12} = 1.0 (stability factor)

$\phi M_u = \phi K_1 K_4 K_6 K_9 K_{11} K_{12} f'_b \frac{2(\mathrm{EI})_{eff}}{\gamma_t E_t h_t}$, ϕM_u = 80.4 E+6Nmm

K_{11} = 0.958 (size factor for tension)

and the applied bending stress is $\sigma_{b,t} = \frac{E_t h_t M^*}{2(\mathrm{EI})_{eff}.}$, $\sigma_{b,t} = (50.7E-08)M^*$

Timber axial capacity

$\phi N_u = \phi K_1 K_4 K_6 K_9 K_{11} K_{12} f'_t A_t$, , $\phi N_u = 0.32E+06N$

and the applied axial stress is; $\sigma_{t,t} = \frac{\gamma_t E_t a_t M^*}{(\mathrm{EI})_{eff}.}$,

$\sigma_{t,t} = (26.9E-08)M^*$, $N^*_t = \sigma_{t,t} A_t = 3.22E-03M^*$ and the

Check combined stresses, 1E-08M*+1.244E-08M* < 1.0

$\frac{N^*_t}{\varphi N_u.} + \frac{M^*}{\varphi M_u}$

Substituting the above values in the equation;

,

Hence, M* < 1/ 2.244E-08 < 44563.3 kNmm

The equivalent load at four point loading test should not exceed; $M^* = (P_{tot}/2)\ a$ (where: $a = L/3$), $P_{tot} < 46.1$ kN

Shear connector strength

$\Phi = 0.8$ (capacity factor for notches)

$K_1 = 0.86$ (short term test 5 hours for connection)

$\phi N_j = \phi K_1 K_4 K_6 Q_k$

$Q_k = 59.5$(average strength) $\phi N_j = 40.94\ kN$

At the support (x=0) ,

$V^* = P_{tot}/2$ (four point loading)

$Q^* = \gamma_c E_c A_c a_c S_{\min} V^* / (EI)_{eff}$, = 2.256V*, and $\varphi N_j \geq Q^*$, hence,

$40.94E+03 \geq 1.88V^*$

$P_{tot} = 36.3$ kN

Figure 100 Connector close to the right support before (right) and after (left) failure for B-4N

Figure 101 Connector at L/4 from the left support before (left) and after (right) failure for B-4N

Figure 102 Failure patterns on the LVL for B-4N

Figure 103 all the four connectors' investigation after failure for B-4N (N1 left end support, N2 left at L/4, N3 right at L/4 and N4 right support).

Figure 104 Connector close to the right support for B-NS.

Table 44: Results of bending test on LVL joist cut from the TCC beam (B-4N) after the ultimate test with 1260 mm clear span.

	Width	Depth	Peak Load	Stiffness	E
Specimen	mm	mm	kN	P/Δ	Gpa
LVL_B_4N_1	48.00	70.00	10.03	484	12348
LVL_B_4N_2	48.00	70.00	8.62	462	12291
LVL_B_4N_3	48.00	70.00	10.03	477	11836
		Mean	**9.56**	**474**	**12158**
		Stdev	**0.8**	**11.2**	**280.3**
		CoV	**9%**	**2%**	**2%**

Table 45: Results of bending test on LVL joist cut from the TCC beam (B-NS) after the ultimate test with 1260 mm clear span.

	Width	Depth	Peak Load	Stiffness	E
Specimen	mm	mm	kN	P/Δ	Gpa
LVL_B_NS_1	48.00	70.00	8.02	512	13672
LVL_B_NS_2	48.00	70.00	8.01	480	13576
LVL_B_NS_3	48.00	70.00	8.00	472	12128
		Mean	**8.01**	**488**	**13125**
		Stdev	**0.0**	**21.2**	**864.6**
		CoV	**0%**	**4%**	**7%**

Table 46: Results of tension test on LVL joist cut from the TCC beam (B-4N) after the ultimate test with 1000 mm clear length between the grips.

	Width	Depth	Peak Load	E	Tensile strength
Specimen	mm	mm	kN	Mpa	Mpa
LVL_B_4N_T_1	48.0	70.0	137.2	11578.1	40.8
LVL_B_4N_T_2	48.0	70.0	127.0	11548.7	37.8
LVL_B_4N_T_3	48.0	70.0	119.9	11546.4	35.7
		Mean	**128.0**	**11557.7**	**38.1**
		Stdev	**8.7**	**17.7**	**2.6**
		CoV	**6.8%**	**0.2%**	**6.8%**

Table 47: Results of tension test on LVL joist cut from the TCC beam (B-NS) after the ultimate test with 1000 mm clear length between the grips.

	Width	Depth	Peak Load	E	Tensile strength
Specimen	mm	mm	kN	Mpa	Mpa
LVL_B_NS_T_1	48.0	70.0	114.2	13307.8	34.0
LVL_B_NS_T_2	48.0	70.0	133.2	13288.1	39.6
LVL_B_NS_T_3	48.0	70.0	103.5	13341.5	30.8
		Mean	**117.0**	**13312.5**	**34.8**
		Stdev	**15.0**	**27.0**	**4.5**
		CoV	**12.8%**	**0.2%**	**12.8%**

Appendix H

This annex presents the calculations of the design loads for the timber composite beams in accordance to AS/NZS 1170.

Table 48: Design load for L6-01 and L6-03 beams according AS/NZS 1170

Loading		
AS/NZS 1170 (Ultimate Limit State)		
ULS (a) combination: 1.35G	1.17 kN/m	selfweight and permanent loading (permanent)
ULS (c) combination: 1.2G + 1.5Q	3.74 kN/m	selfweight, permanent & imposed loading (instantaneous&short term)
ULS (b) combination: 1.2G + 0.6Q	2.12 kN/m	selfweight, permanent & imposed loading (long term)
AS/NZS 1170 (Serviceability Limit State)		
SLS combination: G	0.87 kN/m	selfweight & permanent loading(permanent)
SLS (a) combination:G+Q	2.67 kN/m	imposed loading (instantaneous)
SLS (b) combination:G+ 0.7Q	2.13 kN/m	imposed loading (short-term)
SLS (c) combination: G+0.4Q	1.59 kN/m	imposed loading (long-term)
SLS combination: 1.0 kN	1.00 kN	imposed 'impact' loading (vibration)

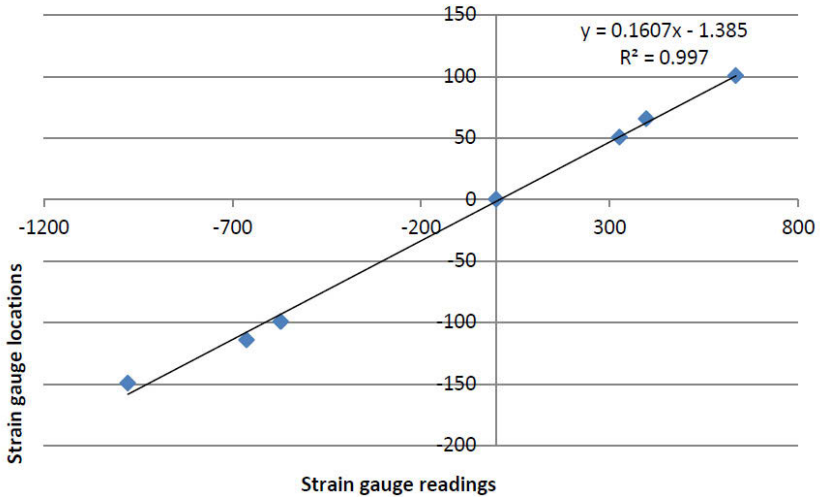

Figure 105: Strain distribution along the beam cross section during short-term test (Zabihi 2012)

Table 49: The transformed section properties of the timber composite beams

Charactristics of the Transformed Section		
Total Depth	250	mm
E_x	13200	N/mm^2
$\bar{y}$	97.6	mm
I_x	317121891.1	mm^4
EI_x	4.18601E+12	Nmm^2
Z_{top}	40488958905	mm^3
Z_{bottom}	28551306650	mm^3

Table 50: The analytical long-term deflection for L6-01 and L6-03 beams using GAMMA method and Euro code 5

Seviceability Limit State deflection					
Span	6000.0	mm	$\Delta = \frac{5\left(G^* + \varphi w^*_{imp}\right)L^4}{384(EI)_{ef}}$		
Long term limit (L/150 to L/300)	40.0	mm			
Calculated delfections					
Instantaneous					
Effective modulus of timber					
E_x (Nmm^2)	13200				
$_{Ix}$ (mm^4)	317121891.1	EI	4.19E+12		
Serviceability load, q	2.10	Kpa			
Self wt G	270.00	N/m			
SLS (a) combination:G+q	1530.00	N/m	1.53 N/mm		
Deflection due to instant load, t= 0 day	6.17	mm			
Long-term deflection due to creep, t= end of life					
Effective modulus of timber					
E_x (Nmm^2)	13200				
Duration	Service class		K_{def}	$K_2 = 1+K_{def}$	
long-term action	3		2	**3**	
$Ex_{ef} = E_x /(1+K_{def})$, (Nmm^2)	4400.00	the creep coeff for timber = 2 according to AS1170			
$_{Ix}$ (mm^4)	317121891.1	EI	1.3953E+12		
Serviceability load	2.10	kpa	1000N/m^2		
SLS (c) combination: (G+q)	1530.00	N/m	1.53 N/mm		
Deflection due to creep, t= end of life	18.50	mm			

Comparison	Beam L6-01	Beam L6-03			
	EC-5	EC-5			
Instantaneous deflection	6.17	6.17			
Total deflection at time t	18.50	18.50			

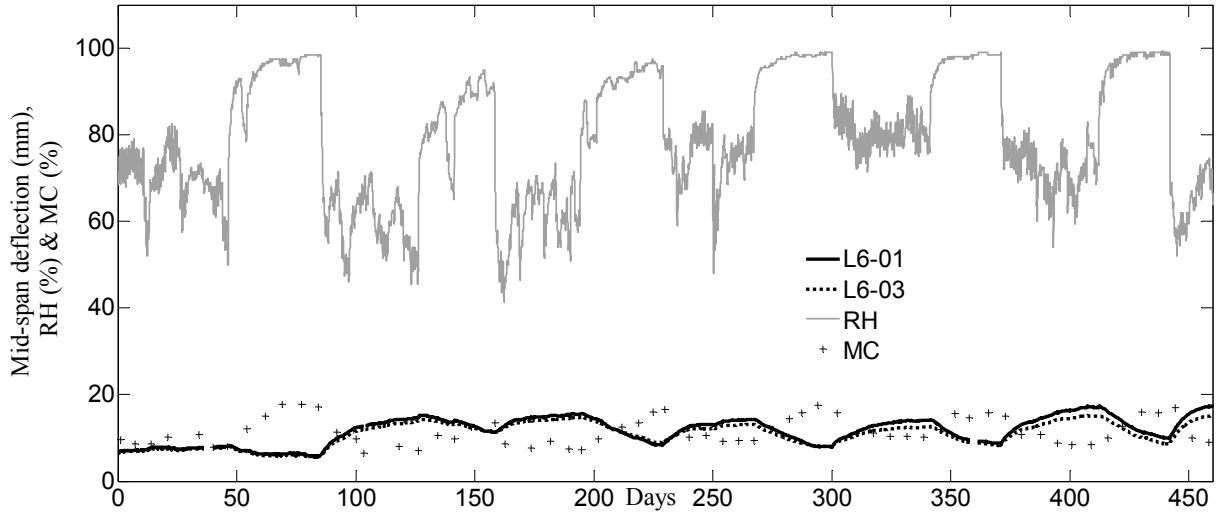

Figure 106: Relationship between the Mid-span deflection, moisture content and relative humidity of the chamber for timber only floor beams.